

AN ASSESSMENT OF SOIL EROSION USING RUSLE MODEL:
A CASE STUDY FROM THE MARMARA REGION

by

Alkor Ezer

Integrated B.S. and M.S. Program in Teaching Physics, Boğaziçi University, 2015

Submitted to the Institute of Environmental Sciences in partial fulfillment of

the requirements for the degree of

Master of Science

in

Environmental Sciences

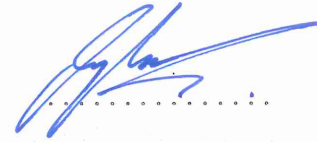
Boğaziçi University

2019

AN ASSESSMENT OF SOIL EROSION USING RUSLE MODEL:
A CASE STUDY FROM THE MARMARA REGION

APPROVED BY:

Assoc. Prof. Dr. Başak Güven
Thesis Advisor



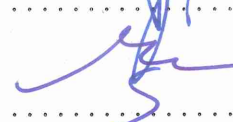
Prof. Dr. Levent Kurnaz
Thesis Co-Advisor



Assoc. Prof. Dr. Aslı Doğru



Prof. Dr. Mete Tayanç



DATE OF APPROVAL: 27/06/2019



TO MY FAMILY AND THE JOY OF LIFE...

ACKNOWLEDGEMENTS

I would like to express my sincere gratitude to my advisor Assoc. Prof. Dr. Başak Güven for her expert guidance, full support, understanding and encouragement, and thank my co-advisor Prof. Dr. Levent Kurnaz for supporting me on climate change throughout my thesis progress. I would also like to thank to the rest of my thesis committee: Assoc. Prof. Dr. Aslı Dođru, Prof. Dr. Mete Tayanç for their insightful comments, and I really hope to keep contact and work with them during my PhD. In addition, I am grateful to Assoc. Prof. Dr. Aslı Dođru for introducing me GIS and Remote Sensing techniques at Kandilli Observatory. Also, I am grateful to Assist. Prof. Dr. Berat Haznedarođlu for his guidance and patience during formatting my thesis.

I cordially thank to Dr. Şeyma Merve Kaymaz for training me in GIS and RS. I would like to thank to Dr. Aslı Sabuncu for helping me to create better maps for my research. I thank to Selen Gökçe for motivating me and being always there. I thank to Tufan Turp for his effort and help on creating R Factor maps. I also thank to Nazan An and all colleagues from IKLIMBU Laboratory for being a part of my thesis progress. In addition, I am especially indebted to my boss Şükrü Yiđit who have been always supportive of my career goals, and also I thank to all my colleagues from Veritas Education and Consultancy.

Last but not least, I would like to acknowledge with gratitude, the support and love of my dear family. They all kept me going, and this thesis would not have been possible without them. I am very much thankful to my aunt Necla Ezer who have always been the most dedicated person for me to achieve my educational goals, and I am very glad to be her nephew. I present my thanks and gratitude to my namesake, my grandmother Alkor Ezer, who is always with her joy and purity at every stage of my life. I would like to thank my mum Sema Ezer and my dad Halef Ezer for their unconditional and pure love. I would like to thank my sister and my confidant Ayça Ezer for encouraging me to be mature and strong. I would like to thank to my grandma Miyase Ürkmez. I commemorate and thank my grandfathers, Şadan Ürkmez and İhsan Ezer with longing, may the light with them...

Many thanks to my family and all the other precious people for making me feel deeply rooted on this Planet...

ABSTRACT

AN ASSESSMENT OF SOIL EROSION USING RUSLE MODEL: A CASE STUDY FROM THE MARMARA REGION

Soil is a vital resource for life. Soil erosion is one of the most serious natural problem caused by degrading land, agricultural and other human induced activities. The aim of this study is to predict the soil loss in the Marmara Region as a result of climate change. To achieve this, the **Revised Universal Soil Loss Equation (RUSLE)** is used and soil loss maps of the region are produced by the the help of remote sensing and geographic information systems techniques. While soil loss maps are produced between the years 1989 and 2017, future projections of soil erosion are also investigated for the period between years 2020 and 2049. For climate projections two scenarios of the Regional Climate Model are used: RCP 4.5 and RCP 8.5. The results showed that, when compared to the historical data, soil erosion risk in the future will increase in the Marmara Region. The soil loss results for the time interval 2020-2049 of the scenario RCP 8.5 is 61% higher than the results of the scenario RCP 4.5. Also, the results based on the historical data of the Regional Climate Model showed that the soil loss ranged from 0 to 24.298 Mg. ha⁻¹. year⁻¹ during the time interval 1989 -2017 in the Marmara Region, and the average soil loss is estimated as 12.2 Mg. ha⁻¹. year⁻¹.

ÖZET

RUSLE MODELİNİ KULLANARAK TOPRAK EROZYONUNUN DEĞERLENDİRMESİ: MARMARA BÖLGESİ VAKA ÇALIŞMASI

Toprak yaşam için hayati bir kaynaktır. Toprak erozyonu ise arazi kayıpları, tarımsal ve diğer insan kaynaklı faaliyetlerden kaynaklanan ciddi bir doğal sorundur. Bu çalışmanın amacı, Marmara Bölgesi'nde iklim değişikliğine bağlı toprak kaybını hesaplamaktır. Bu amacı gerçekleştirmek için çalışmada, Yenilenmiş Evrensel Toprak Kaybı Eşitliği Modeli (YETKE) kullanılmış olup, bölgenin toprak kaybı haritaları hazırlanırken uzaktan algılama ve coğrafi bilgi sistemleri tekniklerinden yararlanılmıştır. Toprak kaybı haritaları 1989 ve 2017 yılları arası için üretilirken, 2020 ve 2049 yılları arası için gelecek toprak erozyonu projeksiyonları da yapılmıştır. İklim projeksiyonları için Bölgesel İklim Modelinin iki senaryosu kullanılmıştır: RCP 4.5 ve RCP 8.5. Sonuçlar, tarihsel verilerle karşılaştırıldığında, gelecekte Marmara Bölgesi'nde toprak erozyonu riskinin artacağı öngörülmüştür. RCP 8.5 senaryosunun sonuçlarına göre 2020-2049 zaman aralığındaki toprak kaybı, RCP 4.5 senaryosunun sonuçlarından %61 daha yüksektir. Bölgesel İklim Modelinin tarihsel verilerine dayanan sonuçlar, toprak kaybının 0 ile 24.298 Mg.hektar⁻¹.yıl⁻¹ arasında olduğunu göstermiştir. Ayrıca, Marmara Bölgesi'nde 1989 - 2017 arasındaki zaman aralığında ortalama toprak kaybının 12.2 Mg.hektar⁻¹.yıl⁻¹ olduğu hesaplanmıştır.

TABLE OF CONTENTS

ACKNOWLEDGEMENTS	iv
ABSTRACT	v
ÖZET	vi
TABLE OF CONTENTS	vii
LIST OF FIGURES	ix
LIST OF TABLES	xi
LIST OF SYMBOLS/ABBREVIATIONS	xii
1. INTRODUCTION.....	1
1.1. Aim of the Study.....	2
1.2. Objectives of the Study.....	3
2. LITERATURE REVIEW.....	4
2.1. Soil Erosion Models (SOMs)	8
2.2. Geographical Information Systems (GIS) and Remote Sensing (RS) Techniques	10
2.3. Climate Change and Climate Models (CMs)	11
2.3.1. A Regional Climate Model System: RegCM	13
2.3.2. ERA Interim	14
3. MATERIALS AND METHODS	15
3.1. Description of the Study Area	15
3.1.1. Climate and Vegetation of The Study Area.....	16
3.2. RUSLE Model Application	18
3.2.1. RUSLE Model Description	18
3.2.2. RUSLE Factors.....	22
3.2.2.1. Rainfall Erosivity Factor (R)	22
3.2.2.2. Soil Erodibility Factor (K).....	25
3.2.2.3. Slope Length (L) and Slope Steepness (S) Factors	26
3.2.2.4. Land Cover and Management Factor (C)	32
3.2.2.5. Conservation Support Practice Factor (P)	36
4. RESULTS AND DISCUSSIONS	37
4.1. R Factor	37
4.2. K Factor	50
4.3. LS Factor	55

4.4. C Factor58

4.5. Soil Loss60

5. CONCLUSION66

REFERENCES68

APPENDIX A: FAO SOIL UNITS79

APPENDIX B: THE FAO SOIL UNITS FOR TURKEY80

APPENDIX C: THE SOIL CONTENT PROPERTIES OF FAO SOIL84



LIST OF FIGURES

Figure 3.1. The Map of the Marmara Region with its 11 Districts.....	15
Figure 3.2. Overlay of the RUSLE model.....	19
Figure 3.3. A Schematic Approach to the Workflow of the RUSLE Model.....	21
Figure 3.4. Demonstration of the values used in LS calculations.....	27
Figure 3.5. Flow Chart of LS Factor.....	28
Figure 3.6. Flow Direction Map for Marmara Region created in ArcGIS.....	29
Figure 3.7. Flow Accumulation Map for Marmara Region created in ArcGIS.....	30
Figure 3.8. Marmara Region DEM Map (created in SRTM DEM).....	31
Figure 3.9. Normalized Difference Vegetation Index of the Marmara Region (NDVI).....	34
Figure 4.1. RCM Modified Fournier Index Variability During 1989-2017.....	40
Figure 4.2. ERA-Interim Modified Fournier Index Variability During 1989-2012.....	41
Figure 4.3. RCP 4.5 Modified Fournier Index Variability During 2020-2049.....	42
Figure 4.4. RCP 8.5 Modified Fournier Index Variability During 2020-2049.....	43
Figure 4.5. R Factor Map Marmara HIST 1989-2017.....	44
Figure 4.6. RFactor Map Marmara ERA-Interim 1989-2017.....	45
Figure 4.7. RCP 4.5 R Factor Map 2020-2049 of the Marmara Region.....	46

Figure 4.7. RCP 8.5 R Factor Map 2020-2049 of the Marmara Region.....	47
Figure 4.9. MFI and R Factor Results for the Marmara Region, Turkey.....	49
Figure 4.10. RUSLE Model K Factor Map created in ArcGIS for Marmara Region.....	53
Figure 4.11. Marmara Region Slope Map.....	56
Figure 4.12. RUSLE Model LS Factor Map created in ArcGIS.....	57
Figure 4.13. C Factor Map of the Marmara Region.....	59
Figure 4.14. Soil Loss Historical Map of the Marmara Region (Historical data between the years 1989-2017).....	61
Figure 4.15. Soil Loss RCP 4.5 Map of the Marmara Region (2020-2049).....	62
Figure 4.16. Soil Loss RCP 8.5 Map of the Marmara Region (2020-2049).....	63
Figure 4.17. Soil Loss Map ERA-Interim of the Marmara Region.....	64

LIST OF TABLES

Table 2.1. The relationship between Intensity of Rainfall and Soil Loss.....	5
Table 2.2. The effect of Slope Percentage and Intensity of Rainfall on Soil Erosion.....	6
Table 2.3. The List of Soil Erosion Models (SOMs).....	8
Table 2.4. Types of Representative Concentration Pathways (RCP's).....	12
Table 3.1. Soil erosion risk classification based on average erosion rate estimated by RUSLE.....	20
Table 3.2. RUSLE Model Factors with their abbreviations, units, and sources.....	22
Table 3.3. The erosivity classes by Fournier Index (F) and modified Fournier Index (F_M).....	24
Table 3.4. C Factor Marmara Region: Land use and Land Cover Classes.....	35
Table 4.1. K Factor Table for the Marmara Region.....	50

LIST OF SYMBOLS/ABBREVIATIONS

Symbol	Explanation	Unit
A	Mean Annual Soil Loss	Mg.ha ⁻¹ .year ⁻¹
C	Crop Management Factor	
E	Total Storm Energy	MJ.ha ⁻¹
F	Fournier Index	mm
F _M	Modified Fournier Index	mm
I30	Maximum 30 Minutes Intensity	MJ.ha ⁻¹
K	Soil Erodibility	Mg.h.MJ ⁻¹ .mm ⁻¹
L	Slope Length	m
LS	Slope Length and Steepness	m
MFI	Modified Fournier Index	mm
OC	Organic Carbon %	
P	Conservation Support Practice	
<i>P</i>	Mean Annual Rainfall amount	mm
<i>P_i</i>	Mean Annual Rainfall Amount For a Month	mm
<i>P_{max}</i>	Monthly Average Amount of Rainfall of the Most Rainy Month	mm
R	Rainfall Erosivity	MJ.mm.ha ⁻¹ .year ⁻¹
S	Slope Steepness	
SAN	Sand (%)	
SIL	Silt (%)	
SNI	Sand Content Subtracted from 1 and Divided by 100	
Abbreviation	Explanation	
AGNPS	Agricultural Non-Point Source Pollution Model	
ANSWERS	Areal Nonpoint Source Watershed Environment Response Simulation	
CDO	Climate Data Operator	
CREAMS	Chemicals, Runoff, and Erosion from Agricultural Management Systems	

cm	Centimeter
cm ²	Squared Centimeter
cm ³	Cubic Centimeter
CMs	Climate Models
CORINE	Coordination of Information on the Environment
DEM	Digital Elevation Model
ECMWF	European Centre for Medium-Range Weather Forecasts
ECPs	Extended Concentration Pathways
EGEM	Ephemeral Gully Erosion Model
EPIC	Erosion Productivity Impact Calculator
ERA-INTERIM	European Centre For Medium-Range Weather Forecasts Data Reanalysis Interim Version
EROSION2D/3D	2D Rainfall Erosion Model
ETM	Enhanced Thematic Mapper
EU	European Union
EUROSEM	European Soil Erosion Model
GAMES	Guelph Model for Evaluating The Effects of Agricultural Management Systems on Soil Erosion and Sedimentation
GFDL-ESM2M	Geophysical Fluid Dynamics Laboratory Geophysical Fluid Dynamics Laboratory
GeoWEPP	Geospatial Interface for the Water Erosion Prediction
GHGs	Greenhouse Gases
GIS	Geographical Information Systems
GLEAMS	Groundwater Loading Effects of Agricultural Management Systems
gr	Gram
FAO	Food and Agriculture Organization of the United Nations
ha	Hectare
HadGEM2	Hadley Global Model 2
HadGEM2-ES	Hadley Centre's "Standard" Climate Model
IAMs	Integrated Assessment Models
ICONA	Institute for Nature Conservation
ICTP	Abdus Salam International Centre for Theoretical Physics
IKLIMBU	Centre for Climate Change and Policy Studies of Boğaziçi University

IPCC	Intergovernmental Panel on Climate Change
IR	Infrared
KINEROS	Kinematic Runoff and Erosion Model
km	Kilometer
km ²	Squared Kilometers
LISEM	Limburg Soil Erosion Model
LUCC	Land Use and Cover Change
MADALUS	Mediterranean Desertification and Land Use
MOSES	Modular Soil Erosion Systems
MPI-ESM-MR	Meteorological Research Institute Earth System Model Version
NASA	National Aeronautics and Space Administration
NCAR	National Center for Atmospheric Research
NDVI	Normalized Difference Vegetation Index
NETCDF	Network Common Data Form
NIR	Near Infrared
Ns	Nanosecond
SOMs	Soil Erosion Models
Ppm	Part Per Million
RCM	Regional Climate Model
RCPs	Representative Concentration Pathways
RS	Remote Sensing
RUSLE	Revised Universal Soil Loss Equation
SRES	Special Report on Emission Scenarios
SRTM	Shuttle Radar Topography Mission
STORM	Storage Treatment Overflow Runoff Model
SWAT	Soil and Water Assessment Tool
t	Tone
TIN	Triangulated Irregular Network
TM	Thematic Mapper
UK	United Kingdom
USA	United States of America
USGS	The United States Geological Survey
USLE	Universal Soil Loss Equation
UTM	Universal Transverse Mercator
Yr	Year

W	Watt
WATEM/SEDEM	Water and Tillage Erosion Model
WEPP	The Water Erosion Prediction Project
WGS	Whole Genome Sequencing



1. INTRODUCTION

The majority of the landscapes of the earth is made up of soil. Soil plays a significant role in the natural ecosystem (Singer and Warkentin, 1996), and is a major natural resource to support life on Earth. Moreover, being one of the most important cornerstones of the life processes in nature, together with water and air, has been seen as an indispensable source of life for securing basic food production. Therefore, the soil is considered to be the most important element in meeting the basic needs of food, feed and fuel, and in the continuation of all terrestrial life (Blanco and Lal, 2008).

Soil erosion is an important social and economic problem and an essential factor in assessing ecosystem health and function. Soil erosion is the most common form of soil degradation worldwide (Bridges and Oldeman, 1999). Soil erosion can lead many adverse influences on water quality, hydrological systems, agricultural activities, and these environmental problems caused by soil erosion have long been recognized as severe problems for human sustainability (Lal, 1998). Soil erosion is a diffusion process occurring and varying from spatial characteristics over a typical landscape (Khare et. al., 2016). The present form of the Earth's surface is being shaped with the effect of naturally occurring physical phenomenon (Das, 2002). Indeed, we as humanity are situated on a landscape which is mostly product of erosion. For example, the Quaternary landscapes of Iowa were formed over the time period of the last 10,000 and 20,000 years (Ruhe, 1969), which might be accepted as relatively young, whereas the topsoil surfaces of the Appalachian Mountain were formed more than millions of years ago (Thornbury, 1965).

Even one single drop of water reaching the soil surface in microseconds have importance to observe the mechanism of nature, and how the natural events are interrelated. In a former research on soil erosion, the impact pressures of raindrops on a soil surface were recorded at a rate of one data point per 500 ns (5×10^{-7} second) in order to experiment those few microseconds of peak impact pressures (Nearing et al., 1987). In a more recent study, Nearing et al. (2017), also investigated the soil erosion on various spatial scales ranging from millimeters for raindrops to megameters for continents.

The factors controlling the soil erosion rate and magnitude include vegetation, fraction cover, rainfall intensity, run-off, land-use and land cover. Thus, the amount of soil loss is dependent upon intensity, duration and frequency of precipitation events, and these factors are likely to be affected

by climate change, slope gradient, vegetation fraction cover, etc. Therefore, it is obvious that the risk of soil erosion can be assessed based on the inter-related processes of the slope, vegetation cover, and land-use type for rill and sheet erosion of the study area (Zhang et. al., 2010). It is difficult to estimate the amount of soil erosion due to complicated interplay of many factors, such as land cover, soil structure, topography, climatic conditions, as well as human induced activities. Indeed, besides biophysical factors, socio-economic and political factors may also affect soil erosion (Ananda and Herath, 2003). Recently, especially with the help of Geographical Information Systems (GIS) and Remote Sensing (RS) techniques, analytical models such as Universal Soil Loss Equation (USLE) and Revised Universal Soil Loss Equation (RUSLE) have successfully been applied on national, regional, and watershed scales for the analysis of soil loss (Kinnell, 2000; Erdoğan et al., 2005).

Today, soil erosion became one of the most important world-wide environmental issue. In Turkey, 54 % of forest areas, 59 % of agricultural land, and 64 % of pastures experience severe erosion. In the future, it is expected that Turkey will face even more severe soil erosivity due to its topographical structure and the impacts of climate change (Tağıl, 2007). In addition to physical factors, human induced effects are too high to be underestimated. Especially, forest destruction, industrialization, urbanization, unproductive land use, and grazing activities have striking roles on soil erosion.

To sum up, the estimated average soil loss for Turkey is $6.14 \text{ t ha}^{-1} \text{ y}^{-1}$ (Çakal et al., 1997), the average values for soil loss vary from region to region in Turkey. For example, the soil loss in the Mustafakemalpaşa River in the Marmara Region of Turkey was estimated $11.2 \text{ Mg. ha}^{-1} \text{ year}^{-1}$ (Ozsoy G et al., 2012).

1.1. Aim of the Study

The aim of the study is to predict the soil loss of the Marmara Region with Revised Universal Soil Loss Equation (RUSLE) Model by using remote sensing (RS) and geographical information system (GIS) techniques for the time interval 1989-2017, and also to predict the future soil loss of the region in a changing climatic conditions by using RCP 4.5 and RCP 8.5 future scenarios of Regional Climate Model (RCM) for the time interval 2020-2049.

1.2. Objectives of the Study

- 1) Assessing the current and historical situation of soil erosion on the Marmara Region for the years 1989-2017
- 2) Projection of soil erosion due to the RCP 4.5 and RCP 8.5 scenarios of the Regional Climate Model for the years 2020-2049
- 3) Development of incorporation of GIS and Remote Sensing Techniques with the RUSLE Model



2. LITERATURE REVIEW

The problem of land use and land cover changes (LUCC), and soil erosion have been the two of the most worldwide discussed environmental topics in recent decades (Latocha et al., 2016). This situation is essentially caused by increasing human impact on the environment, which leads loss of natural vegetation. Due to human induced activities, forested areas are turned to arable lands, creating a situation that causes increase of soil erosion from slopes (Yang et al., 2003). Majority of the research about soil erosion and land use and cover changes focuses on the consequences of anthropogenic degradation of the environment, such as the mechanization of agriculture (Martinez et al., 2000). Soil erosion can lead many environmental problems. Firstly, it induces the reduction in farmland surfaces. Secondly, it causes refilling of lakes and dams. These two results of soil erosion make it an environmental problem, which degrades grounds, induces a modification of their porosity, deterioration of fertile land surfaces, and reduction in agricultural production (Gaubi et al., 2016). Moreover, soil erosion has adverse influences on water quality, and hydrological systems (Lal, 1998)

Since the beginning of the Industrial Revolution, the concentration of carbon dioxide in the Earth's atmosphere has increased by 30 %, also between one-third and one-half of the land surface has been transformed by human induced activities, and also more than half of the accessible surface freshwater is consumed by humanity (Vitousek et al., 1997). By considering these cases and other various environmental issues, it becomes obvious that we live on a human-dominated planet. There is well-established, and scientifically proved relationship between climate and soil erosion, and this relationship have been studied by many researchers in order to reveal the probable outcomes of climate change on soil erosion (Langbein and Schumm, 1958). When it comes to one of the major influences on soil erosion, impact of climatic changes, particularly the changed precipitation trend is the most outstanding one. The International Panel on Climate Change (IPCC) defines climate change as a change in the state of the climate that can be identified by changes in the mean and/or the variability of its properties, and that persists for an extended period, typically decades or longer. That is to say, climate change is any change in climate by considering a period of time, whether due to natural variability or as a result of human induced activity. Due to environmental changes in 21th century it is expected that the future climate change will affect the frequency, magnitude, and extent of soil erosion (Pruski and Nearing, 2002a). Due to climatic changes erosive nature of precipitation events are increasing. Another influence of climate change on soil erosion rates is through changes in plant amount and composition. Climatic changes influence plant growth, which may affect

surface runoff and soil erosion. Thus, it can be interpreted that the relationship between environmental processes are complex with many interconnected and interwoven parts, which may affect one another, resulting in a domino effect (Pruslu and Nearing, 2002b). For example, research suggests that due to the increase in atmospheric carbon dioxide via human induced activities, the plant production and the plant transpiration rates change, which can lead to an increase in soil surface canopy cover, as well as biological ground cover (Rosenzweig and Hillel, 1998).

There are several natural factors affecting soil erosion such as wind, temperature, humidity, but among all these triggering factors, the most prominent one can be considered as precipitation (Doğan et al., 1976). Soil loss is directly related with the erosive nature of the rainfall, and the effect of it on removing the soil from topsoil. Thus, intensity of rainfall is important in terms of analyzing the erosivity of the soil. This can be demonstrated by the Fournier Index, which gives the correlation between the intensity of rainfall and soil loss.

This is later supported by Morgan (1991) with a study, which includes 183 different meteorological stations used for climatic data collection. The results of the study showed that 5 fold increase in the amount 5 duration of precipitation (mm/ha) caused 13 times increase in soil loss amount (Morgan, 1991). The relationship between the Intensity of Rainfall and Soil Loss derived from Morgan's (1991) study is provided in Table 2.1:

Table 2.1. The relationship between Intensity of Rainfall and Soil Loss (Morgan, 1991).

Maximum Rainfall (5 minutes intensity) (mm/ha)	Frequency of Precipitation Events	Average Soil Loss (kg/m²)
0-25.4	40	0.37
25.4-50.8	61	0.60
50.9-76.2	40	1.18
76.3-101.6	19	1.14
101.7-127.0	13	3.42
127.1-152.4	4	3.63
152.5-177.8	5	3.87
177.9-254.0	1	4.79

Scientists have studied the relationship between the rainfall and erosion via laboratory experiments, on site data collection, or using GIS based models. For example, Fox and Bryan (1999) carried out an experimental study in South Ontario, Canada, using grey and brown luvisols (50% sand, 20% silt, 28% clay) in landscapes having 100 x 40 x 10 cm³ volume. The main objective of the study was to observe the relationship between rainfall and soil loss on these artificially created landscapes. The applied artificial rainfall was set to 38.2 - 56.3 mm/h (millimeter per hour),

with an approximate value of 49.1 mm. The density and thickness of the soil were 1.29 gr/cm³ and 2 cm, respectively. The results of the study showed the rainfall erosivity factor (R) of the model RUSLE was reliable, and observed rainfall erosivity values were in agreement with the modeled R factor. Another experimental study by Römken et al. (2011) observed various precipitation events in different landscape slopes using artificial soil blocks having 3.7 x 0.61 x 0.23 m³ volume. In this study, Gredana Silt, comprised of 18% clay, 80% silt and 2% sand was used, and the soil blocks were inclined by 2%, 8% and 17%. The applied artificial rainfall was in four different magnitudes; 15, 30, 45, and 60 mm/h. The results of the study are outlined in Table 2.2.

Table 2.2. The effect of Slope Percentage and Intensity of Rainfall on Soil Erosion (Römken et al., 2011).

Intensity of Rainfall (mm/hour)	The Slope Percentage		
	2%	8%	17%
15	0.01	0.01	0.05
30	0.13	0.08	1.74
45	0.19	0.24	1.89
60	0.40	0.67	1.44
Sum:	0.73	1.00	5.12

By considering the results of this particular study, it can be stated that drainage and soil surface topography have direct effects on the topsoil loss. Results indicated smooth topsoil surfaces had less soil loss, when compared to rough topsoil surfaces (Römken et al., 2011).

Soil structure class, stability of soil structure, soil organic carbon content, the fraction of clay, sand and silt, as well as the mineral content of the soil are the soil characteristics, which affect soil erosion (Lal, 1994). The large soil blocks are more resistive to move, and the small soil blocks are more resistive to be separated into tinier particles. Among other soil contents, the least resistive soil contents are silts and fine sands. According to a study by Richter and Negendak (1977), the least resistive soil to erosion had 40-60% silt content. Evans (1980) studied the relationship between the erosivity and the clay content of the soil in theoretical manner. Results suggested that soils, which have less than 2% organic content can be defined as erosive soils. On Earth the most soil structures contain less than 15% organic content. According to Voroney and colleagues (1980), the erosivity of the soil and the increase in the organic content are directly proportional if the soil have more than 10% organic content. So, the increase in organic content in the soils having more than 10% organic content causes a linear increase in erosivity. Figuerido and Peosen (1998) investigated the effects of stones, placed on the topsoil, on the formation of soil erosion. The researchers designed the

experiment with the metal blocks having 612 cm² area, and they covered the topsoil with the soil having 17%, 30%, 66% grit sand stones. The blocks were left on 10% slope under 240 mm rainfall. Results of the experiment indicated positive relationship between rocky soil surfaces and infiltration, and negative relationship between rocky soil surface and surface flow and flow accumulation. It can be concluded from the study that the stones on the topsoil affect the rainfall impact on the soil and the flow rate.

Fu et al. (2000) investigated the effect of change in land use and slope on soil erosion rate in semi-arid part of China, the Shaanxi Region. The study area was 2.02 km², with an average annual precipitation of the study was undertaken for the time period 1984-1996, and the results showed that an increase in forested and agricultural lands by 7% (from 36% to 43%), lead to a decrease in soil erosion rate by 24% (from 11.886 ton/km²/year to 8.979 ton/km²/year). Kosmas et al. (1997) performed a study investigating the land use and vegetation cover effects on surface flow and soil loss in the areas selected from the Mediterranean countries; Portugal, France, Spain, Italy, and Greece. The authors realized that for time periods, which the topsoil became devoid of plants, higher rates of soil loss were observed. When vegetation was lacking, the test areas which are subject to 200mm annual rainfall exhibit no risk for soil erosion, whereas areas having 700 mm and higher annual rainfall are evaluated as risky in terms of soil erosion, with erosion rates ranging from 15 and 90 ton/km²/year. In areas, where the plants were grown in semi-natural conditions such as olives, soil loss was at least 0.8 tons / km² / year. The soil loss amounts were recorded for the areas covered with shrubs and heaths as 6.7 tons. km⁻² year⁻¹. In addition, the soil loss was recorded for the areas covered with vineyards and eucalyptuses as 142.8 and 23.8 tons. km⁻² year⁻¹ respectively.

There is a study from Büyükçekmece Basin of the Marmara Region by Karaburun et al. (2009). In the study of Karaburun et al. (2009), the RUSLE Model was used to calculate soil loss. The RUSLE factors of the Büyükçekmece basin were produced as five raster layers. The average land loss in the basin was calculated as 2,4 tonne per year. Moreover, in another study by Doğan (2002), he analyzed the data of 96 stations belonging to many years in the country and calculated the R values of these stations. From these calculations, the precipitation of Black Sea, Marmara, Aegean and Mediterranean coastlines is quite high. 15 It is observed that low snowfall in the mountains, mountain ranges and highlands with low erosive power falls. The places where the R value is high (erosive potential) are generally where the amount of precipitation is high and the rain is in the form of rain. Although Rize has the highest R value with 481.385 t / ha and Marmaris with 522.178 t / ha, Aksaray is located between 13.693 t / ha and Van having the lowest R value with 17.625 t / ha R value.

2.1. Soil Erosion Models (SOMs)

In long term, the interest of hydrologist, geomorphologist, agronomist, environmental scientists and other earth science disciplines in soil erosion and sediment transport has led to the development of many SOMs including variety of purposes. The main perspectives of SOMs are creating simulations for analyzing the effects of watershed variables on soil erosion, conservation planning in agricultural lands, site-specific assessments, and project evaluation (Foster, 1990; Albaladejo and Stocking, 1989). Classifying SOMs into mutually exclusive types is very difficult, but can be determined by combining characteristics such as spatial scales, process, duration, hydrological processes, and model output (Witinok, 1988).

There are many qualitative and quantitative methods for the risk assessment of soil erosion. According to the perspectives of many scientists working on this field, the main purpose is to illustrate the qualitative maps includes the soil erosion parameters, and triggering factors. There are several models and methods to assess the soil erosion. Among all the soil erosion assessment methods the most striking ones are USLE (Wischmeier and Smith, 1978), RUSLE (Renard et al., 1997), EPIC , ANSWERS (Beasley et al., 1981), CORINE (CORINE, 1992), ICONA (ICONA, 1997), WEPP (Nearing et al. 1989 & Flanagan et al. 2007), GeoWEPP (Minkowski, 2007), CREAMS (Knisel, 1980), GLEAMS (Leonard et al., 1987), AGNPS (Young, 1986), EGEM (Woodward, 1999), EUROSEM (Morgan et al., 1998), SWAT (Arnold et al., 1988), STORM (USACE, 1977), KINEROS (Woolhiser et al., 1990) etc. In the Table 2.3. there is a list of the most common soil erosion model:

Table 2.3. The List of Soil Erosion Models (SOMs).

	Model Acronym and Full Name	References
1	USLE/RUSLE Universal Soil Loss Equation/ Revised Universal Soil Loss Equation	(Wischmeier and Smith, 1978) (Renard et al., 1991)
2	SLEMSA Soil Loss Estimator Model for South Africa	(Stocking and Elwell, 1973)
3	CREAMS Chemical Runoff and Erosion from Agricultural Management System	(Knisel, 1980)
4	GLEAMS Groundwater Loading Effects of Agricultural System	(Leonard et al., 1995) (Knisel and Turtola, 2000)

5	EPIC Erosion Productivity Impact Calculator	(Williams et al., 1983)
6	KYERMO Kentucky Erosion Model	(Hirschi and Barfield, 1988)
7	WEPP Water Erosion Prediction Project	(Nearing et al., 1989) (Flanagan et al., 2007)
8	EROSION 2D/3D 2D Rainfall Erosion Model	(Schmidt et al., 1999)
9	MADALUS Mediterranean Desertification and Land Use	(Kirkby et al., 1988)
10	GAMES Guelph Model for Evaluating the Effects of Agricultural Management Systems on Soil Erosion and Sedimentation	(Rudra et al., 1986)
11	EUROSEM European Soil Erosion Model	(Morgan et al., 1998)
12	LISEM Limburg Soil Erosion Model	(De Roo, 1996) (De Roo et al., 1996)
13	ANSWERS The Areal Nonpoint Source Watershed Environment Response Simulation	(Beasley et al., 1980)
14	SWAT Soil and Water Assessment Tool	(Gassman, et al., 2007)
15	AGNPS Agricultural Non-Point Source Pollution Model	(Young, 1986)
16	STORM Storage Treatment Overflow Runoff Model	(USACE, 1977)
17	CORINE Coordination of Information on the Environment	(CORINE, 1992)
18	GeoWEPP Geospatial Interface For The Water Erosion Prediction	(Minkowski, 2007)
19	ICONA Institute for Nature Conservation	(ICONA, 1997)

Any Soil Erosion Model (SOMs) is bound to have some strengths and limitations due to the reason that model creators and developers contribute different philosophical aspects and mostly

develop models for specific environmental conditions (Grunwald and Frede, 1999). Mostly, soil erosion models have been developed mainly for agricultural parts of North America and Europe. In these landscapes biophysical environmental factors (e.g. climate, soil, topography, land use), socio-cultural agricultural practices (e.g. cropping and management practices), are indicative for the soil erosion models. When the models are compared, the models covering the mid-altitudes have traditionally conducted on farming fields that indicates short slope lengths with moderate, relatively evenly distributed slope angles. Actually, the slopes exceeding 16% are rare effective to analyze soil erosion because such lands are not most commonly cultivated in temperate regions (El-Swaify, 1997), and also studies of the regions having slopes greater than 50% are rare (McCool et al., 1987; Nearing, 1997). Yet, slope is one of the most important factor affecting soil erosion rates (Zingg, 1940; Desmet and Govers, 1995).

In this study RUSLE (Revised Universal Soil Loss Equation) model is used. Revised Universal Soil Loss Equation (RUSLE) (Renald et al. 1997) is an empirical erosion model which was founded on the Universal Soil Loss Equation, USLE (Wischmeier and Smith 1978). American scientists developed the Universal Soil Loss Equation (USLE) (Wischmeier and Smith, 1978) as a technique for assessing erosion and evaluating the likely effects of different soil conservation practices. Assessment of soil erosion by RUSLE model requires using remote sensing and GIS (Geographical Information Technology). In the model, there are five different major factors used in order to formulate soil erosion loss. The factors are symbolized with R, K, L, S, C, P. The factor R represents rainfall patterns, K represents type of soil, L&S together represents topography conditions, C represents crop management system, P represents. These all factors are taken from the model USLE/RUSLE (Renard et al., 1997). The multiplication of these five factors give the soil loss.

2.2. Geographical Information Systems (GIS) and Remote Sensing (RS) Techniques

In this study, ArcGIS software is used as geographical information system software, and also, Landsat will be used as the satellite to take remote sensing images to visualize the Marmara Region, and also make some calculations and analysis through the region. Firstly, ArcGIS as geographical information (GIS) technology is used in order to build a framework for gathering, managing, and analyzing data. ArcGIS integrates different types of data, also it analyzes spatial location and forms layers of information into visualizations. Moreover, Landsat is a US (NASA and USGS) satellite remote sensing program, and also it was first civil Earth-observing satellite program. It started to

operate with the first Landsat satellite's launch in 1972 with the name Landsat1, and is continuing with Landsat 8, still operational.

2.3. Climate Change and Climate Models (CMs)

This study also aims at evaluating the soil loss under a changing climate. To serve this purpose, Regional Climate Model is used to make future climate projections of the Marmara Region, hence to investigate the effect of climate change on soil erosion. With the industrial revolution and human induced activities global climate change has been a global issue, and in order to prevent, reduce, and coordinate the possible consequences of global climate change, the World Meteorological Organization (WMO) and the United Nations Program in Environment was established 'The Intergovernmental Panel on Climate Change' (IPCC) in 1988 (Gürkan et al., 2016). Currently, IPCC act as one of the most important organizations coordinating the actions on climate change. One of the most important action of IPCC is indicating the possible outcomes of climate change for the future of humanity. In other words, it is aimed to coordinate the creation of possible scenarios for the future. According to Gregory and Duran (2001), a 'Scenario' is a story depicting some future events. A scenario is not an estimate of the future; as defined in (IPCC, 2000). In climatic researches, socio-economic and emission scenarios are significant to indicate how the future may evolve with respect to altering socio-economic, technologic, energy and environmental conditions. The environmental status is generally based on changes in land use practices and emissions of the green house gases (GHGs). The socio-economic and emission scenarios are used as input for climate model runs and they form a basis for assessment of possible climatic impacts and mitigation options, as well as associated costs (Vuuren et al., 2011). In order to make reliable comparisons among various studies, it is better to use a common set of scenarios with scientific communities, by this way a cumulative understanding can be developed easily. Looking at the history of socio-economic and climatic scenarios, one can conclude that a number of scenarios have performed a significant role, including the IS92 scenarios developed by Leggett et al. (1992) and, more recently, the scenarios from the Special Report on Emission Scenarios (SRES) (Nakicenovic et al., 2000). Indeed, Moss et al. (2010) suggests that, the research communities all around the world need new scenarios to create new understandings. As first, in order to run and evaluate the results of current generation climate models, more detailed information is needed than the previous scenario sets (Vuuren et al., 2011). Also, there is an increasing demand in the scenarios exploring the effects of different climate policies, and these types of scenarios should allow the scientists to investigate the 'costs' and 'benefits' of long term climate goals. In order to carry out a detailed investigation of the climatic issues, interdisciplinary approach to integrate information is necessary to aid the scientists

to get more reliable results. There is the need for new generation approach, and new climatic and socio-economic approaches to give countenance to the International Panel on Climate Change (IPCC). The scientific communities should develop new strategies and scenarios for future climate change assessments (IPCC, 2007). The IPCC community left new scenario development responsibility to the research communities (Vuuren et al., 2011). The IPCC adopts a 3-phase design process (Moss et al., 2010):

- i. Development of a scenario set containing emission, concentration and land use trajectories – referred as ‘representative concentration pathways’ (RCPs).
- ii. A parallel development phase with climate model runs, and development of new socio-economic scenarios.
- iii. A final integration and dissemination phase.

Table 2.4. Types of Representative Concentration Pathways (RCP's) (Based on IPCC, 2007).

Name of RCP's	Radiative Forcing	Time	Pathway Shape	Concentration (ppm)	Emissions (Kyoto Protocol's greenhouse gases)
RCP 8.5	>8.5 W/m ²	at stabilization after 2100	Rising	> 1370 CO ₂ eq in 2100	Rising continues until 2100
RCP 6.0	6.0 W/m ²	at stabilization after 2100	Stabilization without overshoot	850 CO ₂ eq (at stabilization after 2100)	Decline in the last quarter of century
RCP 4.5	4.5 W/m ²	at stabilization after 2100	Stabilization without overshoot	650 CO ₂ eq (at stabilization after 2100)	Decline from the mid-century
RCP 3-PD*	3.0 W/m ²	peak at before 2100 and then decline	Peak and decline	peak at 490 CO ₂ eq before 2100 and then decline	Decline in the first quarter of century

The main goal of the development of the representative concentration pathways is to provide possible development trajectories for the main forcing agents of climate change, suitable with current scenario literature that allows subsequent analysis by both Climate Models (CMs) and Integrated Assessment Models (IAMs). Climate modelers will use target time series to investigate future concentrations and emissions of GHGs, air pollutants, land use change from 4 different representative concentration pathways shown in the figure above (Vuuren et al., 2011). With a parallel way, IAMs will explore a range of various new technologies, socio-economic and policy futures that could result in change of a particular concentration pathway, and magnitude of climate

change. Thus, the development of representative concentration pathways will allow climate modelers to make new procedures of their experiments in a parallel approach with the development of emissions and socio-economic scenarios, and this parallel process will show the overall scenario development process (Moss et al., 2010).

2.3.1. A Regional Climate Model System: RegCM

The Regional Climate Model system RegCM, originally developed at the National Center for Atmospheric Research (NCAR), is maintained in the Earth System Physics (ESP) section of the International Center for Theoretical Physics (ICTP) (ICTP, URL). RegCM1 was developed as first version of the model in 1989 and since then major updates implemented in 1993 (RegCM2), 1999 (RegCM2.5), 2006 (RegCM3) and most recently 2010 (RegCM4). The latest version of the model system (RegCM4), is now fully supported by the ESP. This version has major upgrades in many cases such as the structure of the codes, previous and post processors, and some new physical parameterizations. The model can be applicable to any region on the Earth, with grid spacing of up to about 10 km (hydrostatic limit), and for a wide range of studies, from process studies to paleoclimate and future climatic simulation (ICTP, URL).

The efforts to solve the negative impacts of rapid climate change have been developing. Climate models are the best tools in these efforts to foresee how the climate system will react to the negative climatic forces. Climate models are downscaled using Dynamic Downscaling Methods. The model data are getting higher resolution and real-like output results. In this study, based on HadGEM2-ES/RegCM4.3.4 global/regional models' outputs both RCP4.5 and RCP 8.5 scenarios. Precipitation data values of 10m x 10m grid center of surface area were calculated, analyzed and produced maps in ArcGIS10.4 software.

HadGEM2-ES Global Circulation Model outputs which is produced with RCP 4.5 and RCP 8.5 concentration scenarios have been used in the study. Future precipitation projections with 10 m x 10 m grid size for the Marmara Region have been produced from these outputs, for a period between the years 2020-2049, using by RegCM4.3.4 Regional Climate Model and dynamic downscaling method.

2.3.2. ERA Interim

ERA-Interim is the latest global atmospheric reanalysis produced by the European Centre for Medium-Range Weather Forecasts (ECMWF) (Berrisford et al., 2009). The ERA-Interim project was ruled in part to provide a new atmospheric reanalysis to replace ERA-40, which will extend back to the early part of the twentieth century (Berrisford et al., 2009). In this study the ERA-Interim data were used in order to check the R factor in the RUSLE Model for soil erosion analysis of the Marmara Region, with the aim of considering different data sources for the similar time interval.



3. MATERIALS AND METHODS

3.1. Description of the Study Area

Marmara region is located in the northwest part of Turkey, covering 8.6% of the total area of Turkey, with an approximate area of 72.845 km² occupying, and having more than 23 million people (Doğan et al., 2007). Marmara region gets its name from a landlocked sea belonging to the region, which is neighboring to the Black Sea and the Aegean Sea through the straits. It is the smallest but the most densely populated region among the seven geographical regions of Turkey. The region includes 11 cities, namely İstanbul, Bursa, Edirne, Kocaeli, Balıkesir, Kırklareli, Tekirdağ, Çanakkale, Bilecik, Sakarya and Yalova. regarded as the center of main industrial sites in production of food, textile, cement, paper, house furniture, leather, petrochemical, automotive and ship construction products.



Figure 3.1. The Map of the Marmara Region with its 11 Districts.

The region is the most industrialized region among the other regions in Turkey, and the one third of the Turkish national industry has been situated in the region. Turkey has a rapidly growing population, especially in the last few decades. The population of Turkey was approximately 13.6 million in 1927, and it has increased approximately five fold in 73 years reaching approximately to 67.8 million, in 2000. Moreover, according to the projections of the U.S. Census Bureau, the population of Turkey can reach up to 82 205 000, by 2025. Being a major city in the Marmara Region, Istanbul is the most populated city in Turkey, also the economic potential of the city is the highest among other cities of the country. Thus, the Marmara Region has densest population among the other seven regions of Turkey (DIE, 2007; U.S. Census Bureau, 2007). In the basis of the 2000 Census data, human population of the Marmara Region was 17.3 million with an increase rate of 27%, yet the increase rate was 18.34% for Turkey, between the years 1990 and 2000. The location map of the Marmara Region is illustrated in Figure 3.1.

The Marmara Sea is the smallest inland sea of Turkey, connected with other two largest seas by the straits, the Bosphorus from the Black Sea side, and the Dardanelles from the Mediterranean side. Marmara Region is situated between $39^{\circ} 00' 00''$ - $42^{\circ} 00' 00''$ north latitude, and $26^{\circ} 00' 00''$ - $31^{\circ} 00' 00''$ east longitude. Thanks to the geostrategic position as a consequence of being very close to Europe, having the Bosphorus and Dardanelles Straits as a passage from the Black Sea and the Aegean Sea, the region has significant importance in industry, commerce, tourism and transportation. Rapid increase in economic developments, industrialization and urbanization arose in the Marmara Region after 1980s, as a consequence of migration from other regions and countries. This huge amount of human population density have resulted in various ecological changes especially in agricultural, forest areas. Majority of the forests and agricultural lands within the region have been transformed into urbanized areas. Istanbul as a capital has been affected from huge immigration, the city population was 3 million in 1970s, it became 7.4 million in 1990s, rising up to 12 million in 2007 (Kaya et al., 2007). The current population of the city is 15.07 million. Bursa, another important city of the Marmara region had a population of 275 953 in 1970, and reached to 1 194 687 in 2000.

3.1.1. Climate and Vegetation of The Study Area

Turkey is located between mid-latitude temperate climate zone and subtropical climate zone. Due to the diverse topographical structure, Turkey has various climatic regimes. Simply, the climate of Turkey is a Mediterranean-type macro climate (Iyigün et al., 2013). Turkey belongs to the risky group in terms of the potential effects of climate change and global warming. The climatic

studies indicated that there is a tendency to increase in the average annual and seasonal surface temperatures, as well as the temperature at night for the last twenty years, when there is a decrease in the number of days with frost (Altınsoy et al., 2011; Sen et al., 2012; Türkeş 2011).

Turkey as a country belongs to a region described as having a warm and moderate climate (Erinc, 1984). Turkey has 7 sub-regions, which are Aegean, Black Sea, Central Anatolia, Eastern Anatolia, Marmara, Mediterranean, and Southeast Anatolia. These sub-regions are very diverse in terms of climatic conditions. Among the coastal regions of Turkey, the Aegean and Mediterranean have cool, rainy winters, having also moderately hot and dry summers. However, the Black Sea Region receives the highest amount of precipitation among other regions in the country. When it comes to average temperature values, the highest temperature is observed in the south-east part of Turkey, particularly in summer times. Towards the north-west and north-east parts of the country the temperature values decrease gradually, however the decrease in temperature values are smoother during summer with the continental effects of the inner regions. In the low altitudes, the coastal regions are warmer than the inner regions, which are generally separated by mountains with high altitudes. In general, the coastal parts of the Mediterranean Region have the highest average temperatures, followed by the Aegean, the eastern parts of the Black Sea, and the coastal parts of the Marmara Region. In addition, in the Eastern Anatolia due to continental effects and high altitudes, decrease in temperatures are observed (Tayanc et al., 1998). As an interference, the distribution of temperature variability is dependent upon the extension of the continental and topographical impacts. The Mediterranean Region are affected by subtropical air masses, this situation leads to observation of highest temperatures during winter, when compared to the other regions in Turkey. On the other hand, the lowest temperature values are recorded in the Northeastern Anatolian Plateau. The climatic structure of the Marmara Region acts as a bridge between the Black Sea Climate and Mediterranean Climate. The region is divided into four sub-regions, which are namely: Yıldız, Ergene, Çatalca-Kocaeli, and South Marmara. The sub-region Yıldız is the part of the Marmara Region having the highest slope due to the Mountains. The Yıldız Mountains are located towards to the Black Sea and have a Black Sea Climate. Some parts of the mountains towards the inner catchments have drier climate that represents the Mediterranean Climate. When the Black Sea and the Mediterranean Climates are compared, the Black Sea Climate has lower temperatures in both winter and summer, and generally experiences rainfall events more frequently than the Mediterranean Climate of the coastal parts of Turkey. In the Black Sea Region, forests dominate along the coastal parts of the region, however, in the inner catchments of the region vegetation cover spreads sparsely. Another sub-region of the Marmara Region is Ergene, the Ergene Plains covers the most part of this sub-region. The vegetation type of the Ergene is sparsely

vegetated due to dry climate. This part of the region is favorable for agricultural activities, and the farm products of the Ergene are mostly potato, rice, grape, wheat, sunflower, and tobacco. When it comes to the sub-region Çatalca-Kocaeli, this part of the region have two peninsulas situated at the eastern and western parts of the Bosphorus. In this section of the Marmara Region there are low plateaus, and also forests are located in the Black Sea coast of the sub-section. However, the forests are sparsely distributed in the southern parts of the sub-region Çatalca-Kocaeli and the climate is drier. The Adapazarı Plain is one of the most important agricultural land of this section, and it is mainly representative of the farm products such as beet, sunflower, potato, and linen. Lastly, the Southern Marmara, which is situated in the southern part of the region, also including the Gallipoli Peninsula, has medium height mountains, and also many plains, which are favorable for agricultural activities. The Uludağ Mountain is the highest mountain of the region.

3.2. RUSLE Model Application

3.2.1. RUSLE Model Description

Revised Universal Soil Loss Equation (RUSLE) (Renald et al., 1997) is an empirical erosion model, which is revised based on the Universal Soil Loss Equation, USLE (Wischmeier and Smith, 1978). The model USLE is developed by the United States Department of Agriculture (USDA) in 1978. The most remarkable difference between the models USLE and RUSLE is the model RUSLE includes a computer program to make calculations easier, and it also includes the data analysis component. The model RUSLE investigates how landuse, soil and topography may affect the soil erosion that originates from rainfall and surface runoff (Renard et al.,1997). The USLE model was originally designed for soil loss prediction in croplands on gently sloping topography (Wischmeier and Smith, 1978). However, RUSLE has been widely applied to estimate soil erosion loss, and the model has applications in different landuse conditions, such as rangelands, forests, and disturbed areas (Renard et al., 1997). Moreover, in order to predict soil erosion loss, and its spatial distribution, GIS and remote sensing technologies are commonly used to provide better accuracy in larger geographical areas (Millward and Mersey, 1999; Wang et al., 2003).

Five major factors; i. rainfall pattern (R), ii. type of soil (K), iii. topography (LS), iv. crop system (C), and v. management practices (P) are included in the USLE/RUSLE to compute approximate annual average soil erosion, through the equation below (Renard et al., 1997):

$$A = R \times K \times LS \times C \times P \quad (3.1)$$

where A is the the mean annual loss in (ton/ha/year), R is the rainfall and runoff erosivity factor (in MJ/ha/mm/yr), K is the soil erodibility factor (in ton/MJ/mm), LS is the slope and length of slope factor, C is the cropping management factor, and P is the erosion control and practice factor.

In this study, following the derivation of these factors, which will be discussed further below, all five parameters are mapped in GIS raster format; so, the estimates of average annual soil is acquired at the pixel grid level (30m x 30 m grid cell size). The overlay of the RUSLE model and the schematic approach to the workflow of the RUSLE model utilized in this study are illustrated in Figures 3.2 and 3.3., respectively. Detailed information on RUSLE Model factors including sources are summarized in Table 3.2. Soil erosion risk classification estimated by RUSLE is obtained from the literature (Li et al., 2014; Tang et al., 2015), which the details are provided in Table 3.2.

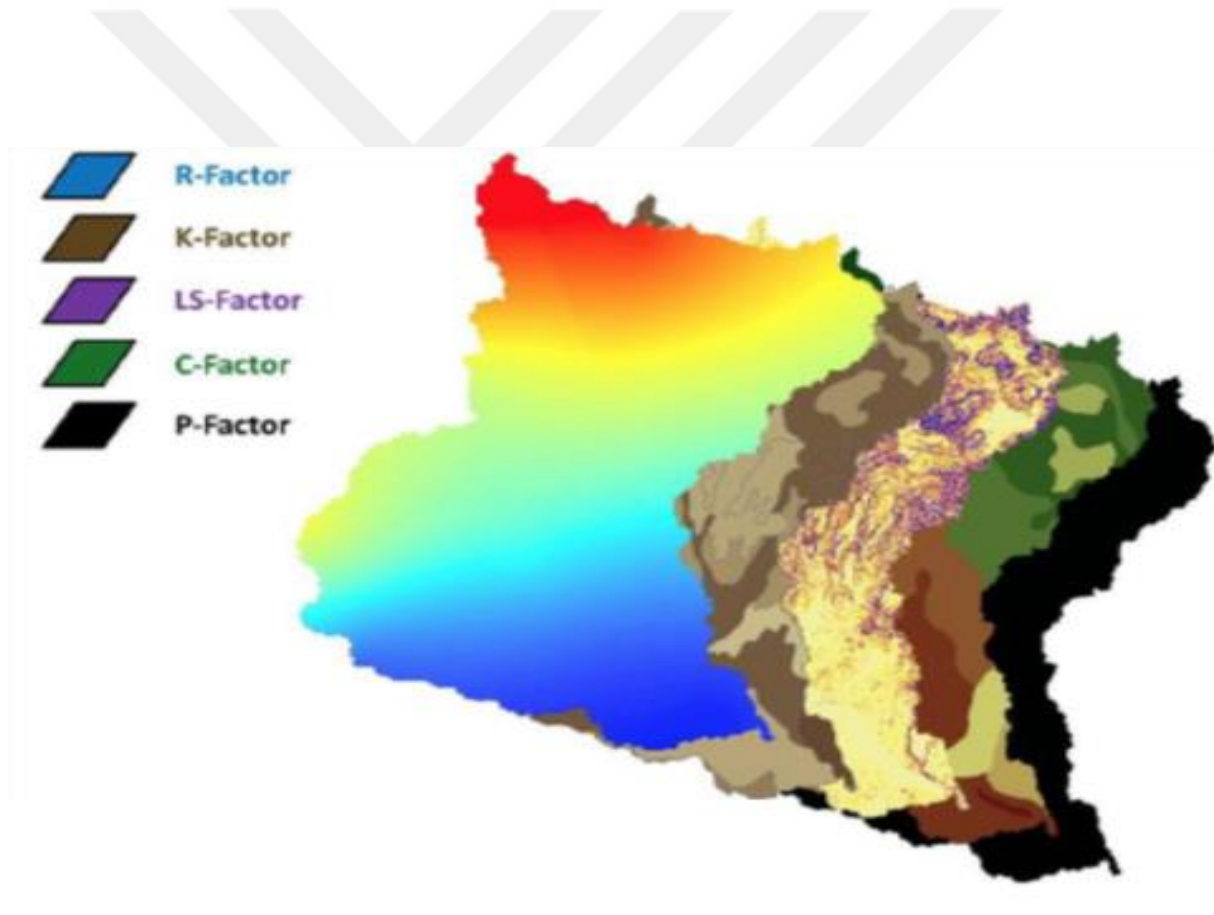


Figure 3.2. Overlay of the RUSLE model.

Table 3.1. Soil erosion risk classification based on average erosion rate estimated by RUSLE (Li et al., 2014; Tang et al., 2015).

Soil Loss (A) (t ha⁻¹ year⁻¹)	Erosion Risk
< 5	Very low
5 - 25	Low
25 – 50	Moderate
50 - 80	Severe
80 - 150	Very severe
> 150	Extremely severe



Figure 3.3. A Schematic Approach to the Workflow of the RUSLE Model.

Table 3.2. RUSLE Model Factors with their abbreviations, units, and sources.

DATA TYPE	ABBREVIATION	UNIT	SOURCE
Rainfall Erosivity	R	$\text{MJ}\cdot\text{mm}\cdot\text{ha}^{-1}\cdot\text{year}^{-1}$	GIS Based Erosivity Map
Slope Length	L	m	DEM (Slope Length and Gradient Map)
Soil Erodibility	K	$\text{Mg}\cdot\text{ha}\cdot\text{h}\cdot\text{ha}^{-1}\cdot\text{MJ}^{-1}\cdot\text{mm}^{-1}$	GIS Based Soil Map
Slope Steepness	S	dimensionless	DEM (Slope Length and Gradient Map)
Crop Management	C	dimensionless	Landsat Images
Conservation Support Practice	P	dimensionless	Landsat Images
The Mean Annual Soil Loss	A	$\text{Mg}\cdot\text{ha}^{-1}\cdot\text{year}^{-1}$	GIS based Map of Soil Loss
Precipitation	<i>P</i>	mm	Historical data, RCP4.5 & RCP8.5 Scenarios of the Regional Climate Model

3.2.2 RUSLE Factors

3.2.2.1. Rainfall Erosivity Factor (R): Rainfall is one of the main drivers of soil erosion. The erosive force of rainfall is defined as rainfall erosivity. Also, rainfall erosivity is expressed as the aggressiveness of the rain to cause soil erosion (Lal, 1990). The R factor is calculated for 29-year period including the years between 1989 and 2017. The data of the mean annual precipitation regarding 1989-2017 for the study area is provided by İklimBU Center for Climate Change and Policy Studies of Boğaziçi University. The climate projections are done using Regional Climate Model. In addition, the precipitation data has 10 km x 10 km resolution. Moreover, in order to make future projection of soil erosion between the years 2021 and 2049, the rainfall data run under two climatic scenarios with the help of the Regional Climate Model RegCM4.3.4. In order to make projection of the precipitation data RCP4.5 and RCP8.5 scenarios, the outputs of a Global Circulation Model (HadGEM2–ES) were used.

Because of the reason that it is hard to find reliable and adequate data for the pluviograph and rainstorm, the general approach used to estimate the R factor by using mean annual and monthly rainfall data from the meteorological stations located in the study area (Arnoldus 1977, 1980; Renard and Freimund, 1994; Lu and Yu, 2002). In order to estimate R factor by using monthly and

annual rainfall data, Arnoldous (1980) introduced an index which is called Modified Fournier Index (MFI).

The Fournier index modified by Arnoldous (1980) is calculated by the equation below:

$$F_M = \sum_{i=1}^{12} \frac{P_i^2}{P} \quad (3.2)$$

where, P_i is the mean rainfall amount (mm) for month i , and P is the mean annual rainfall amount (mm).

The Modified Fournier Index estimated by Arnoldous (1980) has importance to calculate R factor. The MFI and R Factor are directly proportional to each other, and they are linearly correlated. For this study, the precipitation data of the time interval 1989-2017 for the Marmara Region were collected, and the MFI was estimated for each grid of the data provided by the climate model. Also, the MFI for the projected data by the Regional Climate Model were calculated for the two different climatic scenarios. To estimate the R Factor using the calculated MFI for each grid station, the following equation including R-MFI relationship, as suggested by Irvem and others (2007) for the basins climatologically similar to Turkey.

$$R = 0.1215 \times \text{MFI}^{2.2421} \quad (3.3)$$

where,

P_i : monthly rainfall in mm,

P : annual rainfall in mm

(The unit of R factor (rainfall erosivity) is $\text{Mj.mm.ha}^{-1}.\text{yr}^{-1}$).

The MFI and R Factor value was calculated with the equations above for each grid station by using the Regional Climate Model data. The values of rainfall erosivity risk can be classified based on the Fournier rainfall erosivity index. In order to classify the erosivity risk in Marmara Region the Fournier rainfall erosivity index, and its modified version is used. The assessment of rainfall erosivity is based on the Fournier (1960) index and the Fournier modified index (Arnoldous, 1980).

The Fournier index is calculated according to the equation below:

$$F = \frac{P_{\max}^2}{P} \quad (3.4)$$

where,

P_{\max} : monthly average amount of precipitation of the most rainy month in mm,

P : average annual quantity of precipitation in mm.

Table 3.3. The erosivity classes by Fournier Index (F) and modified Fournier Index (F_M) based on the (Fournier, 1960) & (Arnoldus, 1980).

Erosivity class	F	Modified Erosivity Class	F_M
Very low	0-20	Very low	0-60
Low	20-40	Low	60-90
Moderate	40-60	Moderate	90-120
Severe	60-80	High	120-160
Very severe	80-100	Very high	> 160
Extremely severe	> 100		

In this study, HadGEM2 (Hadley Global Model 2) RCP 4.5 and RCP 8.5 scenarios of global climate modeling is used as an input data of regional climate model. Radioactive forcing in 2100 emission scenario of RCP 8.5 (possibly bad scenario for humanity or worst case scenario) and RCP 4.5 (better but still bad scenario or optimistic scenario) will be 8.5 W/m^2 (watt/metersquared) and 4.5 W/m^2 respectively. RegCM4.3.4 Regional Climate Model has been used to dynamic spatial resolution of 10 km. The study involves projection of precipitation events that are produced by using regional climate model (RegCM4.3.4) with dynamic downscaling method based on RCP4.5 and RCP8.5 scenarios from outputs of a Global Circulation Models (HadGEM2-ES.). HadGEM2 is a comprehensive Earth-System Model developed by Hadley Centre of UK Met Office.

The main purpose of the study is to determine future spatial distributions of precipitation events over the Marmara Region domain. For this aim, we used regional climate model (RegCM4.3.4) of the Abdus Salam International Centre for Theoretical Physics (ICTP) to downscale the outputs of HadGEM2-ES to 10 km grid resolution for the Marmara Region. In order to make future projection over the region for the period of 2021-2049 with respect to baseline period of 1989-2017, the worst case emission pathway RCP8.5 and the optimistic emission pathway RCP 4.5 are chosen.

Moreover, the ERA-Interim re-analysis data was used to get the R factor results for the time interval 1989-2012. ERA-Interim is the latest global atmospheric reanalysis created by the European Centre for Medium-Range Weather Forecasts (ECMWF) (Berrisford et al., 2009). The data provided by ERA-Interim was used in order to check soil erosion of the Marmara Region by considering different data sources.

3.2.2.2. Soil Erodibility Factor (K): K factor is an empirical measure of soil erodibility depends on intrinsic soil properties (Fu et al. 2006). The K factor values are predicted with the help of

information about soil properties, such as soil texture, content of organic matter, soil structure and permeability (Renard et al., 1997; Ferreira and Panagopoulos, 2014). Wishmeier and Smith (1978) were developed a monogram to obtain the K factor (equation 3.5) on the basis of the percentages of silt, very fine sand, and organic matter, soil structure and permeability.

$$K = \frac{(2.1 M^{1.14}(10^{-4})(12-a) + 3.25 (b-2) + 2.5 (c-3)) \times (0.1317)}{100} \quad (3.5)$$

where a = % of organic matter

b = non-dimensional code related to soil structure class

c = non-dimensional code related to soil permeability class

M = (% silt + % very fine sand) or (100 - %clay)

And also, unit of K factor is t. h. MJ⁻¹ mm⁻¹.

$$K = 0.0034 + 0.0405 \times \exp\left(-0.5 \left[\frac{\log D_g + 1.659}{0.7101}\right]^2\right) \quad (3.6)$$

where:

D_g is the geometrical particle diameter, based on the fractions of the texture classes and arithmetic means of the particle diameter of each texture class.

$$K = \frac{SAN + SIL}{CLA} \times \frac{1}{100} \quad (3.7)$$

where:

SAN, SIL and CLA are sand, silt and clay percentage, respectively.

$$K = 0.00000748(M) + 0.00448059(b) - 0.0631175(DMP) + 0.010396(REL) \quad (3.8)$$

where:

M: the sum of percentage silt and very find sand multiplied by 100 minus percent clay

b: the non-dimensional code related to the soil structure

DMP: the weighted mean of the particles smaller than 2mm

REL: the ratio between organic matter content and the content of particles between 0.1mm and 0.2mm

$$K = A \times B \times C \times D \times 0.1317 \quad (3.9)$$

where:

$$A = \left[0.2 + 0.3 \exp(-0.0256 SAN (1 - \frac{SIL}{100}))\right] \quad (3.10)$$

$$B = \left[\frac{\text{SIL}}{\text{CLA} + \text{SIL}} \right]^{0.3} \quad (3.11)$$

$$C = \left[1.0 - \frac{0.25 C}{C + \text{EXP}[(3.72 - 2.95C)]} \right] \quad (3.12)$$

$$D = \left[1.0 - \frac{0.70 \text{SN1}}{\text{SN1} + \text{EXP}[-5.41 + 22.9 \text{SN1}]} \right] \quad (3.13)$$

SAN, SIL and CLA represent percent sand, silt and clay respectively. In addition, C and SNI represent organic carbon content, sand content subtracted from 1 and divided by 100 respectively.

3.2.2.3. Slope Length (L) and Slope Steepness (S) Factors: The LS factor represents the rate of soil loss per unit area from a field has 22.13 m slope length and 9% slope. Actually, LS values are not absolute values, but the LS value in a terrain with a slope length of 22.13 m and a slope of 9% is taken as 1 (Wischmeier & Smith, 1978). Slope length (L sub-factor) in the model is the representative of the distance between the source and culmination of inter rill process. The culmination is either the point where slope decreases and the resultant depositional process begins or the point where concentration of flow into rill or other constructed channel such as a terrace or diversion (Wischmeier and Smith, 1978; Renard et al., 1996). Deriving slope by geographic information system (GIS) benefits a wide range of environmental models because slope attributes are frequently needed as input for landslides, land planning and construction, and others (Dunn & Hickey, 1998). The shortcomings of slope length calculation can be solved by using the cumulative uphill length from each cell which accounts for convergent flow paths and depositional areas during the use of the Universal Soil Loss Equation (Hickey, 2000). Similarly, LS factor in the RUSLE are measures of the sediment transport capacity of the flow (Moore and Wilson, 1992).

Slope length (L) and slope steepness (S) factors are representatives of topographic factors affected soil erosion loss. The combination of two factors is called “topographic factor”. The L factor is the ratio of the actual horizontal slope length to the experimentally measured slope length 22.13 m. The S factor is the ratio of the actual slope to an experimental slope 9% (Kim and Julien, 2006). The LS factor is an expression of the effect of topography, particularly hill slope length and the steepness, on rates of soil loss at a determined part.

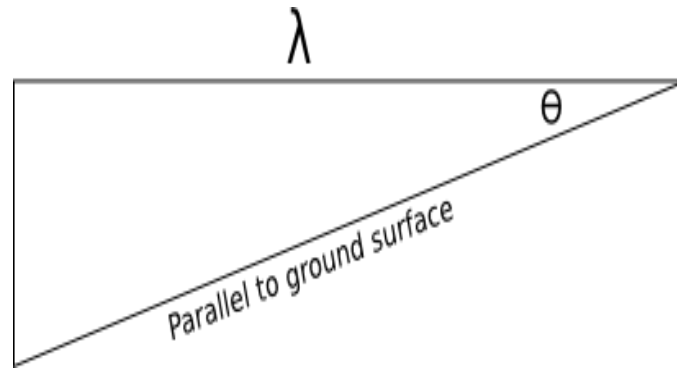


Figure 3.4. Demonstration of the values used in LS calculations.

Calculation of L factor is shown with equation (4) below:

$$L = \left(\frac{\lambda}{22.1} \right)^m \quad (3.14)$$

where,

L is the slope length factor,

λ is the horizontal plot length (as shown in the figure 4), and

m is a variable exponent calculated from the ratio of rill-to-interrill erosion, as described in (Renard, Foster, Weesies, McCool, & Yoder, 1997).

$$\begin{aligned} S &= 10.8 \sin \theta + 0.03, \text{ slope gradient} \leq 9\% \\ S &= 16.8 \sin \theta - 0.50, \text{ slope gradient} > 9\% \end{aligned} \quad (3.15)$$

where,

S is the slope factor, and

θ is the slope angle.

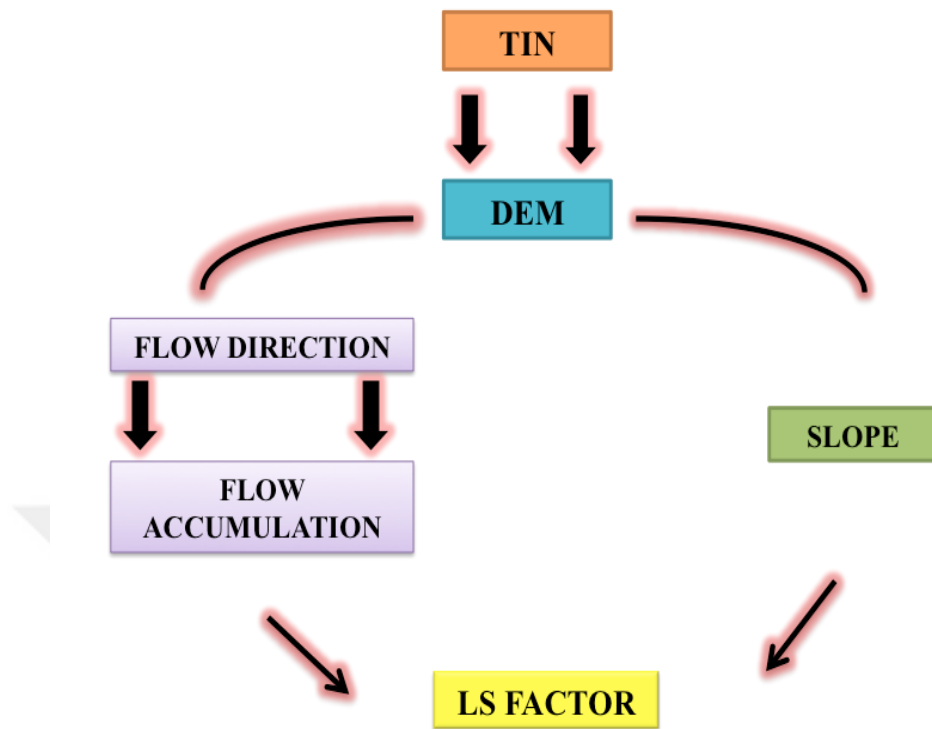


Figure 3.5. Flow Chart of LS Factor.

The value of LS factor is directly proportional with the increase in hill slope length and steepness under the assumption that run-off accelerates and accumulates in the direction of the down slope (Khare et al., 2016).

In this study, in order to estimate LS factor a DEM (Digital Elevation Model) is created in ArcGIS software by digitizing contour lines from topographic maps (Rozos et al., 2013). There is one significant factor that affects the catchment hydrology and soil erosion classification is flow direction which will be determined by “Flow Direction” function of the ArcGIS10.4 software.

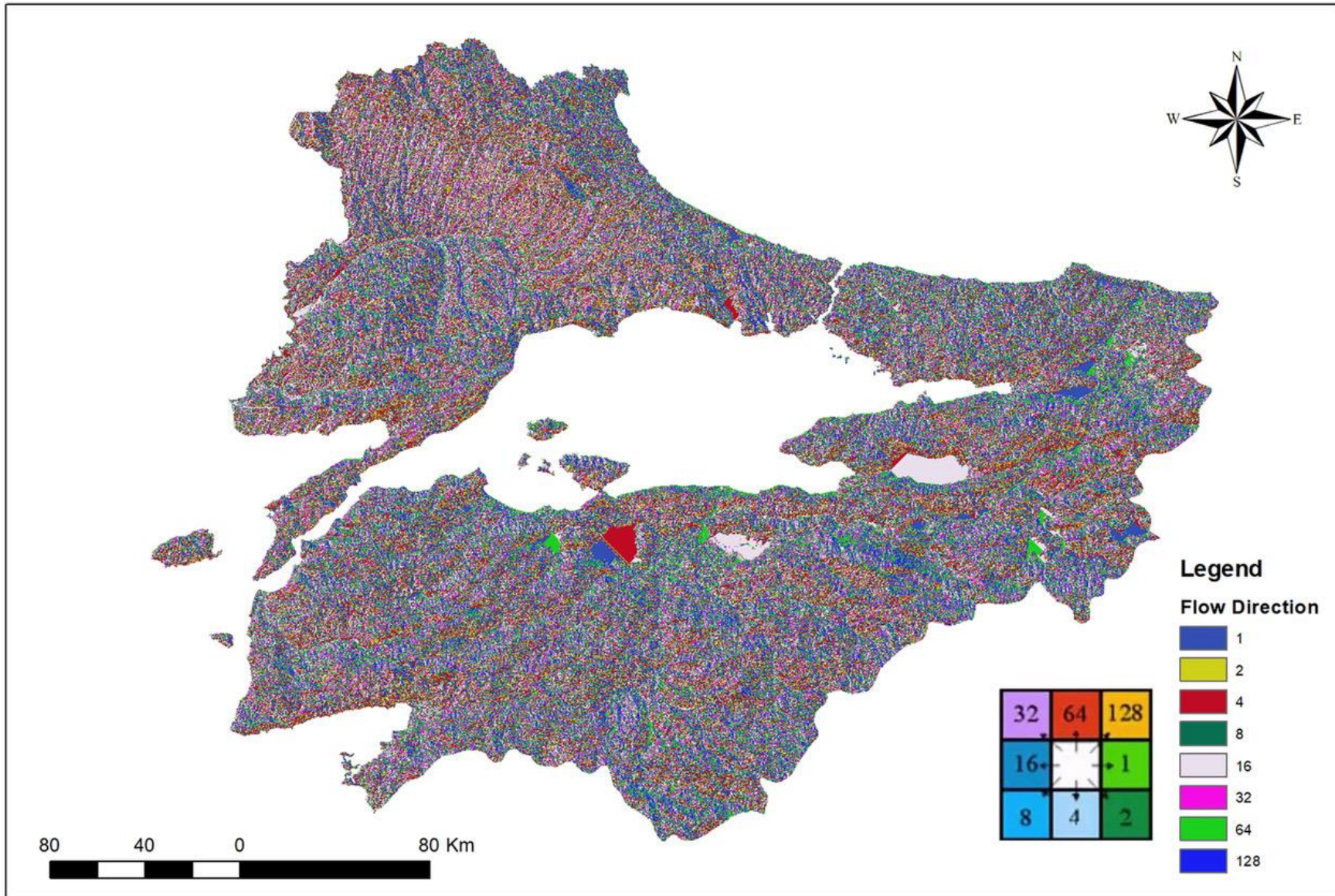


Figure 3.6. Flow Direction Map for Marmara Region created in ArcGIS.

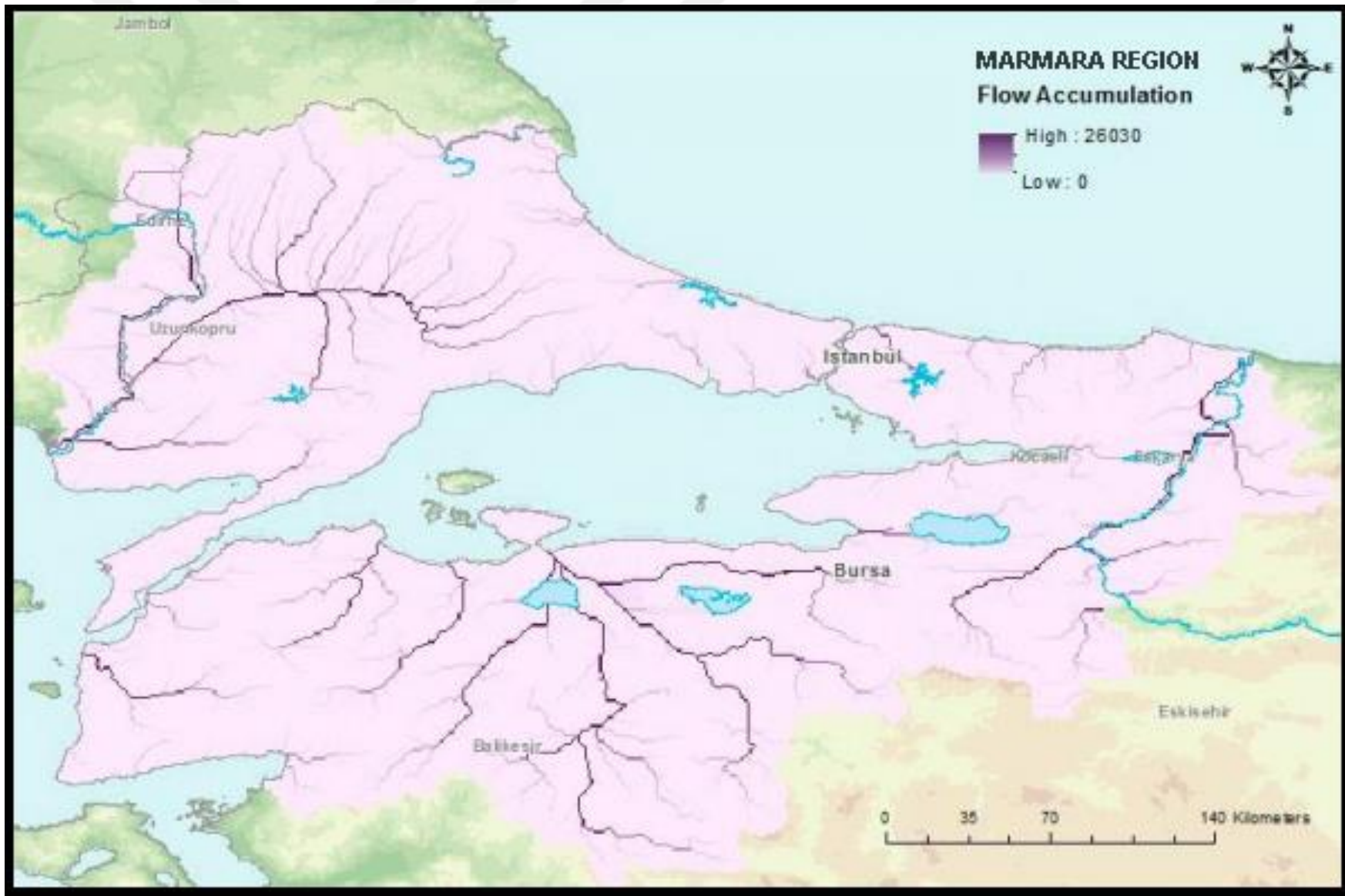


Figure 3.7. Flow Accumulation Map for Marmara Region created in ArcGIS.

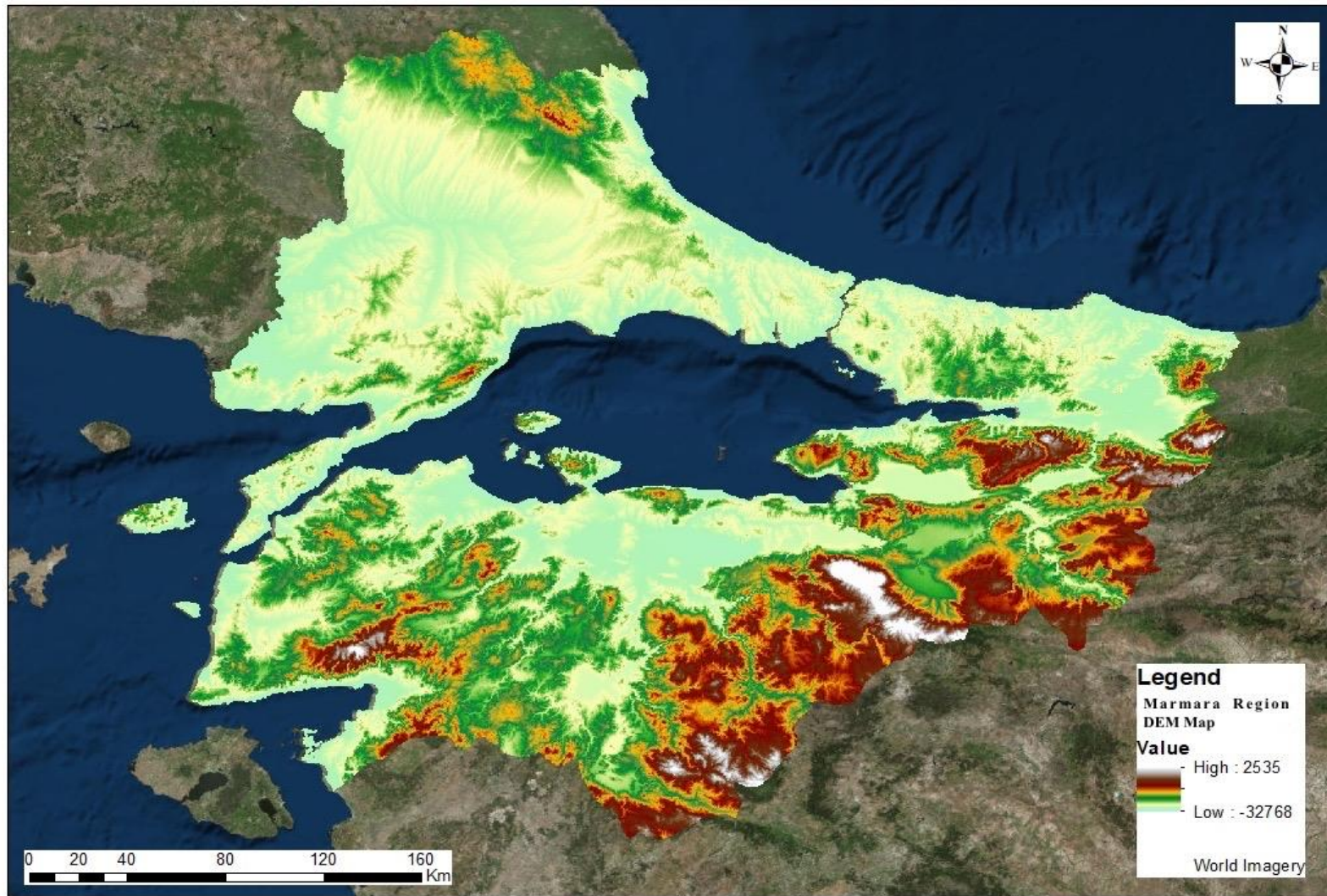


Figure 3.8. Marmara Region DEM Map (created in SRTM DEM).

3.2.2.4 Land Cover and Management Factor (C): There are lots of practices to control soil erosion, among them agricultural and management practices plays important role. For instance, soil loss rates are inversely proportional to increase in vegetation cover. Soil loss rates decrease exponentially as vegetation cover increases (Gyssels et. al., 2005). In addition to vegetation cover, several other land use and management conditions affect soil erosion, such as type of crop, tillage practices, etc. The C factor represents the conditions that can be managed most easily to reduce soil erosion. The land cover and management (C) factor is defined as the ratio of soil loss from land with specific vegetation to the corresponding soil loss from continuous fallow (Wischmeier and Smith, 1978). The crop management factor (C) is the representative of the soil loss ratio under a given crop to that of the base soil (Morgan, 1994). The land cover and management factor (C) represents the effects of cropping and management practices on the soil erosion rate (Renard et al., 1997).

Land cover has significance especially in order to protect soil against rainfall erosion (Zachar, 1982). From a physical perspective, land cover decreases the magnitude of impulse when the raindrops hit the ground, and reduce the flow rate (Çepel, 1997; Gold, 2006). Also, raindrops that fall on the branches and leaves cause the surface flow to be affected (Hoşgören, 2010), and the roots of the plants keep the soil more stable and prevents soil erosion with a considerable extent. There is also some topographic concerns about land cover, soil erosion is less at the hillsides where land cover is denser than the inclined surfaces (Çepel, 1997). So, as the rate of floor coating increases the resistance of land cover increases (Zachar, 1982). To illustrate land cover resistivity, the rate of soil erosion is less in the forestal area than the agricultural areas. The plant management factor is used in both USLE and RUSLE to reflect the effect of crop cultivation and management practices on erosion rates. It is most commonly used factor to compare the proportional effects of treatment factors on soil protection schemes. This factor demonstrates how the soil conservation plan affects the average annual soil loss and how the soil loss potential will deteriorate in time due to the construction activities, crop alternations or other management programs (Renard et al., 1997).

Land cover and mangement actor (C) is used to explain the effects of vegetation, crop cultivation and management practices on erosion. In many cases the C factor remains constant throughout the year. Especially in the last 30 years, satellite imagery and remote sensing techniques and software have been intensively used in soil erosion studies. Today, the images obtained through various satellites are processed in remote sensing software to provide fast, accurate and cheaper information for large areas (Çelik, 2011).

Among the factors of the RUSLE Model the C-factor is perhaps the most important factor with regard to policy and land use decisions, as it represents conditions that can be most easily managed to lower soil erosion (Renard et al., 1991). In the RUSLE model, the C-factor represents how land cover, crops and crop management trigger soil loss to vary from those losses occurring in bare fallow areas (Kinnell, 2010). The bare soil and the construction sites (no vegetation) was taken with a C factor value of 1. The water bodies in the region was taken with a C factor value of 0. In this study, the C factor values for the region ranges from 0 to 1. The remotely sensed data have been used to make estimations of the C factor distribution based on land use and land cover classification results (Millward and Mersey, 1999; Reusing et al., 2000), presuming that the similar land covers have the same C factor values.

In this study, a land use and land cover map of the Marmara Region were prepared from the Landsat satellite images by using remote sensing techniques. The structure of the Landsat TM sensor is primarily designed to monitor the vegetation covering the Earth from space (Lusch, 1999). The resolution of the Landsat images are 30 m x 30 m. From the website <https://earthexplorer.usgs.gov/> the Landsat satellite images were downloaded, for the time interval 1989 to 2018 the satellite images of Landsat 8 OLI/TIRS C1 Level 1, Landsat 7 Enhanced Thematic Mapper (ETM+) C1 Level 1, Landsat 4-5 TM C1 Level 1, Landsat 1-5 C1 Level 1 were selected. Among the satellite images the cloudy, foggy, not clear ones were eliminated. The Landsat TM bands were chosen by considering their function to distinguish between water and vegetation, soil and plant moisture measurement, ice and snow separation from clouds, and thermal changes (Jensen, 2000).

The red, the green and the blue bands of the satellite images were selected in order to examine the vegetation cover of the study area. In ArcGIS software, the composition of these raster form of these three bands 4, 3 and 2 were done in the composite bands tool. After composing the bands on the software, the image analysis tool were used and the processing option was used to make NDVI. This process was completed for each satellite images. Mosaic to new raster tool were used to make all the raster NDVI forms united. Then, the mosaic raster form of NDVI images were clipped according to the area of the study area. Thus, the NDVI map of the Marmara Region was done

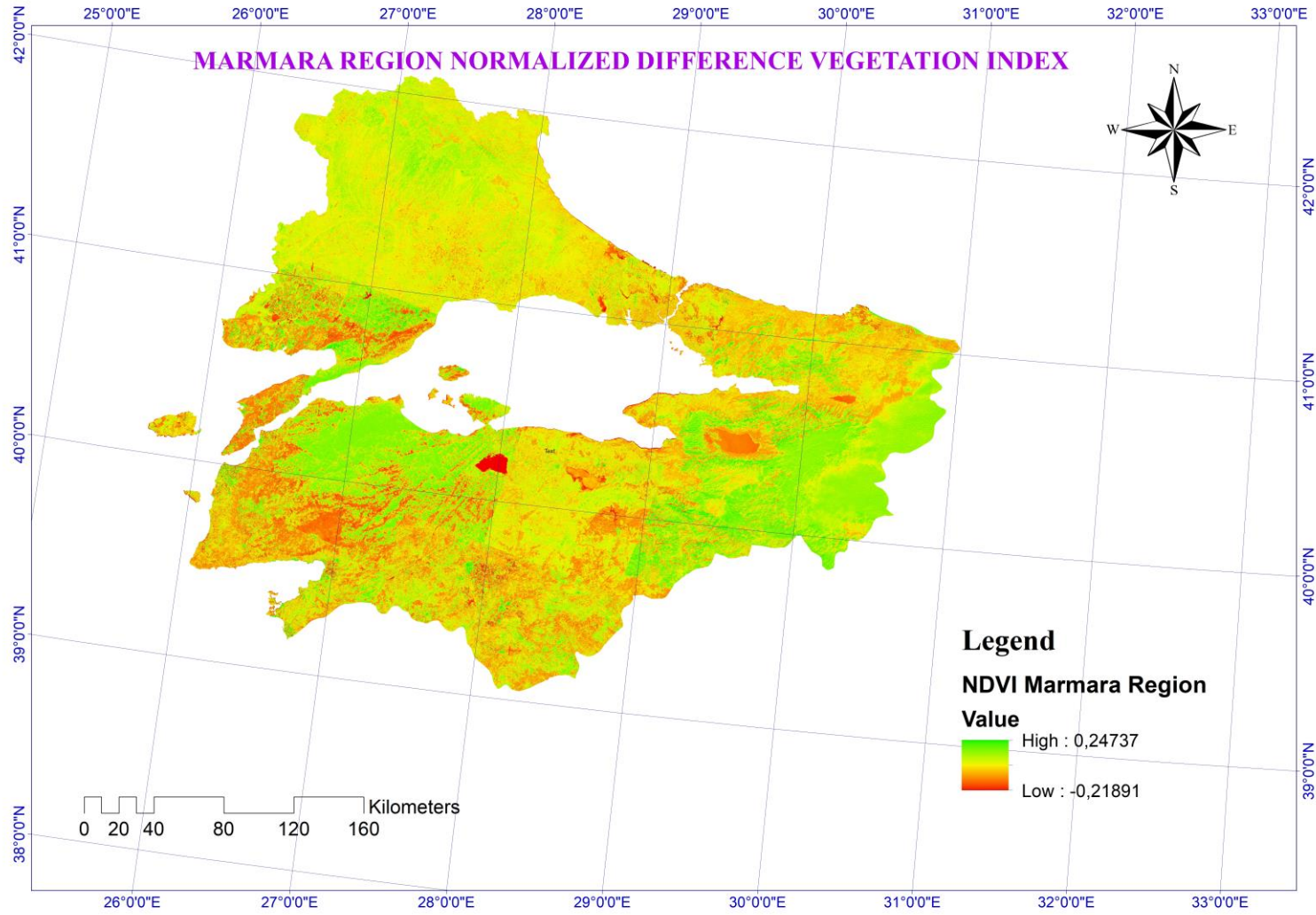


Figure 3.9. Normalized Difference Vegetation Index of the Marmara Region (NDVI).

The Normalized Difference Vegetation Index (NDVI) is one of the vegetation indices that estimate the amount of green vegetation. The spectral reflectance difference between Near Infrared (NIR) and red is used to calculate NDVI. The formula can be expressed as (Jensen, 2000);

$$NDVI = (NIR - red) / (NIR + red) \quad (3.16)$$

where *NIR* is the near-infrared band and *R* is the red band of the image.

The NDVI has been used commonly in remote sensing techniques since its discovery (Jensen, 2005). The NDVI values range from -1.0 to 1.0, where higher values are representatives of green vegetation and low values are representative of other common surface materials.

Table 3.4. C Factor Marmara Region: Land use and Land Cover Classes.

Land Use and Land Cover Classes	C FACTOR
Broad-leaf forest	0.001
Coniferous forest	0.010
Sparsely coniferous forest	0.050
Heathland	0.038
Pasture	0.090
Vineyard and fruit orchards	0.180
Complex cultivation pattern	0.280
Fallow land	0.500
Water body	0.000
Bare rocks and construction sites	1.000

Bare soil is represented with NDVI values which are closest to 0 and water bodies are represented with negative NDVI values (Lillesand et al., 2004; Jasinski, 1990; Sader and Winne, 1992). When it comes to C factor map, the classification of the land use and land cover were done by investigating the parts of the region by selecting bare rocks and construction sites, water bodies, pastures, heathlands, vine yards, forested areas etc. The training sample manager tool were open to draw polygons and classify the parts of the region according to the land use and land cover types. When the classifications were completed and the same classes merged, Interactive Supervised

Classification tool were used in the software. The supervised classification method is a method which requires ground truth information for each land use-land cover category trained the algorithm to extract them (Ganasri et al., 2016).

3.2.2.5. Conservation Support Practice Factor (P): When it comes to conservation/support practice factor P, it is basically the ratio of soil loss with specific support practice to the corresponding loss with up and down the slope tillage (Wischmeier and Smith, 1965). P factor indicates the soil loss rate by considering various cultivated lands. There are contours, cropping, terraces, and these are significant factors that can control soil erosion (Shin, 1999). P factor values can vary from 0 to 1, whereby the value “0” imply a very good manmade soil erosion resistance facility, on the other hand the value “1” represents no manmade resistance to soil erosion resistance facility (Sheikh et al., 2011). In the research area there is no large scale data about the spatial distribution of conservation practices. When it comes to give some examples to the spatial distribution of conservation practices, they are contour ploughing, strip cropping, bank systems or terracing that could decrease the erosive rate of rainfall and run off (Latocha et. al. 2016). Thus, the P factor value for the study area for both historical, present and the future projection data is taken as 1. To take 1 as the P factor value is a common solution where there is not enough conservation support practices for the study area (Latocha et al., 2016).

4. RESULTS AND DISCUSSIONS

4.1. R Factor Maps

In the application part of the Regional Climate Model, the precipitation model data of the Marmara Region obtained for the time interval 01.01.1989 - 31.12.2017, and the time interval of the projected data was chosen as in between 01.01.2020 – 31.12.2049. The projection of historical data prepared for two different scenarios: RCP4.5 and RCP8.5. According to the scenario RCP4.5's future assumptions, radiation power of greenhouse gases is 4.5W/m^2 which is positive one, and also according to RCP8.5's future assumptions, radiation power of greenhouse gases is more than 8.5W/m^2 which is negative one.

The climatic data had netCDF format, and this format was opened in the ArcGIS 10.4 software, and the results of the historical data, and the projected data according to RCP 4.5 and RCP 8.5 projections was arranged both daily and annually. There are 4790 grid stations opened in the ArcGIS 10.4 software, and the grid station data was exported from attribute table to Microsoft Excel to do calculations for annual rate.

The sample data from the meteorological grid stations defined by the Regional Climate Model were analyzed on the software ArcGIS 10.4. The unit of precipitation data was taken in mm. The border of the model data was determined as 25.212563 West, 32.307807 East, 42.954817 North, 37.751721 South. After all of the precipitation data analysis, the formula by Arnoldus (1980) represented in the Equations 3.2 and 3.3 were used for the estimation of R factor using monthly and annual rainfall data.

Rainfall data of the Marmara Region for the time interval 1989-2017 was gathered from the Regional Climate Model, and run to represent the R factor by considering the formula shown in the Equation 3.3. The Equation 3.2 shown in the methodology part represents the Modified Fournier Index, and the MFI was used to calculate the R factor represented in the Equation 3.3 in the methodology part. According to the results gathered by creating maps from the ArcGIS 10.4 software for the Modified Fournier Index of the Marmara Region by considering the data of the Regional Climate Model, the MFI of the Region for the time interval 1989-2017 ranges from 68.5288 to 319.038 mm. According to the formula derived by Fournier (1960) and later modified by Arnoldus (1980), in this study MFI value ranges from 0 to 60 mm represents very low rainfall

erosivity. By clasifying the MFI data, it is concluded that there is no representative area of very low rainfall erosivity in the Marmara Region. The rainfall erosivity ranges from low to extremely severe, and also the parts of the region having extremely severe rainfall erosivity are very less in amount when they are compared with the low rainfall erosivity parts. In the Figure 4.1. the MFI index of the Marmara Region for the time interval 1989 – 2017 is shown, according to the figure especially the cities Balıkesir and Çanakkale have risky parts having extremely severe rainfall erosivity, and especially the cities Kırklareli and Edirne have low rainfall erosivity classes provided by the MFI values.

When it comes to the results of the R factor provided by the data of the Regional Climate Model, the distributions to the values of the factor is similar to the distribution of the MFI for the same time interval. Thus, it can be deduced that the MFI results and the R factor results are directly proportional. The R factor calculated with the historical data of the model ranges from 1587,77 to 49939 Mj.mm.ha⁻¹.year⁻¹. According to the results, Çanakkale, Balıkesir, and Bursa having the highest R factor among the other cities of the region. When it is the compared to the findings of study Ozsoy et al. (2012) analyzing the soil erosion in the Mustafakemalpaşa River Basin of the Marmara Region for the time interval 1964 - 2005, the MFI results of the study ranges from 41.4 to 93.4 mm, and also the R factor results ranges from 51.3 to 3179 Mj.mm.ha⁻¹.year⁻¹. It can be concluded that the results of the study by Ozsoy et al. (2012) show the Mustafakemalpaşa River Basin in Bursa city of the Marmara Region have rainfall erosivity classes range from very low to moderate. Also, according to the study of soil erosion analysis in Kuseyr Plateau of Turkey by Özşahin et al. (2014), the findings for the R factor ranges from 309.73 to 674.52 Mj.mm.ha⁻¹.year⁻¹. According to the case of the study by Özşahin et al. (2014) for minimum and maximum elevations the R values 309.73 - 370.52 and 613.72 – 674.52 MJ.mm.ha⁻¹.year⁻¹, and also in this study the R factor calculated according to levels of elevation by considering data from meteorological stations by applying to the whole area using the interpolation method.

In addition to the results of the R factor of the Marmara Region, in this study the ERA-Interim data was used in order to check the R factor in RUSLE Model for soil erosion analysis of the Marmara Region with the aim of considering different data sources for the similar time interval. The time interval for the ERA-Interim data was selected from 1989-2012, there was no opportunity to complete the time interval gap from 2013 to 2017. However, as it is indicated above, there is similar time interval chosen to compare rainfall erosivity of the region. According to the results taken from the ERA-Interim data, the MFI value ranges from 40.7382 to 187.883 mm which is very close to the results taken from the results of the historical data of the region. Then, it became a

satisfactory comparison between different rainfall data set for the Marmara Region. Also, according to the results of the ERA-Interim data the rainfall erosivity ranges from very low to extremely severe. Moreover, the results the R values created by the ERA-Interim rainfall data range from 494.722 to 15235.7 MJ.mm.ha⁻¹.year⁻¹. The R factor values created by the ERA-Interim data sets are lower than the R factor values created by the historical data of the Marmara Region.

According to the scenario the RCP4.5's future assumptions radiation power of greenhouse gases is 4.5W/m² which is positive one, and also according to RCP8.5's future assumptions radiation power of greenhouse gases is more than 8.5W/m² which is negative one (IPCC, 2007). The SI unit W/m² is representative of the physical phenomena "intensity" which means power divided by area. In the Figure 4.3. the Modified Fournier Index (Arnoldous, 1980) during 2020-2049 range from 64,888 to 272,357 mm. This range shows that according to scenario, the Representative Concentration Pathways 4.5 results the rainfall erosivity during the 2020-2049 years ranges from low to moderate class. Also, there is a significant finding from the results that the MFI value of the historical data gives greater MFI values than the RCP 4.5 scenario's results. Moreover, due to optimistic scenario (IPCC, 2007) RCP 4.5 results the cities Balıkesir, Çanakkale, Bursa and Sakarya of the Marmara Region have extremely severe erosive parts when they are compared to the other cities in the region.

In addition to the MFI values taken by the projection of the climatic data with RCP 4.5 scenario, the R factor values of the RCP 4.5 scenario range from 1404.85 to 35026.7 MJ.mm/ha.year. The results of the RCP 4.5 for R values are less than the historical data's results. In the Figure 4.7. the RCP 4.5 R factor map during 2020-2049 time period for the Marmara Region is shown, there are some parts of the cities Çanakkale, Balıkesir, Bursa, Sakarya and Istanbul have highest R factor values among the other cities in the region. However, especially Çanakkale and Balıkesir have the greatest R values both with the results of the MFI and R factor results for the same time interval of the scenario RCP 4.5.

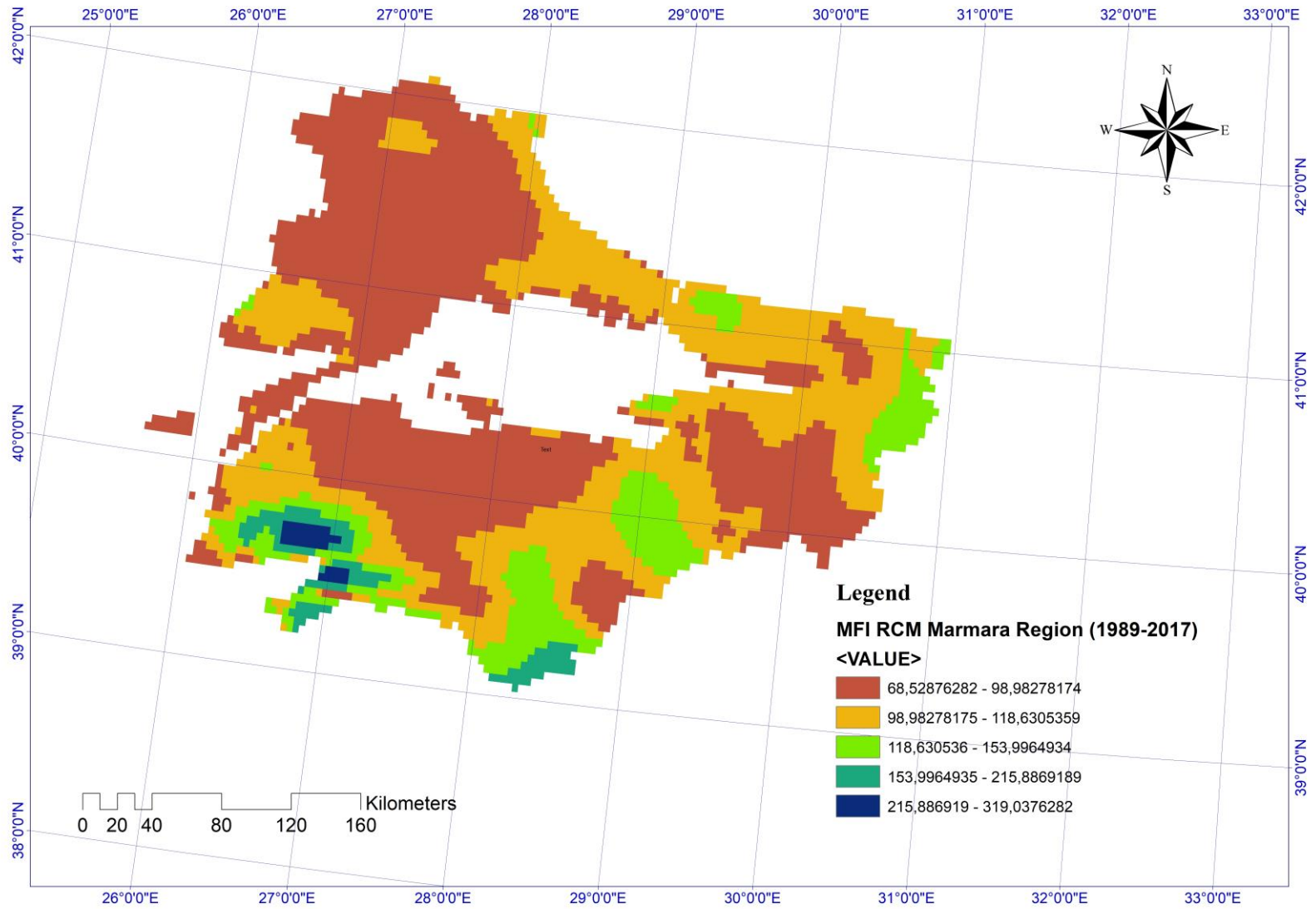


Figure 4.1. RCM Modified Fournier Index Variability During 1989-2017.

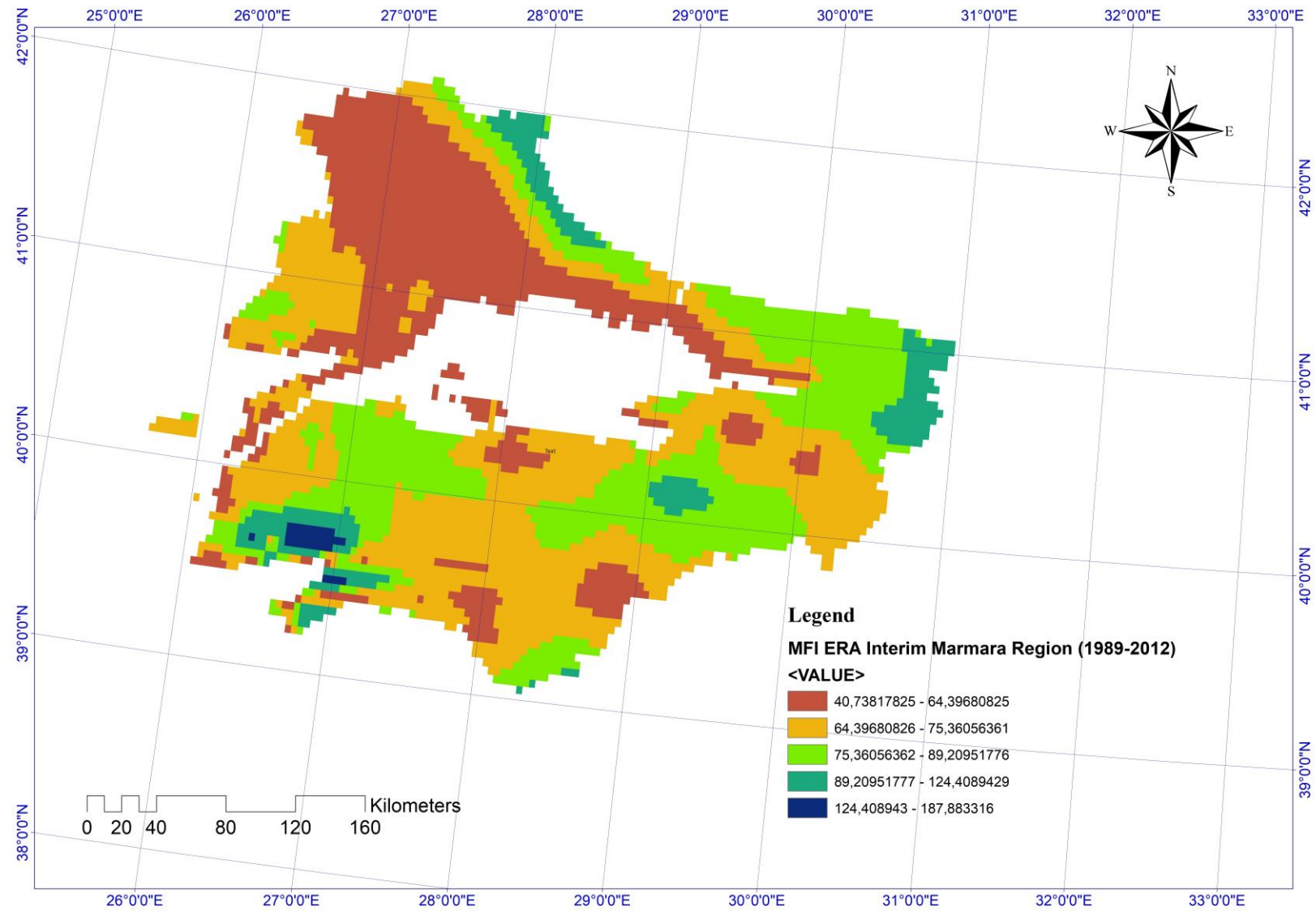


Figure 4.2. ERA-Interim Modified Fournier Index Variability During 1989-2012.

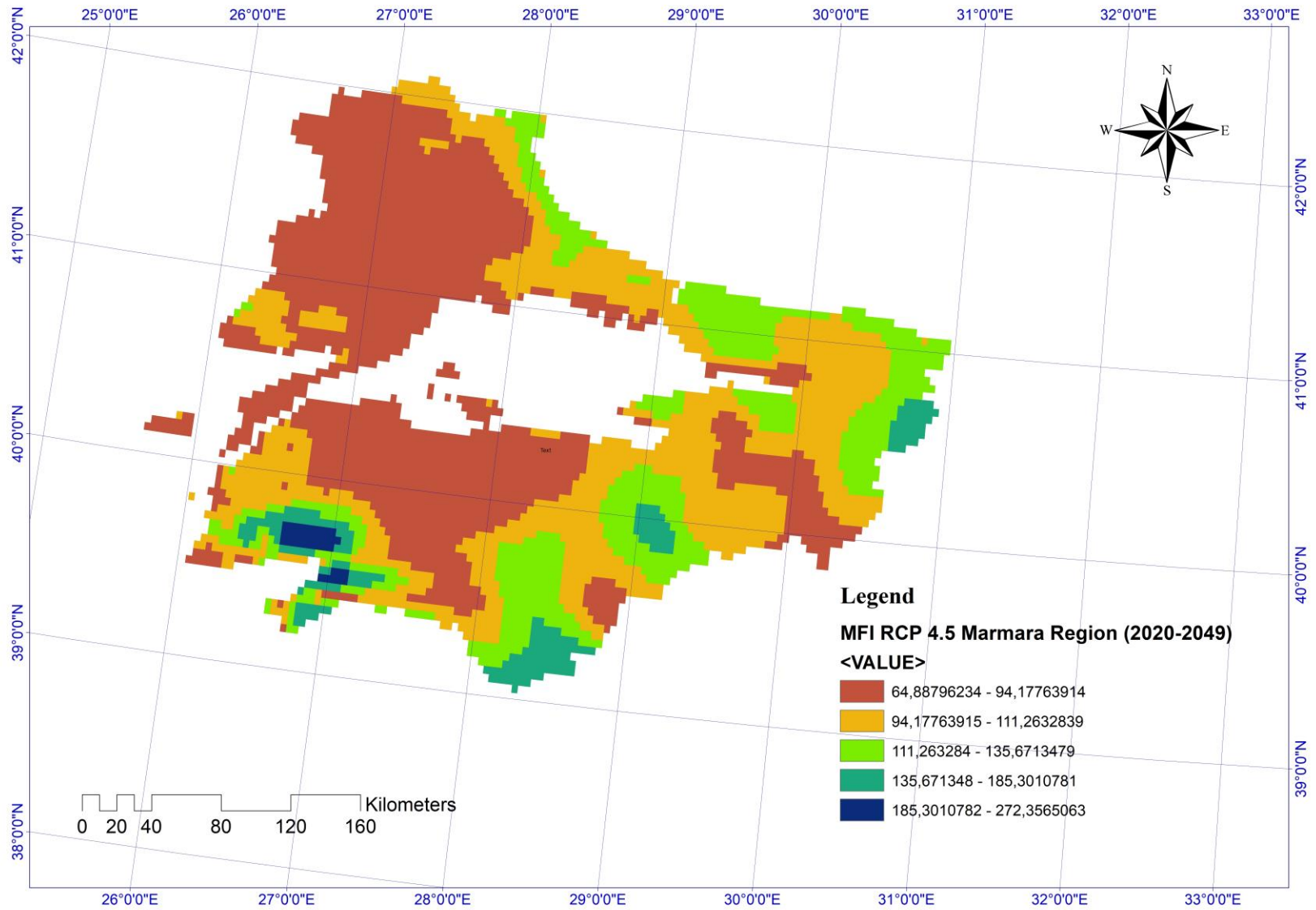


Figure 4.3. RCP 4.5 Modified Fournier Index Variability During 2020-2049.

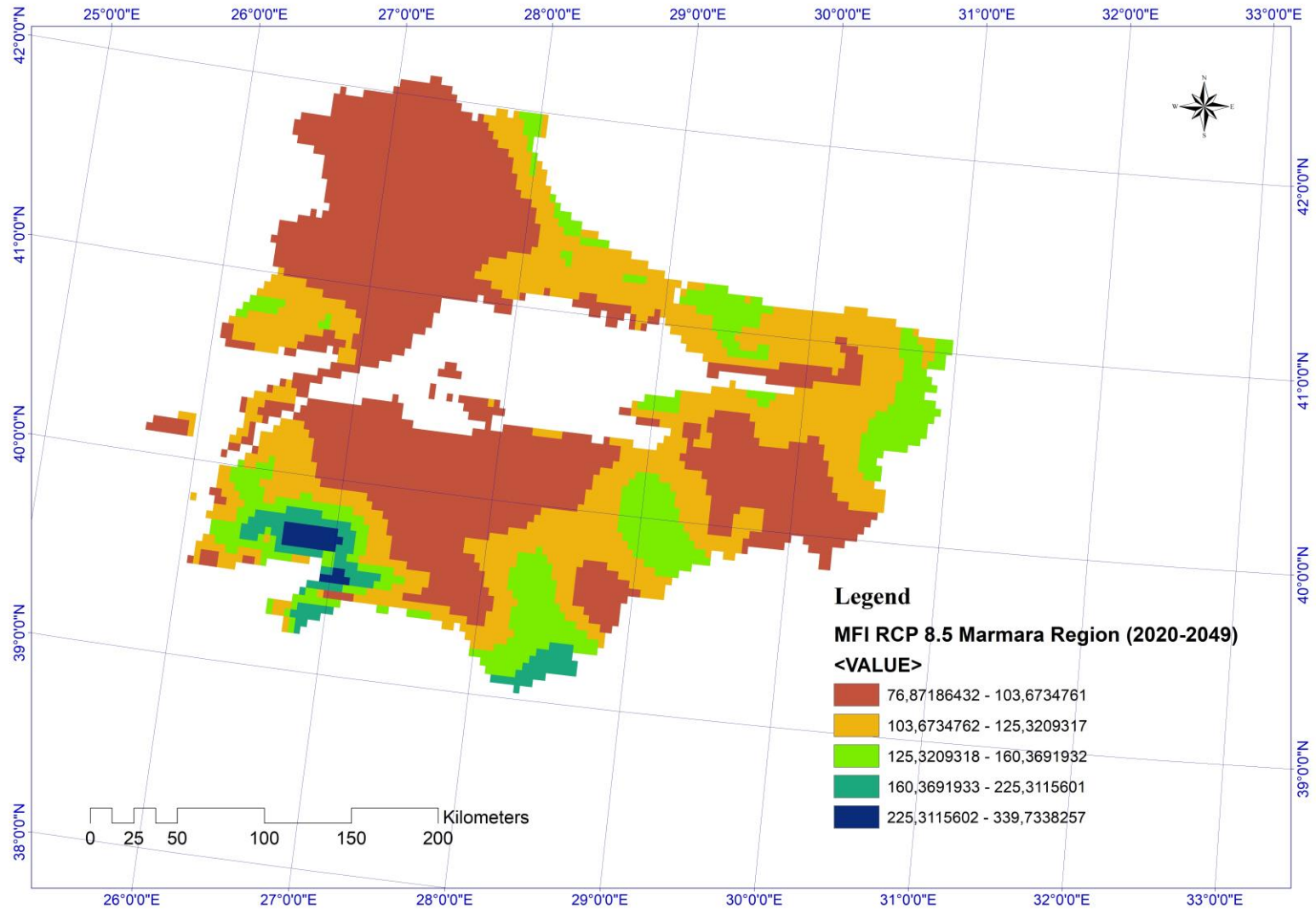


Figure 4.4. RCP 8.5 Modified Fournier Index Variability During 2020-2049.

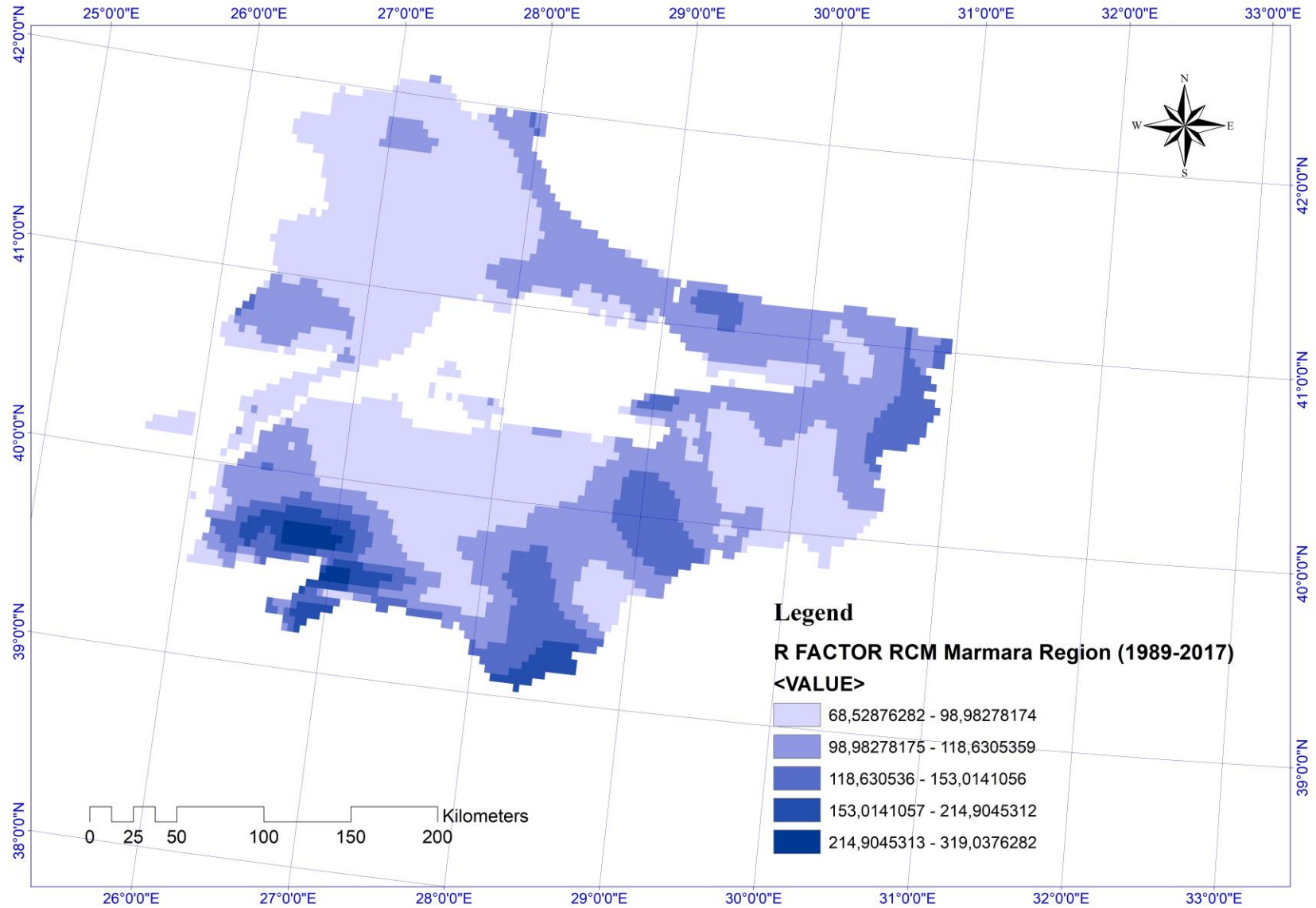


Figure 4.5. R Factor Map Marmara HIST 1989-2017.

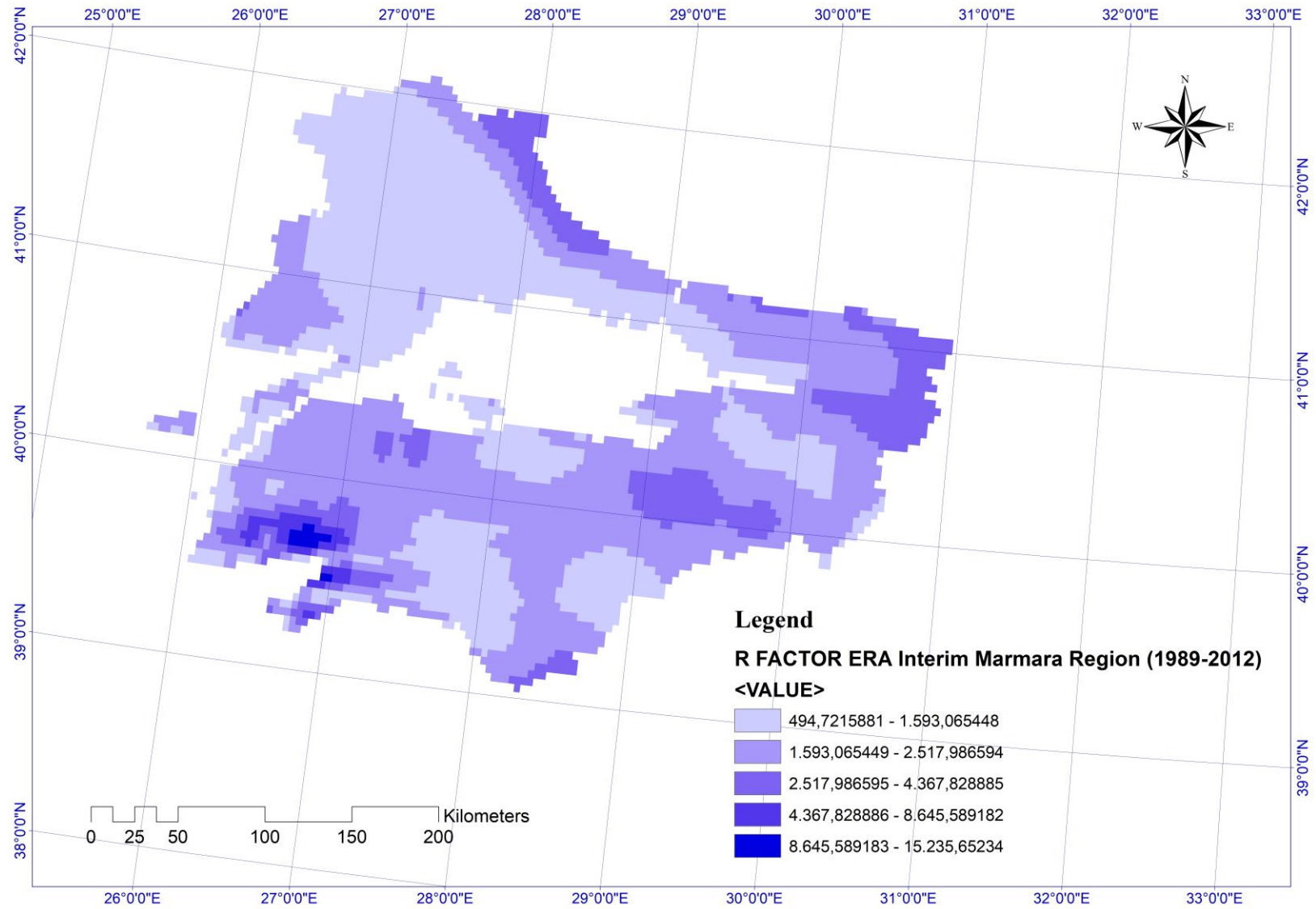


Figure 4.6. RFactor Map Marmara ERAINTERIM 1989-2017.

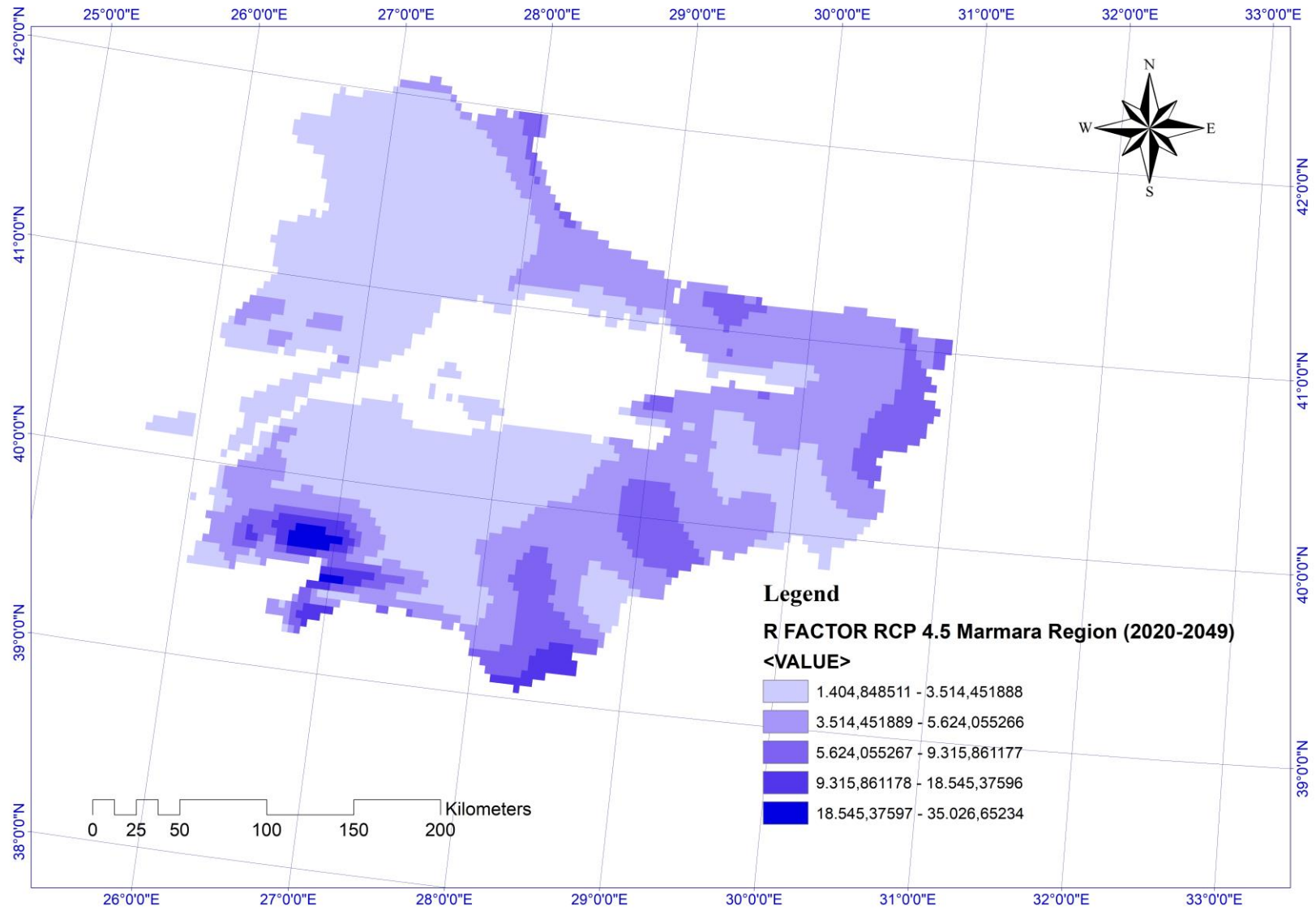


Figure 4.7. RCP4.5 R Factor Map 2020-2049 of the Marmara Region.

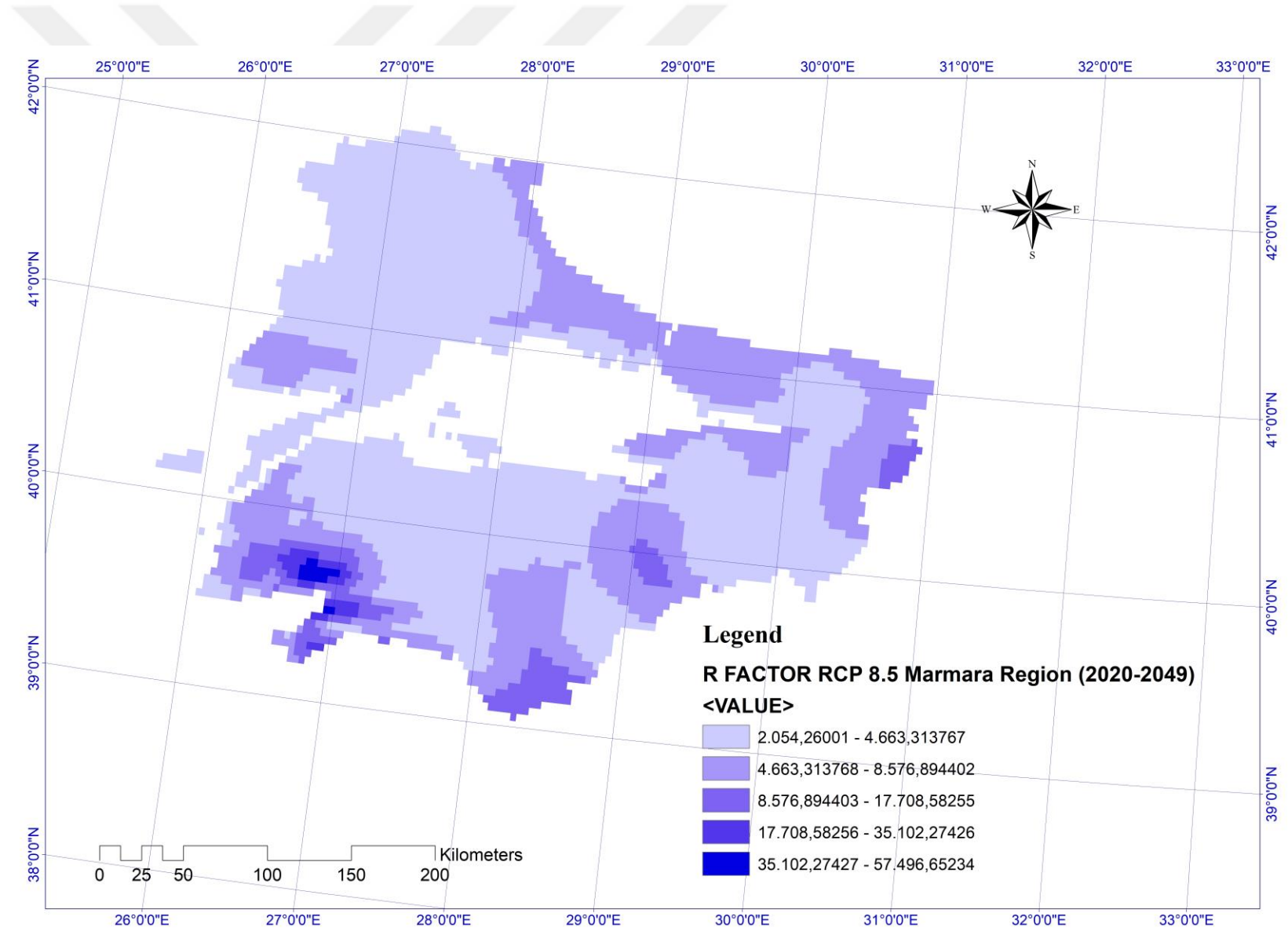


Figure 4.8. RCP 8.5 R Factor Map 2020-2049 of the Marmara Region.

According to the RCP8.5's future assumptions radiation power of greenhouse gases, it is more than 8.5W/m^2 which is negative one (IPCC, 2007), the results of the MFI are obtained and shown in the Figure 4.1.7. The MFI values of the RCP 8.5 during the time interval 2020-2049 range from 76, 8719 to 339.734 mm. This projection values show that the rainfall erosivity during the time interval 2020-2049 of the RCP 4.5 scenario foresee represent the range from low rainfall erosivity class to extremely severe rainfall erosivity class for the Marmara Region. Also, the MFI values of RCP 8.5 foresee the same risky places which demonstrate extremely severe rainfall erosivity class such as the cities Çanakkale, Balıkesir, and Bursa.

In order to take the final results for the R factor, the projected data of RCP 8.5 scenario for the region was run. The R factor values of RCP 8.5 scenario for the time interval 2020 - 2049 range from 2054, 26 to 57496,7 MJ.mm/ha.year. This range of the R factor results become the highest range among the historical data, ERA-Interim data, RCP 4.5 scenario results. It can be also deduced from the results of RCP 8.5 scenario for the time interval 2020 -2049, it foresees higher rainfall erosivity than the RCP 4.5 scenario's results. Thus, it might be said that according to the worst case scenario emission, the soil loss of the Marmara Region will be higher.

Finally, the datum of the maps were chosen as D_WGS 1984, and also spatial reference system were chosen as UTM Zone 35 N. Moreover, the standard deviation of the R factors results for RCM data for 1989-2017, ERA-Interim data for 1989-2012, RCP 4.5 data for 2020-2049, and RCP 8.5 data for 2020-2049 are 23.31836, 956.26716, 2402.46450, and 3690.13246 mm respectively.

R FACTOR AND MFI RESULTS

The MFI values of the historical data of the Regional Climate Model (1989-2017) range from 68.5288 to 319.038 mm

The R factor values of the historical data of the Regional Climate Model (1989-2017) range from 1587.77 to 49939 MJ.mm.ha⁻¹.year⁻¹

The MFI values of the ERA-Interim data (1989-2012) range from 40.7382 to 187.883 mm

The R factor values of the ERA-Interim data (1989-2012) range from 494.722 to 15235.7 MJ.mm.ha⁻¹.year⁻¹

The MFI values of the RCP 4.5 scenario data of the Regional Climate Model (2020-2049) range from 64.888 to 272.357 mm

The R factor values of the RCP 4.5 scenario data of the Regional Climate Model (2020-2049) range from 1404.85 to 35026.7 MJ.mm.ha⁻¹.year⁻¹

The MFI values of the RCP 8.5 scenario data of the Regional Climate Model (2020-2049) range from 76.8719 to 339,734 mm

The R factor values of the RCP 8.5 scenario data of the Regional Climate Model (2020-2049) range from 2054.26 to 57496.7 MJ.mm.ha⁻¹.year⁻¹

Figure 4.9. MFI and R Factor Results for the Marmara Region, Turkey

4.2. K Factor

Table 4.1. K Factor Table for Marmara Region (Soil Type Classification & RUSLE Model Calculation Result for K Factor).

FID	SOIL TYPE	Sand %	Silt %	Clay %	Organic Content %	A	B	C	D	K_Factor
0	PELLIC VERTISOLS	25.1	12.2	62.7	0.68	0.37065002	3.47729735	0.99720628	0.99999539	0.169267997
1	CHROMIC LUVISOLS	64.3	12.2	23.5	0.63	0.270705562	2.610657056	0.997716674	0.983033772	0.091286898
2	CHROMIC LUVISOLS	64.3	12.2	23.5	0.63	0.270705562	2.610657056	0.997716674	0.983033772	0.091286898
3	CHROMIC LUVISOLS	64.3	12.2	23.5	0.63	0.270705562	2.610657056	0.997716674	0.983033772	0.091286898
4	CHROMIC LUVISOLS	64.3	12.2	23.5	0.63	0.270705562	2.610657056	0.997716674	0.983033772	0.091286898
5	CHROMIC LUVISOLS	64.3	12.2	23.5	0.63	0.270705562	2.610657056	0.997716674	0.983033772	0.091286898
6	CHROMIC LUVISOLS	64.3	12.2	23.5	0.63	0.270705562	2.610657056	0.997716674	0.983033772	0.091286898
7	PELLIC VERTISOLS	25.1	12.2	62.7	0.68	0.37065002	3.47729735	0.99720628	0.99999539	0.169267997
8	CHROMIC LUVISOLS	64.3	12.2	23.5	0.63	0.270705562	2.610657056	0.997716674	0.983033772	0.091286898
9	CALCIC CAMBISOLS	81.6	6.8	11.7	0.44	0.242814283	2.143587009	0.999037953	0.718478976	0.049203601
10	CHROMIC LUVISOLS	64.3	12.2	23.5	0.63	0.270705562	2.610657056	0.997716674	0.983033772	0.091286898
11	PELLIC VERTISOLS	25.1	12.2	62.7	0.68	0.37065002	3.47729735	0.99720628	0.99999539	0.169267997
12	PELLIC VERTISOLS	25.1	12.2	62.7	0.68	0.37065002	3.47729735	0.99720628	0.99999539	0.169267997
13	CALCARIC FLUVISOLS	39.6	39.9	20.6	0.65	0.363124337	2.513831277	0.997521888	0.999897187	0.119910002
14	CALCARIC FLUVISOLS	39.6	39.9	20.6	0.65	0.363124337	2.513831277	0.997521888	0.999897187	0.119910002

15	RENDZINAS	48.5	30.8	20.7	1.74	0.32705185	2.517317066	0.977541731	0.999327645	0.105921
16	ORTHIC LUVISOLS	76	9.9	14.1	0.41	0.251976769	2.257839592	0.999174913	0.862979907	0.0646073
17	CHROMIC LUVISOLS	64.3	12.2	23.5	0.63	0.270705562	2.610657056	0.997716674	0.983033772	0.091286898
18	ORTHIC LUVISOLS	76	9.9	14.1	0.41	0.251976769	2.257839592	0.999174913	0.862979907	0.0646073
19	CHROMIC LUVISOLS	64.3	12.2	23.5	0.63	0.270705562	2.610657056	0.997716674	0.983033772	0.091286898
20	CALCARIC REGOSOLS	63.5	19.2	17.3	0.76	0.280664427	2.391857637	0.996217853	0.985505084	0.086800396
21	CALCARIC FLUVISOLS	39.6	39.9	20.6	0.65	0.363124337	2.513831277	0.997521888	0.999897187	0.119910002
22	ORTHIC LUVISOLS	76	9.9	14.1	0.41	0.251976769	2.257839592	0.999174913	0.862979907	0.0646073
23	ORTHIC LUVISOLS	76	9.9	14.1	0.41	0.251976769	2.257839592	0.999174913	0.862979907	0.0646073
24	ORTHIC LUVISOLS	76	9.9	14.1	0.41	0.251976769	2.257839592	0.999174913	0.862979907	0.0646073
25	PLANOSOLS	19.8	55.2	24.8	4.27	0.439056574	2.65146508	0.974400837	0.999998534	0.149393007
26	EUTRIC CAMBISOLS	36.4	37.2	26.4	1.07	0.367099084	2.699760064	0.990309927	0.999947971	0.129253998
27	CALCIC CAMBISOLS	81.6	6.8	11.7	0.44	0.242814283	2.143587009	0.999037953	0.718478976	0.049203601
28	CALCIC CAMBISOLS	81.6	6.8	11.7	0.44	0.242814283	2.143587009	0.999037953	0.718478976	0.049203601
29	EUTRIC CAMBISOLS	36.4	37.2	26.4	1.07	0.367099084	2.699760064	0.990309927	0.999947971	0.129253998
30	CHROMIC VERTISOLS	24.1	12.2	63.7	0.68	0.37065002	3.47729735	0.99720628	0.99999539	0.171463996
31	CALCARIC FLUVISOLS	39.6	39.9	20.6	0.65	0.363124337	2.513831277	0.997521888	0.999897187	0.119910002
32	ORTHIC LUVISOLS	76	9.9	14.1	0.41	0.251976769	2.257839592	0.999174913	0.862979907	0.0646073
33	CALCARIC FLUVISOLS	39.6	39.9	20.6	0.65	0.363124337	2.513831277	0.997521888	0.999897187	0.119910002
34	ORTHIC LUVISOLS	76	9.9	14.1	0.41	0.251976769	2.257839592	0.999174913	0.862979907	0.0646073
35	PLANOSOLS	19.8	55.2	24.8	4.27	0.439056574	2.65146508	0.974400837	0.999998534	0.149393007
36	LITHOSOLS	58.9	16.2	24.9	0.97	0.284792963	2.654544006	0.992542089	0.994235324	0.098252401

37	PLANOSOLS	19.8	55.2	24.8	4.27	0.439056574	2.65146508	0.974400837	0.999998534	0.149393007
38	LITHOSOLS	58.9	16.2	24.9	0.97	0.284792963	2.654544006	0.992542089	0.994235324	0.098252401
39	CALCIC CAMBISOLS	81.6	6.8	11.7	0.44	0.242814283	2.143587009	0.999037953	0.718478976	0.049203601
40	EUTRIC CAMBISOLS	36.4	37.2	26.4	1.07	0.367099084	2.699760064	0.990309927	0.999947971	0.129253998
41	ORTHIC LUVISOLS	76	9.9	14.1	0.41	0.251976769	2.257839592	0.999174913	0,862979907	0,0646073
42	CALCIC CAMBISOLS	81.6	6.8	11.7	0.44	0.242814283	2.143587009	0.999037953	0.718478976	0.049203601
43	EUTRIC CAMBISOLS	36.4	37.2	26.4	1,07	0.367099084	2.699760064	0.990309927	0.999947971	0.129253998
44	LITHOSOLS	58.9	16.2	24.9	0.97	0.284792963	2.654544006	0.992542089	0.994235324	0.098252401
45	CALCARIC FLUVISOLS	39.6	39.9	20.6	0.65	0.363124337	2.513831277	0.997521888	0.999897187	0.119910002
46	LITHOSOLS	58.9	16.2	24.9	0.97	0.284792963	2.654544006	0.992542089	0.994235324	0.098252401

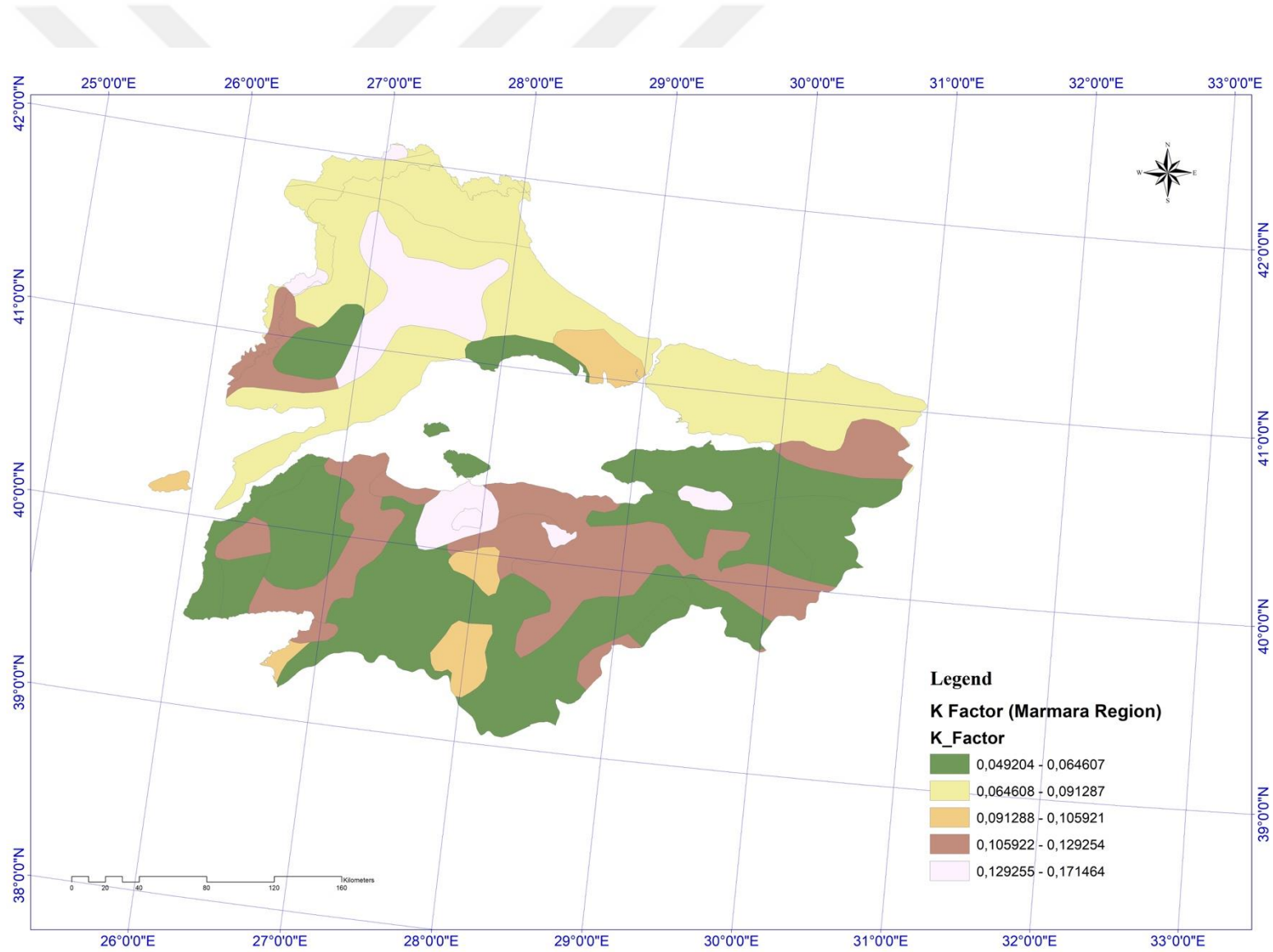


Figure 4.10. RUSLE Model K Factor Map created in ArcGIS for Marmara Region

First of all K factor demonstrates soil erodibility among all the factors of RUSLE Model. The K factor is related to organic matter content, soil texture, soil permeability class, and other various factors, and it is mostly determined by the soil type (Renard et al., 1997). In this study, the open source of the FAO Digital Soil Map of the World (DSMW) was used. The FAO Digital Soil Map of the World is the digitized version of the FAO-UNESCO Soil Map of the World. In the data the soil units estimates are provided of physical (% sand, % silt, % clay, bulk density) and chemical properties in the topsoil and subsoil. For the calculation of K Factor defined by RUSLE Model, the soil data of the Marmara Region was taken in shape file format. In ArcGIS10.4 software, the shape file of the soil data of Marmara Region was open in attribute table, and then exported to Excel file. The symbols used for describing soil content were investigated and the sand, clay, silt and organic content were analyzed. There are many soil types in Marmara Region such as pellic vertisols, chromic luvisols, rendzinas etc. and the soil types are written and classified in the Table 4.1. These soil types have different soil contents in percentage. After organic soil content, sand, silt and clay percentages were separated, A, B, C, and D factors to calculate K factor which are defined in RUSLE Model methodology were calculated in Excel file by using the formulas expressed in methodology part with the Equation 3.10, 3.11, 3.12, and 3.13. The K Factor values range from 0.049204 to 0.171464 Mg/Mj.mm. The higher K factor values are representative of the higher potential of the soil to erode the top soil. The soil type chromic vertisol have the highest K factor value, and it mostly contains clay content. In addition, the pellic vertisol, and the planasols have the second and third highest K factor value respectively.

In the study of Ozşahin et al. (2014), the authors investigate the effects of land use and land cover changes in Kuseyr plateau of Turkey on erosion, and the study area is a part of Mediterranean basin of Turkey. According to the study based on Kuseyr plateau of Mediterranean, the soil groups are alluvial, colluvial, brown forest, non-calcic brown forest, red mediterranean, red brown, and rocky areas. Also, the K factor ranges from 0.001 to 0.065 in the study of Özşahin et al. (2014). In addition to the K factor findings of the other studies, Ozsoy et al. (2012) provides information about the soil types of the Mustafakemalpaşa River Basin in the Marmara Region, and the main soil types in the basin are non-calcic brown forest soils, and brown forest soils. According to the study of Ozsoy et al. (2012) these two great soil groups constitute 85.7% of the basin, but 9.3% is composed of rendzinas, alluvial, colluvial, and brown soils. The 5% part of the Mustafakemalpaşa River Basin is composed of water and bare rocks (Ozsoy et al., 2012). Besides all the soil information given in the study of Ozsoy et al. (2012), the study claim that it is not possible to estimate the K factor for the Mustafakemalpaşa River Basin due to the lack of information, insufficient and old soil maps for the basin.

Finally, the datum of the maps were chosen as D_WGS 1984, and also spatial reference system were chosen as UTM Zone 35 N. Also, the standard deviation of the K Factor results is $0.033508 \text{ Mg.ha.h.ha}^{-1}.\text{MJ}^{-1}.\text{mm}^{-1}$.

4.3. LS Factor

The LS factor is the topographic factor represents the ratio of the soil loss under given condition to that at a site with the standard slope steepness of 9% and slope length of 22.6 m (Ganasri et al., 2016). The L factor represents the slope length, and the S factor represents the slope steepness. The soil loss per unit area increases if the slope length increases. The effect of slope steepness have a greater impact on soil erosion when it is compared to the effect of slope length. Steeper the slope makes soil erosion greater (Ganasri et al., 2016).

In this study, to estimate the LS factor, DEM (Digital Elevation Model) in ArcGIS software was created by digitizing contour lines from topographic maps (Rozos et al., 2013). Geographical Information Systems analyses allow users to make slope steepness (S) and slope length (L) raster covers by various methods (Gaubli et al., 2015). The five steps to calculate the LS factor below were used.

5 Steps taken to calculate the LS FACTOR :

1. Marmara Region DEM
2. Creation of the SLOPE Map on SRTM DEM
3. Flow Direction Map
4. Flow Accumulation Map
5. Discovered LS Algorithm

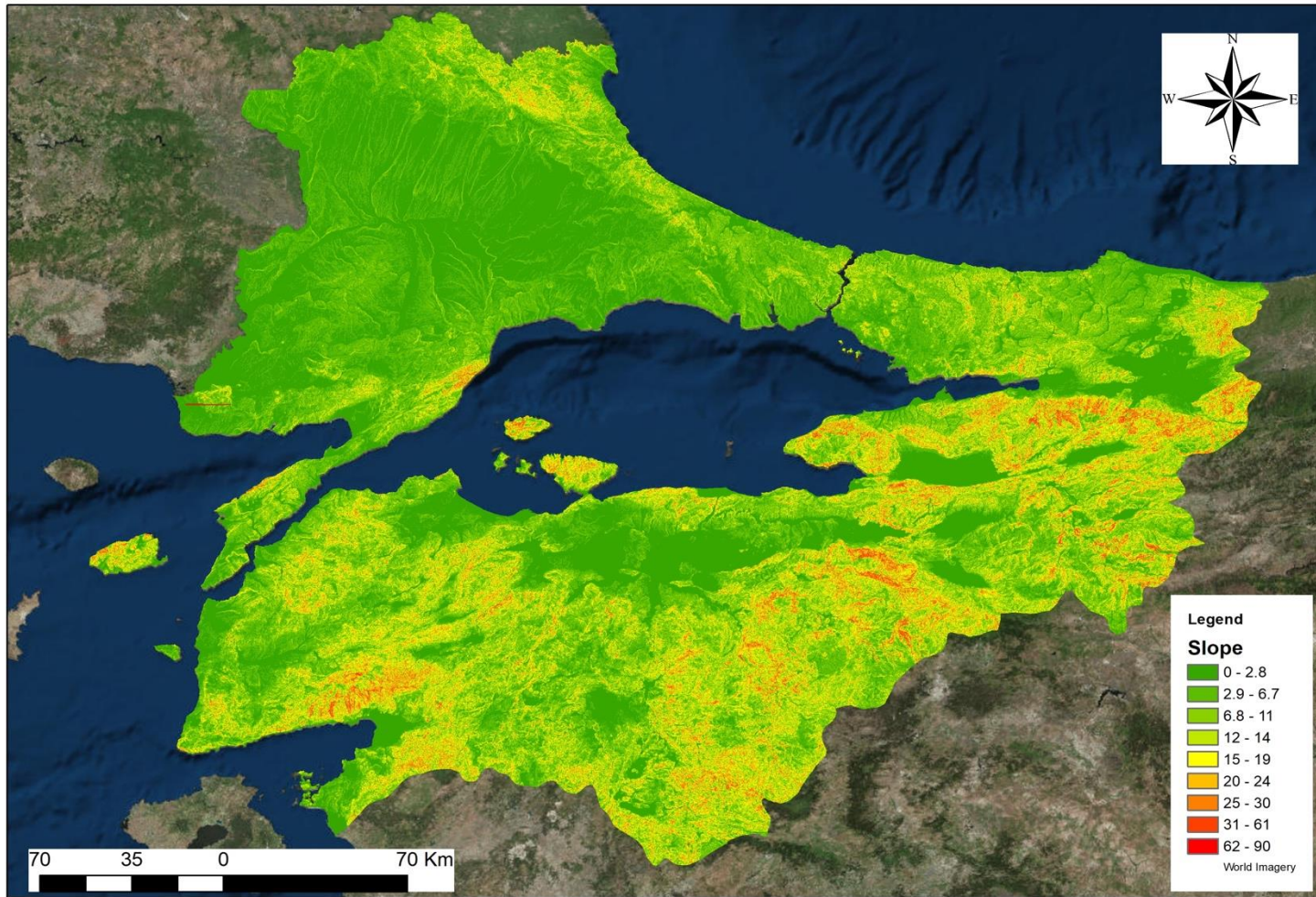


Figure 4.11. Marmara Region Slope Map.

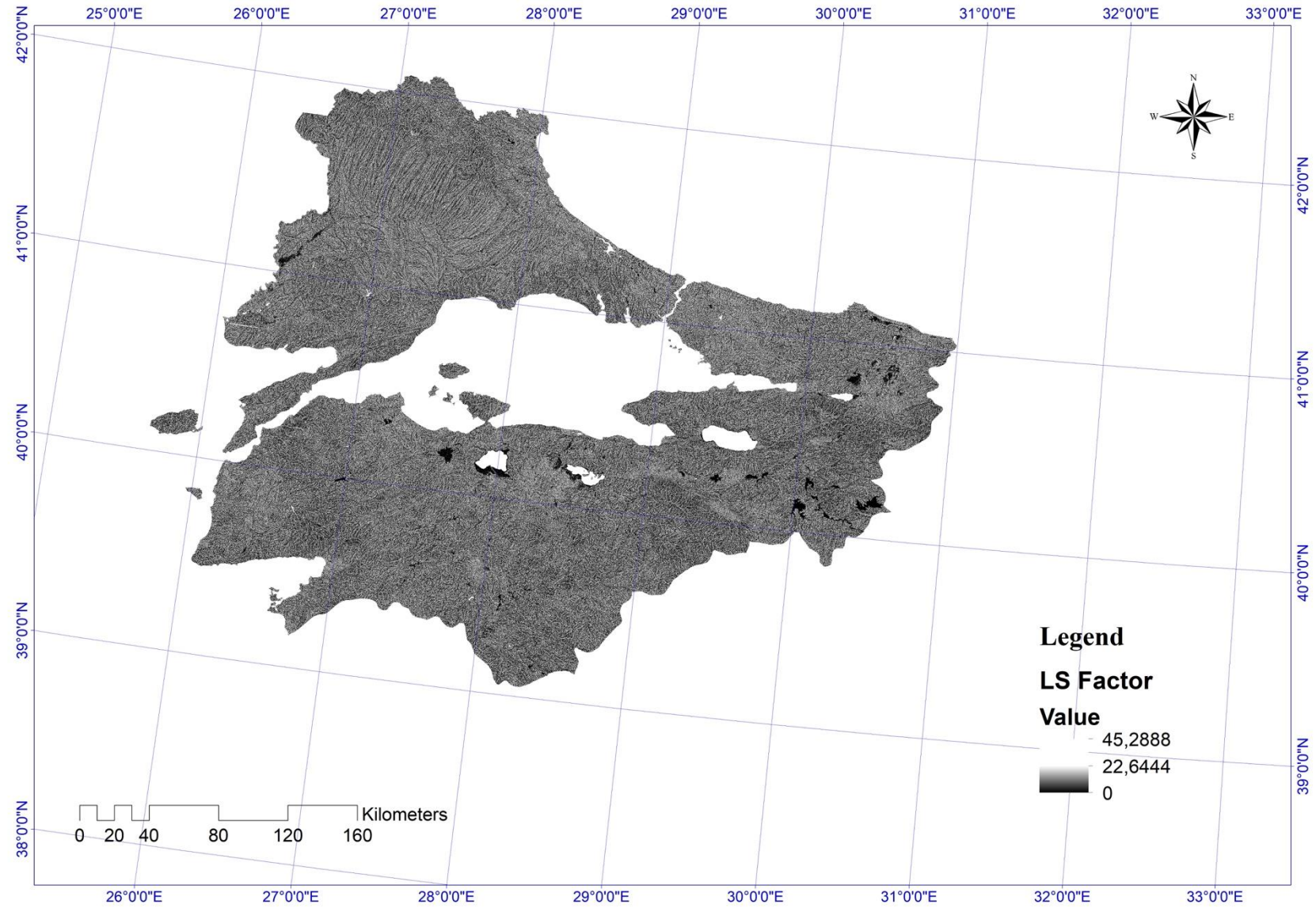


Figure 4.12. RUSLE Model LS Factor Map created in ArcGIS.

Topographic factor includes slope length factor (L) and slope steepness factor (S), they are the representatives of the effect of surface topography on erosion by water action. Slope Length (L) and Slope Steepness (S) were derived by SRTM DEM in 30 m x 30 m resolution in ArcGIS 10.4. In methodology part, Equation 10 and Equation 11 represent the calculation of LS Factor for RUSLE application. In that case, the combined factor LS was computed for the Marmara Region by means of ArcGIS Spatial Analyst Tool extension using DEM. The grid based DEM was generated from contour vector data, and also it was digitized from 1:25000 scale topographic maps with 10 meter intervals (Ozsoy et al., 2012). The DEM was created with the “Topo to Raster” interpolation method in 3D Analyst Tool in the ArcGIS software. In the Figure 4.11., the results of the slope map of the Marmara Region shows that in the most of the region the slope values are in between 0 to 18. According to the LS distribution map of the Marmara Region created in DEM the LS values range from 0 to 45.28888. The east parts of the region is more likely to represent high lands (elevation is approximately 2000 m), especially the north-east parts of the region. When it comes to the results of the other studies have close characteristics with the study area of this study, there are some shared results of them. According to the results of the study by Ozsoy et al. (2012) the LS values of the Mustafakemalpasa River basin of the Marmara Region range from 0.03 to 70.07.

Finally, the datum of the maps were chosen as D_WGS 1984, and also spatial reference system were chosen as UTM Zone 35 N. Also, the standard deviation of the LS Factor results is 0.24735.

4.4. C Factor

C Factor is the crop management factor defined by RUSLE Model, and it is dimensionless factor among others. It depends on the land use pattern of an area. To have the results of these the factor, the literature review were done, and for the application part the Landsat images were downloaded from www.earthexplorer.usgs.gov (USGS). However, it is hard to classify the Landsat satellite images because of some cloudy, foggy, not clear weather images. The clearest ones was chosen and run for the model application. The C factor changes from region to region, so the best fit regional values are being searched. In order to analyze the agricultural, vegetation, urban etc. parts of the Marmara Region, remote sensing technology is essential.

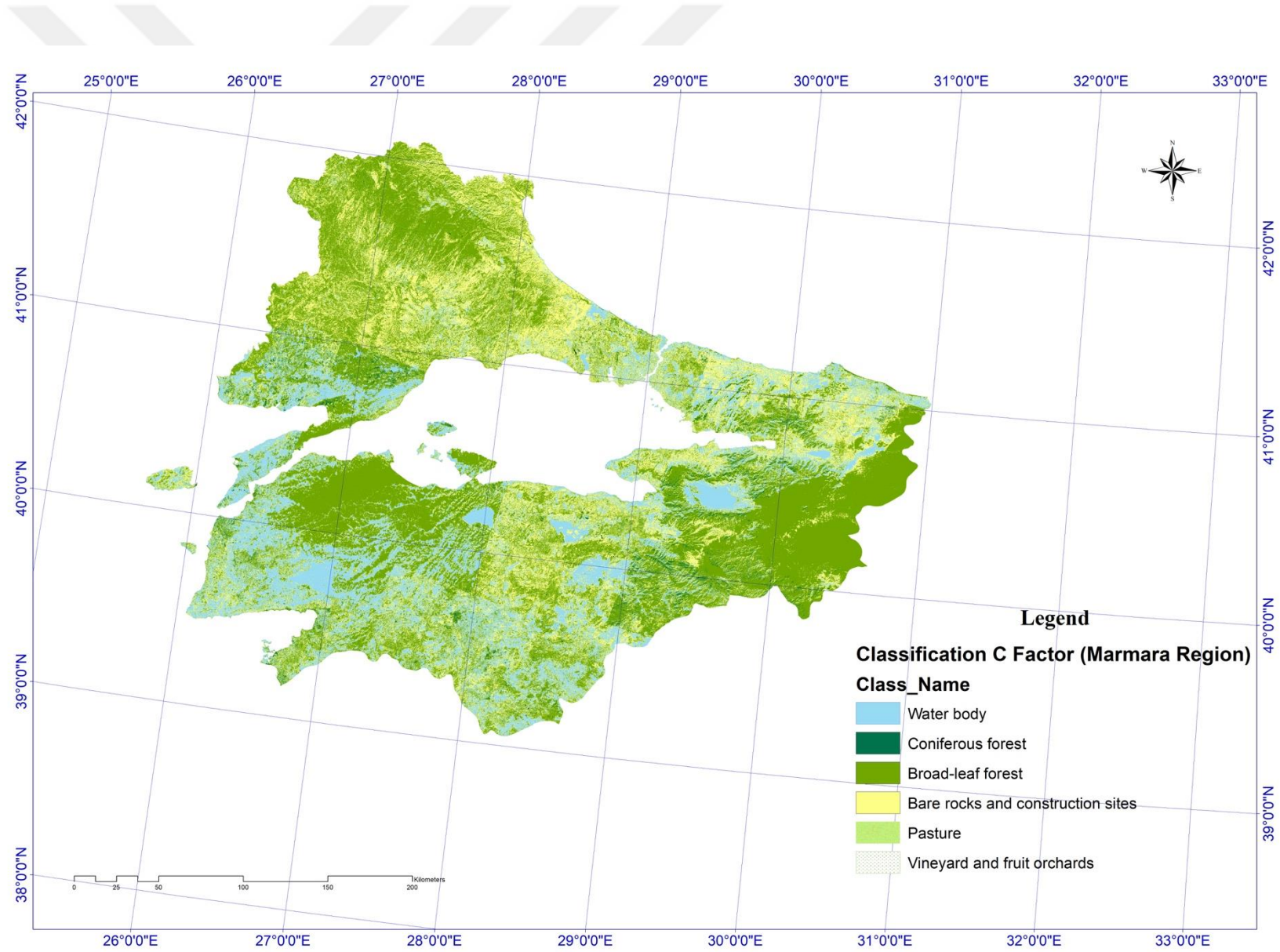


Figure 4.13. C Factor Map of the Marmara Region.

The estimation of the C Factor became the most time spent part of the study, because of the hardness of running the satellite images in ArcGIS software and finding the best fit satellite images for the borders of the region. After fitting the best satellite images for the study area, the red, the green and the blue bands of the satellite images were selected in order to examine the vegetation cover. In ArcGIS software, the composition of these raster form of these three bands 4, 3 and 2 were done in the composite bands tool. After composing the bands on the software, the image analysis tool were used and the processing option was used to make NDVI. This process was completed for each satellite images. Mosaic to new raster tool were used to make all the raster NDVI forms united. Then, the mosaic raster form of NDVI images were clipped according to the area of the study area. Thus, the NDVI map of the Marmara Region was done. Then, classification of C factor for the study area was done with the values shown in the Table 3.4. Finally, the datum of the maps were chosen as D_WGS 1984, and also spatial reference system were chosen as UTM Zone 35 N. Also, Landsat images have 30 m x 30 m resolution.

4.5. Soil Loss

The RUSLE Equation (shown in Eqn.1) was used to calculate the annual average soil loss rate (A) in $\text{Mg} \cdot \text{ha}^{-1} \cdot \text{year}^{-1}$. In order to estimate the soil loss rate in the Marmara Region of Turkey the R, K, LS, C, and P factors found in the earlier sections were multiplied by using the raster calculator function tool of the ArcGIS 10.4 Software (Jinghu and Yan, 2014; Tang et al., 2015).

The results of the raster calculation of five RUSLE Model factors show the estimation of the average rate of soil erosion on every point of the Marmara Region and to elaborate the synthetic soil loss map. By considering the study of Li et al. (2014) there are 6 different soil erosion risk classifications dependent on the soil loss results in $\text{Mg} \cdot \text{ha}^{-1} \cdot \text{year}^{-1}$ shown in Table 3.2. in methodology part.

In this part, the soil loss results of the historical data of the Regional Climate Model showed that the soil loss range from 0 to $24.298 \text{ Mg} \cdot \text{ha}^{-1} \cdot \text{year}^{-1}$ during the time interval 1989 – 2017 in the Marmara Region. The average soil loss is $12.2 \text{ Mg} \cdot \text{ha}^{-1} \cdot \text{year}^{-1}$. According to classifications of the Li et al. (2014) $12.2 \text{ Mg} \cdot \text{ha}^{-1} \cdot \text{year}^{-1}$ is the representative of the low soil erosion risk. Besides, the Modified Fournier Index of the Marmara Region by considering the historical data of the Regional Climate Model, the MFI of the Region for the time interval 1989-2017 ranges from 68.5288 to 319.038mm.

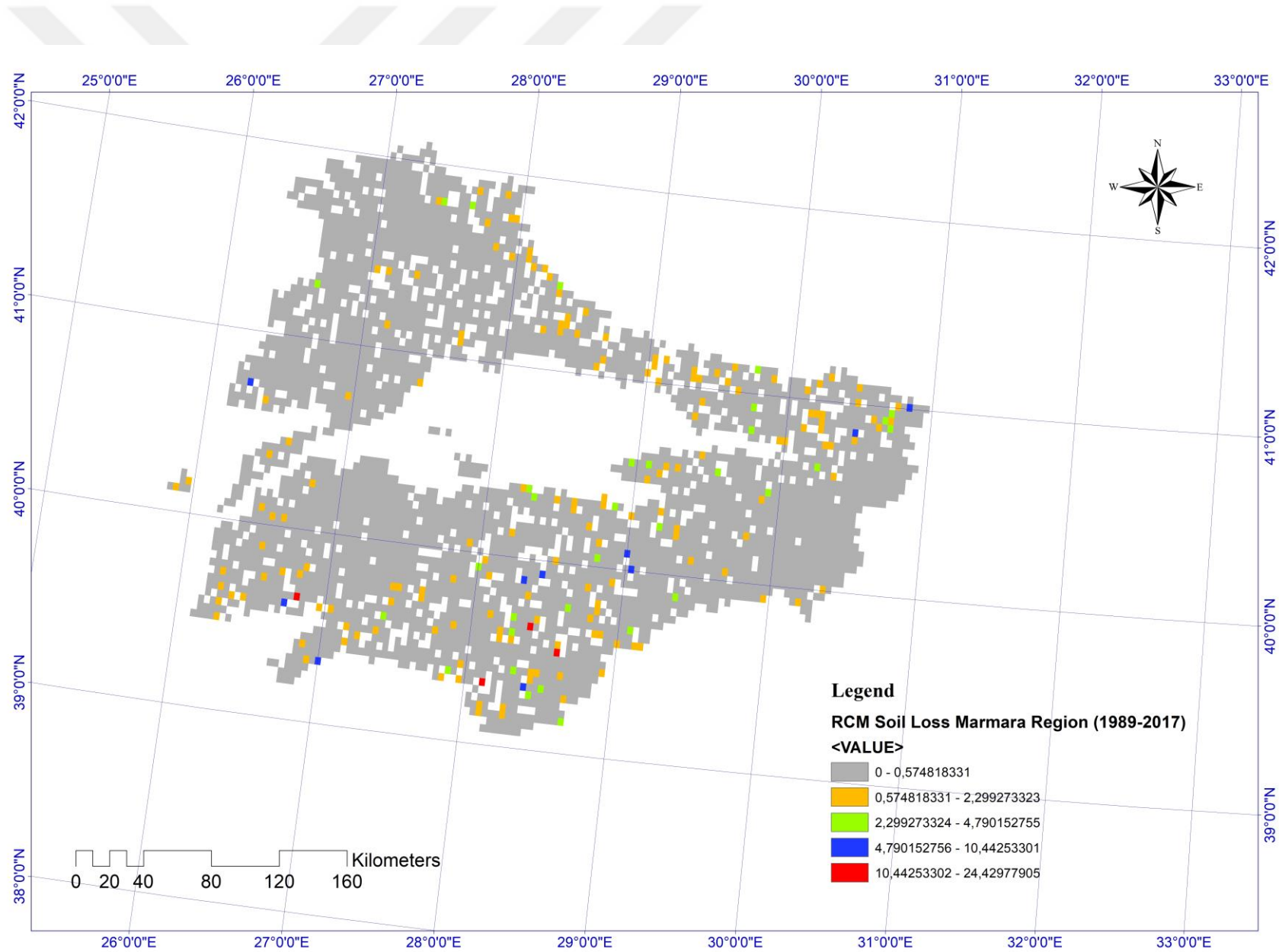


Figure 4.14. Soil Loss Historical Map of the Marmara Region (Historical data between the years 1989-2017).

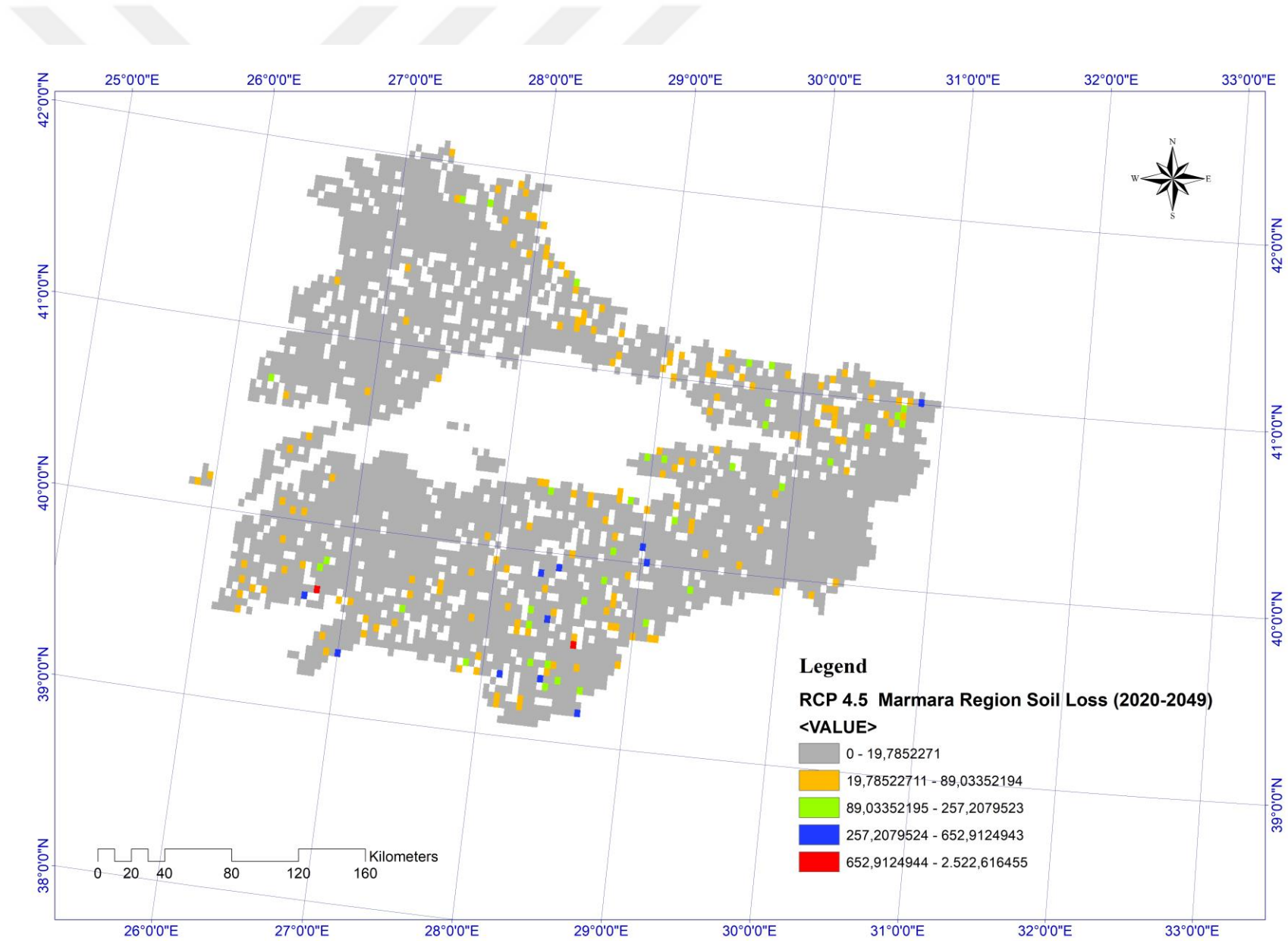


Figure 4.15. Soil Loss RCP 4.5 Map of the Marmara Region (2020-2049).

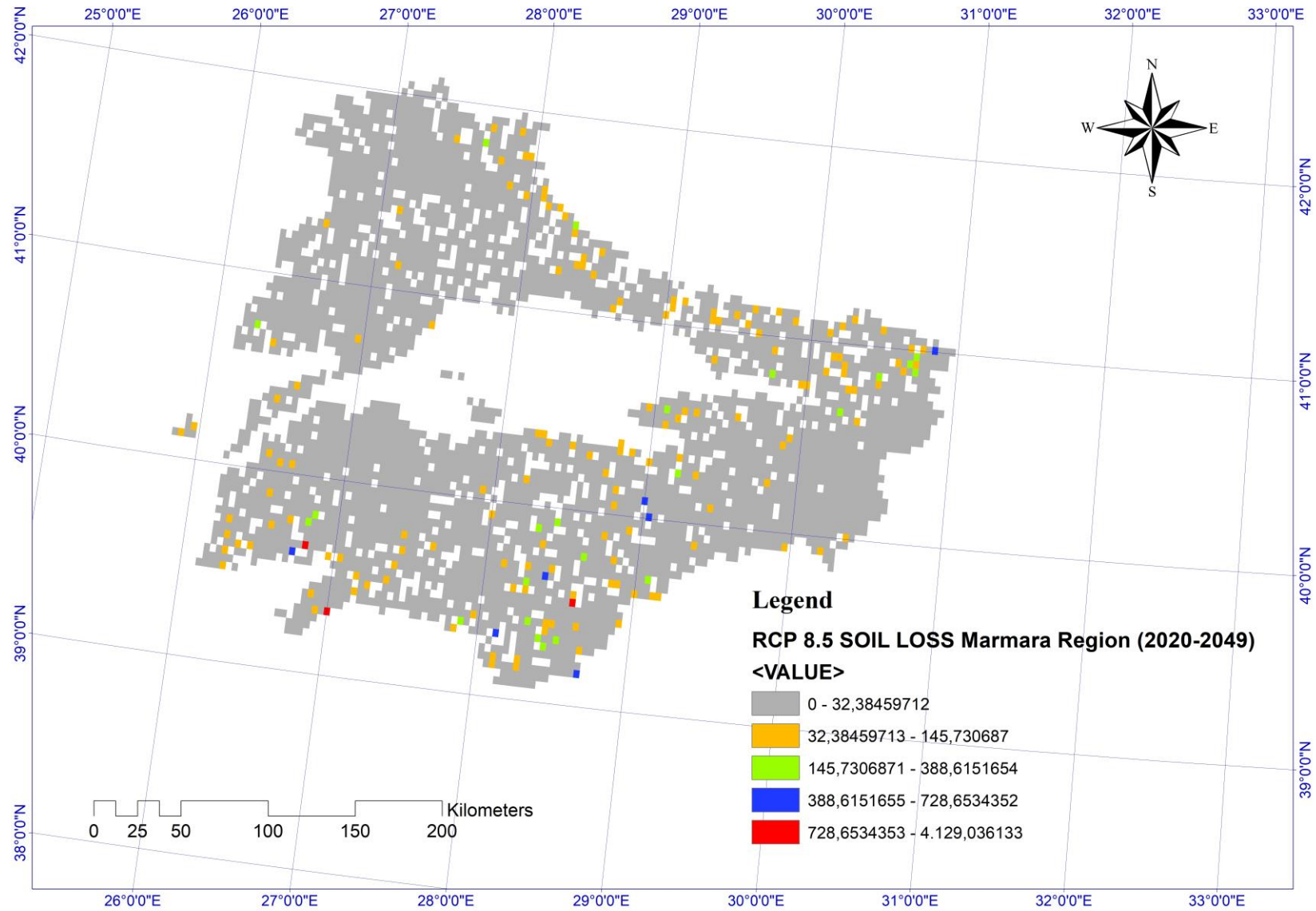


Figure 4.16. Soil Loss RCP 8.5 Map of the Marmara Region (2020-2049).

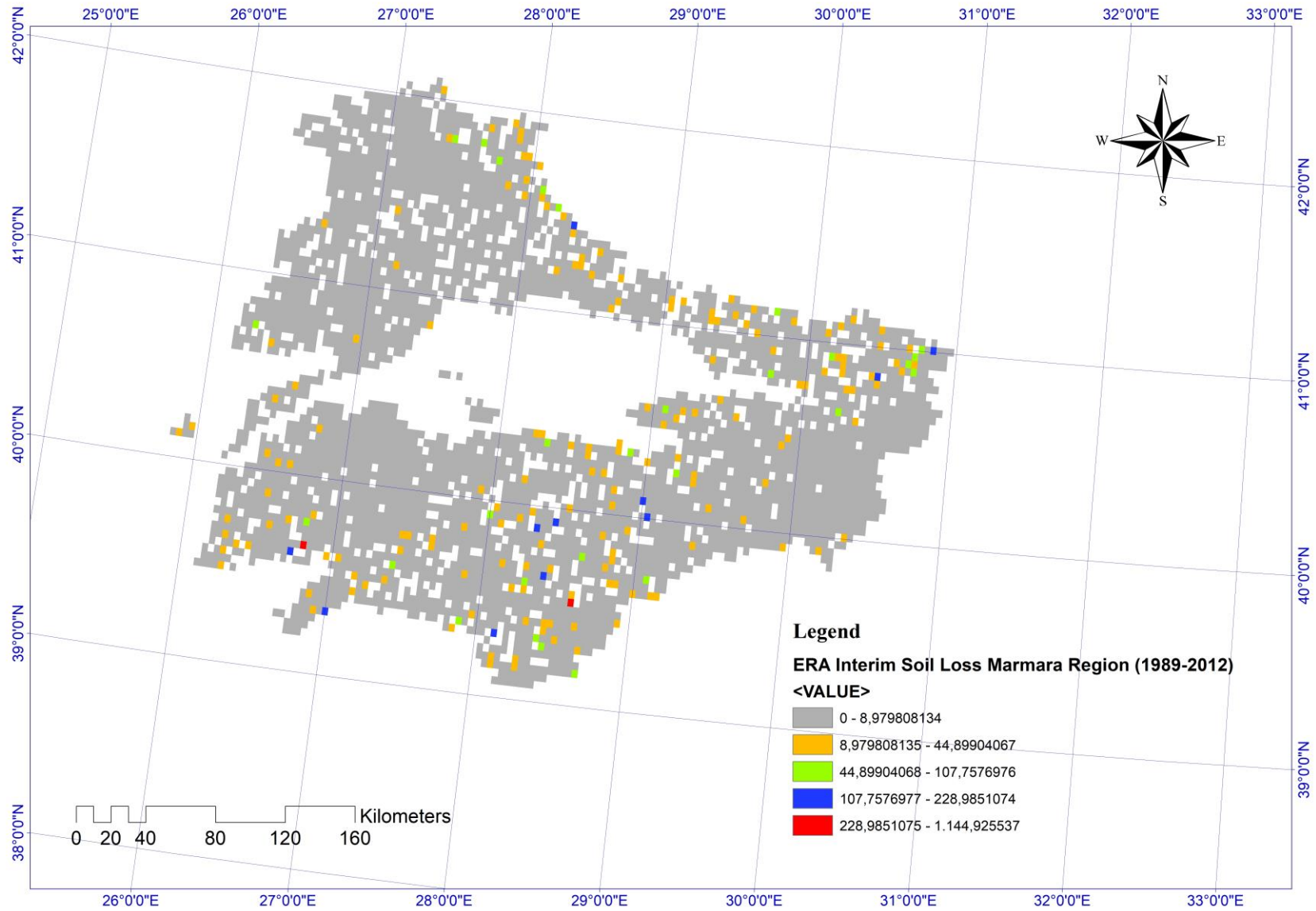


Figure 4.17. Soil Loss Map ERA-Interim of the Marmara Region.

By considering the study done by Arnoldus (1980), the MFI value ranges from 0 to 60 mm represents very low rainfall erosivity, and there is no representative area for the very low rainfall erosivity class in the Marmara Region according to the findings of the study. According to the results the rainfall erosivity ranges from low to extremely severe classes, and also the parts of the region having extremely severe rainfall erosivity are very less in amount when they are compared to the low rainfall erosivity parts. Thus, it is a satisfactory result that the findings from the rainfall erosivity and the soil loss are parallel when the risk classes are compared. Both the results of the MFI and the soil loss shows that the Marmara Region during the time interval 1989- 2017 have low rainfall erosivity and low soil erosion risk. When it comes to the results of the other studies having the similar characteristics, the study by Ozsoy et al. (2012) the average soil loss of the Mustafakemalpaşa River basin of the Marmara Region was found in time interval 1946 – 2005 as 11.2 Mg. ha⁻¹. year⁻¹ which is approximately very similar result with the results of the historical model data of the RegCM.

However, the results taken by the RCP 4.5 scenario and RCP 8.5 scenario are shown over-estimated soil loss results, and they provide extremely high soil erosion risk for both the historical period and the future. Firstly, the ERA-Interim results for the time interval 1989-2012 showed that the soil loss range from 0 to 1144.93 Mg. ha⁻¹. year⁻¹. Secondly, the RCP 4.5 results for the future projection (2020-2049) range from 0 to 2522.62 Mg. ha⁻¹. year⁻¹. Thirdly, the RCP 8.5 results for the future projection (2020-2049) range from 0 to 4129.04 Mg. ha⁻¹. year⁻¹. These over-estimated results for the soil loss calculation of the region are important when it comes to make comparison between the scenarios and the model data. However, their numerical findings most probably shows unrealistic amounts. According to the two scenarios of the Regional Climate Model RCP 4.5 (optimistic), and RCP 8.5 (pessimistic), the future soil loss of the Marmara Region in the changing rainfall events is higher than the results of the historical data. The soil loss results for the time interval 2020-2049 of the scenario RCP 8.5 is 61% higher than the results of the scenario RCP 4.5. As final words, the soil loss results of the historical data of the Regional Climate Model showed that the soil loss range from 0 to 24.298 Mg. ha⁻¹. year⁻¹ during the time interval 1989-2017 in the Marmara Region, and also the average soil loss is 12.2 Mg. ha⁻¹. year⁻¹.

Finally, the datum of the maps were chosen as D_WGS 1984, and also spatial reference system were chosen as UTM Zone 35 N. Moreover, the standard deviation of the soil loss results for RCM data for 1989-2017, ERA-Interim data for 1989-2012, RCP 4.5 data for 2020-2049, and RCP 8.5 data for 2020-2049 are 0.777323, 956.26716, 21.95592, 50.22157 and 75.30263 Mg.ha⁻¹.year⁻¹ respectively.

6. CONCLUSION

Soil is essential for all living organisms on the Earth. Soil is a natural body consisting of layers that are composed of organic contents, weathered minerals, air and water (Bockheim et al., 2005). Also, it is the final product of the combination of the climatic conditions, slope, living organisms (fauna and flora), minerals, and time. Soil erosion is one of the most important environmental threats to the society and the economy in various cases all around the world especially affecting the agriculture. Due to human induced activities the rate of soil erosion is drastically increasing, and global climate change becomes the most striking reason to affects soil erosion negatively (Mondal et al., 2015). With this reason, in this study, the effect of changing climatic conditions on soil erosion was investigated in the perspective of the changing rainfall events by considering the historical data and future climatic scenario data of the Regional Climate Model. The main aim was to develop awareness towards the soil related and climate change oriented environmental issues by emphasizing on the soil erosion risk through the Marmara Region of Turkey. Moreover, the present study was aimed to quantitatively and qualitatively assess soil erosion rates in the Marmara Region of Turkey using RUSLE model in a GIS environment considering various datasets like rainfall, vegetation cover, soil as well as topographic characteristics. The average annual soil erosion rate of the Marmara Region was found to be $12.2 \text{ Mg. ha}^{-1} \cdot \text{year}^{-1}$ for the time interval 1989-2017. The entire area was divided into six soil erosion risk classes ranging from 0 to $24.298 \text{ Mg. ha}^{-1} \cdot \text{year}^{-1}$ (Li et al., 2014; Tang et al., 2015). High intensity precipitation events, high LS factor due to terrain characteristics, increase in human induced activities as well as low vegetation cover on ground can be identified as the major causes of high erosion rates. The findings of the annual soil erosion rate, and all the factors included in the RUSLE Model was compared to the other studies' results especially applied on the Marmara Region and the other areas which has similar climatic and terrain characteristics. to validate both the RUSLE Model and the results of the study. The use of remote sensing and GIS inputs enable us to identify high erosion risk zones, the estimation accuracy and functions of the model can be improved further by providing a rainfall data with higher resolution as well as vegetation cover values using NDVI.

Land cover is a significant factor affecting and linking many parts of the human life and our physical environment. Since the remote sensing techniques has provided a map-like representation of the Earth's surface that is spatially continuous and mostly reliable, and also available at a range of spatial and temporal scales, it has become a powerful source to create land cover data. In the scientific studies including land cover. Digital image processing techniques and geostatistical techniques were applied to derive land cover and vegetation map by using the satellite imagery.

Also, the past and future comparison techniques can be used to improve the study in the future. Since, bringing new understandings and construction the knowledge are very significant in scientific researches.



REFERENCES

- Albaladejo, M.J., Stocking, M.A., 1989. Comparative evaluation of two models in predicting storm soil loss from erosion plots in semi-arid Spain. *Catena* 16, 227-236.
- Altınsoy, H., Öztürk, T., Türkeş, M., Kurnaz, M.L., 2011. Projections of Future Air Temperature and Changes in the Mediterranean Basin by Using the Global Climate Model, Proceedings of the National Geographical Congress with International Participation (CD-R), ISBN 978-975-6686-04-1, 7–10 September 2011, Türk Coğrafya Kurumu, İstanbul University
- Ananda, J., Herath, G., 2003. Soil erosion in developing countries: a socio-economic appraisal. *Journal of Environmental Management*, 68, 343-353.
- Arnold, J.G., Srinivasan, R., Muttiah, R.S., Williams, J.R., 1998. Large area hydrologic modeling and assessment part I: Model development. *Water Research Association*, 34, 73-89.
- Arnoldous, H.M.J., 1977. Methodology used to determine the maximum potential average annual soil loss due to sheet and rill erosion in Morocco. *FAO Soils Bulletin* 34, 39-51.
- Arnoldous, H.M.J., 1980. An Approximation of Rainfall Factor in the Universal Soil Loss Equation. *Assessment of Erosion*. De Boodt M., Gabriels D., (Eds.), Whey, Chichester, U.K., 127-132.
- Beasley, D.B., Huggins, L.F., 1981. *ANSWERS Users' Manual EPA-905/9-82-001*, US EPA, Chicago, Illinois, USA.
- Beskow, S., Mello, C.R., Norton, L.D., Curi, N., Viola, M.R., Avanzi, J.C., 2009. Soil erosion prediction in the Grande River Basin, Brasil using distributed modeling. *Catena*, 79, 49-59, USA.
- Berrisford, P., Dee, D.P., Fielding, K., Fuentes, M., Kallberg, P., Kobayashi, S., Uppala, S.M., 2009. The ERA-Interim Archive, ERA Report Series, 1, European Centre for Medium Range Weather Forecasts, UK.
- Bridges, E.M., Oldeman, L.R., 1999. Global assessment of human-induced soil degradation. *Arid Soil Research Rehabilitation* 13, 319-25.

- Blanco, H., Lal, R., 2008. Principles of Soil Conservation and Management. Springer, USA.
- Bogdanova, C., 1969. Seasonal Fluctuations in the Inflow and Distribution of the Mediterranean Waters in the Black Sea. Academy of Sciences, 131-139, Moscow, USRR.
- Büyükay, M., 1989. The Surface and Internal Oscillations in the Bosphorus Related to Meteorological Forces,. M Sc. Thesis, Middle East Technical University, Turkey.
- Chen, T., Niu, R., Li, P., Zhang, L., Du, B., 2010. Regional soil erosion risk mapping using RUSLE, GIS, and remote sensing: a case study in Miyun Watershed, North China. Environmental Earth Sciences, 63, 533-541.
- CORINE, 1992. Soil erosion risk and important land resources in the Southeastern Regions of the European Community, EUR 13233.
- Correa, S.W., Mello, C.R., Chou, S.C., Curi, N., Norton, L.D., 2016. Soil erosion risk associated with climate change at Mantaro River basin. Peruvian Andes, 110-124.
- Das, G., 2002. Hydrology and Soil Conservation Engineering Including Watershed Management, PHI Publishers, India.
- De Roo A.P.J., Jetten V.G., 1999. Calibrating and validating the LISEM model for two data sets from the Netherlands and South Africa. Catena, 37, 477-493.
- De Roo A.P J., 1996. The LISEM project: an introduction. Hydrological Processes, 10, 1021-1025.
- De Roo A.P.J., Offermans R.J.E., Cremers N., 1996. LISEM: a single-event, physically based hydrological and soil erosion model for drainage basins' sensitivity analysis, validation and application. Hydrological Processes, 10, 1119-1126.
- Evans, R., 1980. Mechanics of Water Erosion and Their Spatial and Temporal Controls: an Empirical Viewpoint. In Kirkby. M.J., Morgan, R.P.C. (Eds), Soil Erosion, Wiley Incorporation, 109.
- Gassman, P.W., Reyes M.R., Green C.H., Arnold J.G., 2007. The soil and water assessment tool:

historical development, applications, and future research directions. *Transactions of the ASABE*, 50: 1211-1250.

Gürkan, H., Arabacı, H., Demircan, M., Eskiöglu, O., Şensoy, S., Yazıcı, B., 2016. Temperature and precipitation projections based on GFDL-ESM2M using RCP4.5 and RCP8.5 scenarios for Turkey. *Coğrafi Bilimler Dergisi*, 14, 77-88.

Ferreira, V., Panagopoulos, T., 2014. Seasonality of soil erosion under Mediterranean conditions at the Alqueva dam watershed. *Environmental Management*, 54, 67–83.

Figueiredo, T., Poesen, J., 1998. Effect of surface rock fragment characteristics on interrill and erosion of the a silty loam soil. *Soil and Tillage Research*, 46, 81- 95.

Flanagan, D.C., Gilley, J.G., Franti, T.G., 2007. Water erosion prediction project (WEPP): development history, model capabilities, and future enhancements. *Transactions of the Asabe*, 50, 1603-1612.

Foster, G. R., 1990. Process-based modelling of soil erosion by water on agricultural land. In, J. Boardman, I.D.L., Foster J.A. (Eds.), *Dearings*, 429-445, New York, John Wiley and Sons Ltd.

Fournier, F., 1960. *Climat Et Erosion*, Ph.D. Thesis, Presses University, France.

Fox, D.M., Bryan, R.B., 1999. The relationship of soil loss by interrill erosion to slope gradient. *Catena*, 38, 211-222

Fu, B., Chen, L., Ma, K., Zhou, H., Wang, J., 2000. The relationships between land use and soil condition in the hilly area of the Loess Plateau in Northern Shaanxi, China. *Catena*, 39, 69-78.

Fu G., Chen S., McCool K.D., 2006. Modeling the impacts of no-till practice on soil erosion and sediment yield using RUSLE, SEDD and ArcView GIS. *Soil Tillage Research*, 85, 38–49.

Gaubı, I., Chaabani, A., Mammou, A., Hamza, M.H., 2016. A GIS-based soil erosion prediction using the revised universal soil loss equation (RUSLE) (Lebna watershed, Cap Bon, Tunisia). *Natural Hazards*, 219-239.

Ganasri B.P., Ramesh H., 2016. Assessment of soil erosion by RUSLE model using remote sensing and GIS: A case study of Nethravathi Basin. *Geoscience Frontiers*, 7, 953-961.

Grunwald, S., Frede, H.G., 1999. Using the modified agricultural non-point source pollution model in German watersheds. *Catena*, 37, 319-328.

Hirschi, M.C., Barfield B.J., 1988. KYEMO- A physically based research erosion model Part I: Model development. *American Society of Agricultural Engineers*, 31, 804-813.

ICONA, 1997. Guidelines for Mapping and Measurement of Rainfall-Induced Erosion Processes in the Mediterranean Coastal Areas, Priority Action Programme Regional Activity Centre, Split, Croatia.

Irvem, A., Topaloglu, F., Uygur, V., 2007. Estimating spatial distribution of soil loss over Seyhan River Basin in Turkey. *Journal of Hydrology*, 336, 30-37.

IPCC, 2001. *Climate Change 2001: The Scientific Basis*. Contribution of Working Group I to the Third Assessment Report of the Intergovernmental Panel on Climate Change, Houghton, J.T., Y. Ding, D.J., Griggs, M., Noguer, P.J., van der Linden, X., Maskell, D., K., Johnson, C.A. (Eds.), Cambridge University Press, Cambridge, United Kingdom and New York, USA, 881.

IPCC, 2007. *Climate Change 2007: The Physical Science Basis*, Contribution of Working Group I to the Fourth Assessment Report of the 111 Intergovernmental Panel on Climate Change, Solomon, S., Qin, M., Manning, M., Marquis, M., Averyt, K., Tignor, M. M. B., Miller, H. L., Chen, Z. (Eds.), Cambridge University Press, Cambridge, United Kingdom and New York, USA.

Iyigun, C., Türkeş, M., Batmaz, I., Yozgatligil, C., Puruçuoğlu, V., Koç, E., Öztürk, M., 2013. Clustering current climate regions of Turkey by using a multivariate statistical method. *Theoretical and Applied Climatology*, 114, 95-116.

Jasinski, M.F., 1990. Sensitivity of the normalized difference vegetation index to subpixel canopy cover, soil albedo, and pixel scale. *Remote Sensing of Environment*, 32, 169-187.

Jensen, J.R., 2000. *Remote Sensing of the Environment: An Earth Resource Perspective*, 77-98, Prentice Hall, New Jersey.

Jensen, J.R., 2005. *Introductory Digital Image Processing: a Remote Sensing Perspective*, 55-62, Prentice Hall, New Jersey.

Jinghu, P., Yan, W., 2014. Estimation of soil erosion using RUSLE in Caijiamiao watershed, China. *Natural Hazards*, 71, 2187-2205.

Kaya S., 2007. Multitemporal analysis of rapid urban growth in Istanbul using remotely sensing data. *Environmental Engineering Science*, 24, 228-233.

Kaya, S., Curran, P.J., 2006. Monitoring urban growth on the European side of the İstanbul metropolitan area: a case study. *International Journal of Applied Earth Observation and Geoinformation*, 8, 18-25.

Karamage, F., Zhang, C., Liu, T., Maganda, A., Isabwe, A., 2017. Soil Erosion Risk Assessment in Uganda. *Forests*, 8, 52.

Khare, D., Mondal, A., Kundu, S., Mishra, P.K., 2016. Climate change impact on soil erosion in the Mandakini River Basin, North India. *Applied Water Sciences*. 7, 2373-2383.

Kim, H.S., Julien, P.Y., 2006. Soil erosion modeling using RUSLE and GIS on the IMHA watershed. *Water Engineering Research*, 7, 1, 29-41.

Kinnel, P.I.A., 2005. Alternative approaches for determining the USLE-M slope length factor for grid cells. *Soil Science Society of America*, 69, 674-680.

Kirkby, M.J., Abrahart R., McMahon M.D., Shoa J., 1988. MEDALUS soil erosion models for global change. *Geomorphology*, 24, 35-39.

Knisel, W.G., 1980. *CREAMS: A Fieldscale Model for Chemical, Runoff, and Erosion from Agricultural Management Systems Conservation Report 26*, Science and Education Administration, USDA, Washington DC, USA.

Lal, R., 1998. Soil erosion impact on agronomic productivity and environment quality: critical reviews. *Plant Sciences*, 17, 319-464.

Langbein, W.B., Schumm, S.A., 1958. Yield of sediment in relation to mean annual precipitation. *Transactions of American Geophysical Union*, 39, 1076–1084.

Latocha, A., Szymanowski, M., Jeziorska, J., Stec, M., Roszczewska, M., 2016. Effects of land abandonment and climate change on soil erosion – an example from depopulated agricultural lands in the Sudetes Mts., SW Poland. *Catena*, 145, 128-141.

Leonard, R.A., Knisel, W.G., Still, D.A., 1987. GLEAMS: Groundwater loading effects of agricultural management systems. *American Society of Agricultural Engineers*, 30, 1403-1418.

Li, X., Zhang, X., Zhang, L., Wu, B., 2014. Rainfall and vegetation coupling index for soil erosion risk mapping. *Soil Water Conservation*, 69, 213-220.

Lu, H., Yu, B., 2002. Spatial and seasonal distribution of rainfall erosivity in Australia. *Australian Journal of Soil Research*, 40, 887-901.

Martinez, C.J.A., Sanchez, B.I., 2000. Impact assessment of changes in land use/conservation practices on soil erosion in the Penedes-Anoia vineyard region (NE Spain). *Soil Tillage Research*, 57, 101-106.

Millward, A.A., Mersey J.E., 1999. Adapting the RUSLE to model soil erosion potential in a mountainous tropical watershed. *Catena*, 38, 109-129.

Minkowski, M., 2007. Advanced GeoWEPP Tools. <http://www.geog.buffalo.edu/renschen/geowepp/documents>. Date accessed May 2019.

Mondal, A., Khare, D., Kundu, S., Mukherjee, S., Mukhopadhyay, A., Mondal, S., 2015. Uncertainty of soil erosion modelling using open source high resolution and aggregated DEMs. *Geoscience Frontiers*, 8, 425-436.

Morgan, R.P.C., 1991. *Soil Erosion and Conservation*, Longman Scientific and Technical, John Wiley and Sons Inc., New York, 255.

Moss, R.H., Edmonds, J.A., Hibbard, K.A., Manning, M.R., Rose, S.K., Vuuren, D.P., Carter, T.R., Emori, S., Kainuma, M., Kram, T., 2010. The next generation of scenarios for climate change research and assessment. *Nature*, 463, 747–756.

Nearing, M.A., Brandford, J.M., Holtz, R.D., 1987. Measurement of waterdrop impact pressures on soil surfaces. *Soil Science Society of America Journal*, 51, 1302-1306.

Nearing, M.A., Foster, G.R., Lane, L.J., Finkner, S.C., 1989. A process-based soil-erosion model for USDA-water erosion prediction project technology. *American Society of Agricultural*, 32, 1587-1593.

Nearing, M.A., Xie, Y., Liu, B., Ye, Y., 2017. Natural and antropogenic rates of soil erosion. *International Soil and Water Conservation Research*, 5, 77-84.

Oliveira, A.H., Aparecida, M., Silva, M.L.N., Curi, N., Neta, G.K., França, D.A., 2013. Development of topographic factor modeling for application in soil erosion models in soil processes and current trends in quality assessment. In Soriano, M.C.H. (Eds), *InTech*, 111-138, New York, U.S.A.

Ozsoy, G., Aksoy, E., Dirim, M.S., Tumsavas, Z., 2012. Determination os soil erosion risk in the Mustafakemalpaşa River Basin, Turkey, using the Revised Universal Soil Loss equation, geographical information system, and remote sensing. *Environmental Management*, 50, 679-694.

Özşahin, E., Uygur, V., 2014. The effects of land use and land cover changes (LULCC) in Kuseyr plateau of Turkey on erosion. *Turk Journal of Agriculture Forestry*, 38, 478-487.

United States Department of Agriculture, Agricultural Research Service, 1997. *Predicting Soil Erosion by Water. A Guide to Conservation Planning with the Revised Universal Soil Loss Equation (RUSLE)*, Agricultural Handbook 703, U.S.A.

Pruski, E.E., Nearing, M.A., 2002a. Climate-induced changes in erosion during the 21st century for eight U.S. locations. *Water Resources Research*, 38, 12-25.

Pruski, E.E., Nearing, M.A., 2002b. Runoff and soil loss responses to changes in precipitation: a computer simulation study. *Journal of Soil and Water Conservation*, 57, 7-16

Rango, A., Arnoldus, H.M.J., 1987. *Amenagement des bassins versants*, Cahiers techniques de la FAO.

Renard, K.G., Foster, G.A., Weesies, G.A., McCool, D.K., 1997. *Predicting soil erosion by water: a guide to conservation planning with RUSLE*, USDA, Agriculture Handbook No.703, Washington, DC.

Renard, K.G., Freimund, J.R., 1994. Using monthly precipitation data to estimate the R factor in the revised USLE. *Journal of Hydrology*, 157, 287-306.

Richter, G., Negendank, J.F.W., 1977. Soil Erosion Processes and Their Measurement in the German Area of the Moselle River. *Earth Surface Process*, 2, 261-278.

Rozos, D., Skilodimou, H.D., Loupasakis, C., Bathrellos, G.D., 2013. Application of the revised universal soil loss equation model on landslide prevention: an example from Euboea (Evia) Island, Greece. *Environmental Earth Sciences*, 70, 3255-3266.

Römken, M.J.M., Helming, K., Prasad, S.N., 2001. Soil erosion under different rainfall intensities, surface roughness, and soil water regimes, *Catena* 46, 103-123.

Rudra, R., Dickinson, W., Clark, D., Wall, G., 1986. GAMES-A screening model of soil erosion and fluvial sedimentation on agricultural watershed. *Canadian Water Resources Journal*, 11, 58-71.

Ruhe, R.V., 1969. *Quarternary landscapes in Iowa*, Iowa State University Press, Ames, Iowa.

Ruhe, R.V., Daniels, R.B., 1965. Landscapes erosion: geologic and historic. *Journal of Soil and Water Conservation*, 20, 52-57.

Schmidt, J., M., Werner A., 1999. Application of the EROSION 3D model to the CATSOP watershed, The Netherlands. *Catena*, 37, 449-456.

Sen, Z., Habib, Z., 2001a. Monthly spatial rainfall correlation functions and interpretations for Turkey. *Hydrology Science Journal*, 46, 525–535.

Sen, Z., Habib, Z., 2001b. Spatial rainfall pattern identification by optimum interpolation technique

and application for Turkey. *Hydrological Sciences*, 32, 85–98.

Sheikh, A., Palria H.S., Alam, A., 2011. Integration of GIS and universal soil loss equation (USLE) for soil loss estimation in a Himalayan watershed. *Recent Research Science and Technology*, 3, 51-57.

Singer M.J., Warkentin B. P., 1996. Soils in an environmental context: an American perspective. *Catena*, 27, 179-189.

Stocking, M.A., Elwell H.A., 1973. Soil erosion hazard in Rhodesia. *Rhodesia Agricultural Journal* 70, 93–101.

Stocking, M.A., Elwell, H.A., 1976. Rainfall erosivity over Rhodesia. *The Institute of British Geographers*, 1, 231-245.

Tağıl, Ş., 2007. Tuzla Çayı havzasında (Biga Yarımadası) CBS-Tabanlı RUSLE modeli kullanarak arazi degradasyonu risk değerlendirmesi. *Ekoloji*, 17, 65, 11-20

Tayanç, M., Dalfes, N., Karaca, M., Yenigün, O., 1998. A comparative assessment of different methods for detecting inhomogeneities in Turkish temperature data set. *International Journal of Climatology*, 18, 561–578.

Tang, Q., Xu, Y., Bennett, S.J., Li, Y., 2015. Assessment of soil erosion using RUSLE and GIS: a case study of the Yangou watershed in the Loess Plateau, China. *Environmental Earth Sciences*, 73, 1715 – 1724.

Thornbury, W.D., 1965. Regional geomorphology of the United States. *Soil Sciences*, 100, 148.

Turp T., Öztürk T., Türkeş M., Kurnaz L., 2014. Investigation of projected changes for near future air temperature and precipitation climatology of Turkey and surrounding regions by using the regional climate model RegCM4.3.5.

Türkeş, M., Tatlı, H., 2011. Use of the spectral clustering to determine coherent precipitation regions in Turkey for the period 1929– 2007. *International Journal of Climatology*, 31, 2055–2067.

US Army Corps of Engineers (USACE), 1977. Storage, treatment, overflow, runoff model "STORM": users' manual, report CPD-7. Hydrologic Engineering Center, Davis, CA, USA.

Vitousek, P., Mooney, H., Lubchenco, J., Melillo, J., 1997. Human domination of Earth's ecosystems. *Science, New Series*, 277, 494-499.

Voroney, R.P., van Venn, J.A., Paul, E.A., 1981. Organic carbon dynamics in crassland soil II. model validation and simulation of the long-terms effects of cultivation and rainfall erosion. *Canada Journal of Soil Science*, 61, 24, 211.

Vuuren, D.P., Edmonds, J., Kainuma, M., Riahi, K., Thompson, A., Hibbard, K., Hurtt, G.C., Kram, T., Krey, V., Lamarque, J.F., Masui, T., Meinshausen, M., Nakicenovic, N., Smith, S.J., Rose, S.K., 2011. The representative concentration pathways: an overview. *Climate Change*, 109, 5-31.

Yang, D., Kanae, S., Oki, T., Koike, T., Musiak, K., 2003. Global potential soil erosion with reference to land use and climate changes. *Hydrology Process*, 17, 2913- 2928.

Young, R.A., 1986. Agricultural nonpoint source pollution model: A watershed analysis tool, Conservation Report 35, Agricultural Research Service, USDA, Morris, Minnesota, USA.

Zhang, X., Zeng, Y., Yan, N., Yuan, C., 2010. Identification of priority areas for controlling soil erosion. *Catena*, 83, 76-86.

Wang, G., Gertner, G., Fang, S., Anderson, A.B., 2003. Mapping multiple variables for predicting soil loss by geostatistical methods with TM images and a slope map. *Photogrammetric Engineering and Remote Sensing*, 69, 889-898.

Williams, J.R., Renard, K.G., Dyke, P.T., 1983. Epic - a New Method for Assessing Erosions Effect on Soil Productivity. *Soil and Water Conservation*, 38, 381-383.

Wischmeier, W.H., Smith D.D., 1978. Predicting rainfall erosion losses-a guide to conservation planning, Agriculture Handbook, No 537. US Department of Agriculture Science and Education Administration, Washington, 163.

Witinok, P.M., 1988. A critical examination of the universal soil loss equation (USLE). *Geographical Perspectives*, 62, 25-54.

Woodward, D.E., 1999. Method to predict cropland ephemeral gully erosion. *Catena*, 37, 393-399

Woolhiser, D.A., Smith, R.E., Goodrich, D.C., 1990. KINEROS, a kinematic runoff and erosion model: documentation and user manual, report ARS77, Agricultural Research Service, USDA, Minnesota, US.



APPENDIX A: FAO SOIL UNITS (DSMW)

J	FLUVISOLS	Q	ARENOSOLS	Z	SOLONCHAKS	K	KASTANOZEMS
Je	Eutric Fluvisols	Qe	Cambic Arenosols	Zo	Orthic Solonchaks	Kh	Haplic Kastanozems
Jc	Calcaric Fluvisols	Ql	Luvic Arenosols	Zm	Mollic Solonchaks	Kk	Calcaric Kastanozems
Jd	Dystric Fluvisols	Qf	Ferralic Arenosols	Zt	Takyrlic Solonchaks	Kl	Luvic Kastanozems
Jt	Thionic Fluvisols	Qa	Albic Arenosols	Zg	Gleyic Solonchaks		
G	GLEYSOLS	E	RENDZINAS	S	SOLONETZ	C	CHERNOZEMS
Ge	Eutric Gleysols			So	Orthic Solonetz	Ch	Haplic Chernozems
Gc	Calcaric Gleysols			Sm	Mollic Solonetz	Ck	Calcaric Chernozems
Gd	Dystric Gleysols	U	RANKERS	Sg	Gleyic Solonetz	Cl	Luvic Chernozems
Gm	Mollic Gleysols					Cg	Glossic Chernozems
Gh	Humic Gleysols						
Gp	Plinthic Gleysols	T	ANDOSOLS	Y	YERMOSOLS	H	PHAEZEMS
Gx	Gelic Gleysols	To	Ochric Andosols	Yh	Haplic Yermosols	Hh	Haplic Phaeozems
		Tm	Mollic Andosols	Yk	Calcaric Yermosols	Hc	Calcaric Phaeozems
R	REGOSOLS	Th	Humic Andosols	Yy	Gypsic Yermosols	Hi	Luvic Phaeozems
Re	Eutric Regosols	Tv	Vitric Andosols	Yl	Luvic Yermosols	Hg	Gleyic Phaeozems
Rc	Calcaric Regosols			Yt	Takyrlic Yermosols		
Rd	Dystric Regosols	V	VERTISOLS				
Rx	Gelic Regosols	Vp	Pellic Vertisols	X	XEROSOLS	M	GREYZEMS
		Ve	Chromic Vertisols	Xh	Haplic Xerosols	Mo	Orthic Greyzems
I	LITHOSOLS			Xk	Calcaric Xerosols	Mg	Gleyic Greyzems
				Xy	Gypsic Xerosols		
				Xl	Luvic Xerosols		

Figure A.1. The abbreviations of FAO Soil Units (DSMW), Part 1.

B	CAMBISOLS	D	PODZOLUVISOLS	A	ACRISOLS	O	HISTOSOLS
Be	Eutric Cambisols	De	Eutric Podzoluvisols	Ao	Orthic Acrisols	Oe	Eutric Histosols
Bd	Dystric Cambisols	Dd	Dystric Podzoluvisols	Af	Ferric Acrisols	Od	Dystric Histosols
Bh	Humic Cambisols	Dg	Gleyic Podzoluvisols	Ah	Humic Acrisols	Ox	Gelic Histosols
Bg	Gleyic Cambisols			Ap	Plinthic Acrisols		
Bx	Gelic Cambisols			Ag	Gleyic Acrisols		
Bk	Calcic Cambisols	P	PODZOLS				
Bc	Chromic Cambisols						
Bv	Vertic Cambisols	Po	Orthic Podzols	N	NITOSOLS		
Bf	Ferralic Cambisols	Pl	Leptic Podzols	Ne	Eutric Nitosols		
		Pf	Ferric Podzols	Nd	Dystric Nitosols		
		Ph	Humic Podzols	Nh	Humic Nitosols		
		Pp	Placic Podzols				
L	LUVISOLS	Pg	Gleyic Podzols				
				F	FERRALSOLS		
Lo	Orthic Luvisols	W	PLANOSOLS	Fo	Orthic Ferralsols		
Lc	Chromic Luvisols			Fx	Xanthic Ferralsols		
Lk	Calcic Luvisols	We	Eutric Planosols	Fr	Rhodic Ferralsols		
Lv	Vertic Luvisols	Wd	Dystric Planosols	Fh	Humic Ferralsols		
Lf	Ferric Luvisols	Wm	Mollic Planosols	Fa	Acric Ferralsols		
La	Albic Luvisols	Wh	Humic Planosols	Fp	Plinthic Ferralsols		
Lp	Plinthic Luvisols	Ws	Solodic Planosols				
Lg	Gleyic Luvisols	Wx	Gelic Planosols				

Figure A.2. The abbreviations of FAO Soil Units (DSMW), Part 2.

APPENDIX B: THE FAO SOIL UNITS FOR TURKEY (DSMW)

Table B.1. The Soil Unit List for Turkey of FAO Soil (DSMW).

FID	SNUM	FAOSOIL	DOMSOI	CNTCODE	CNTNAME	SQKM	COUNTRY	X	Y
7922	3185	Lc104-2/3bc	Lc	223	TU	3293	TURKEY	27	42
7927	3027	Bk49-2c	Bk	223	TU	20057	TURKEY	37	41
7939	3003	Ao111-2bc	Ao	223	TU	14013	TURKEY	33	41
7947	3188	Lc105-2/3ab	Lc	223	TU	11	TURKEY	28	42
7975	6660	Lc105-2/3ab	Lc	223	TU	7221	TURKEY	27	41
8002	3283	Vp72-3a	Vp	223	TU	4423	TURKEY	27	41
8012	3168	Kh35-2ab	Kh	223	TU	2365	TURKEY	34	42
8031	3026	Bk45-2bc	Bk	223	TU	1021	TURKEY	32	41
8038	3090	I-Be-2c	I	223	TU	227	TURKEY	43	42
8044	3016	Be122-2bc	Be	223	TU	8659	TURKEY	34	41
8053	3120	I-Rc-Xk-2c	I	223	TU	12	TURKEY	42	42

8055	3089	I-Bd-2c	I	223	TU	973	TURKEY	42	41
8056	3090	I-Be-2c	I	223	TU	20	TURKEY	43	41
8059	3004	Ao112-2bc	Ao	223	TU	18945	TURKEY	39	41
8060	3096	I-Bh-U-2c	I	223	TU	1505	TURKEY	43	41
8062	3026	Bk45-2bc	Bk	223	TU	14713	TURKEY	32	41
8065	3090	I-Be-2c	I	223	TU	202	TURKEY	42	41
8079	3028	Bk49-2c	Bk	223	TU	1675	TURKEY	42	41
8084	3093	I-Be-c	I	223	TU	20317	TURKEY	42	40
8101	3090	I-Be-2c	I	223	TU	81	TURKEY	43	41
8107	3282	Vp68-3a	Vp	223	TU	28	TURKEY	26	41
8126	3157	Kh1-2ab	Kh	223	TU	983	TURKEY	43	41
8129	3140	Jc49-1/3a	Jc	223	TU	1096	TURKEY	26	41
8133	6494	E23-2bc	E	223	TU	1119	TURKEY	29	41
8139	3206	Lo85-2b	Lo	223	TU	1525	TURKEY	27	41
8144	3188	Lc105-2/3ab	Lc	223	TU	6815	TURKEY	30	41
8151	3098	I-Bh-U-c	I	223	TU	6772	TURKEY	40	41
8157	3168	Kh35-2ab	Kh	223	TU	2500	TURKEY	36	41
8158	3206	Lo85-2b	Lo	223	TU	1003	TURKEY	28	41
8162	3185	Lc104-2/3bc	Lc	223	TU	4197	TURKEY	27	41
8174	3026	Bk45-2bc	Bk	223	TU	4298	TURKEY	35	41
8185	6997	WAT	WR	223	TU	116	TURKEY	43	41
8207	3157	Kh1-2ab	Kh	223	TU	1789	TURKEY	42	41
8217	3157	Kh1-2ab	Kh	223	TU	2768	TURKEY	43	41
8220	3098	I-Bh-U-c	I	223	TU	508	TURKEY	42	41
8227	3139	Jc49-1/3a	Jc	223	TU	1500	TURKEY	30	41
8232	3121	I-Rc-Xk-2c	I	223	TU	5229	TURKEY	34	40
8240	3026	Bk45-2bc	Bk	223	TU	858	TURKEY	36	41
8244	3310	Xk56-2/3ab	Xk	223	TU	86183	TURKEY	34	39
8249	3208	Lo91-2bc	Lo	223	TU	8151	TURKEY	32	41
8266	3157	Kh1-2ab	Kh	223	TU	3691	TURKEY	41	40
8272	3208	Lo91-2bc	Lo	223	TU	4338	TURKEY	30	41
8277	3121	I-Rc-Xk-2c	I	223	TU	950	TURKEY	35	40
8286	3016	Be122-2bc	Be	223	TU	6303	TURKEY	36	40
8287	3208	Lo91-2bc	Lo	223	TU	108	TURKEY	28	41
8318	3208	Lo91-2bc	Lo	223	TU	294	TURKEY	28	40
8326	6997	WAT	WR	223	TU	272	TURKEY	30	40
8330	3121	I-Rc-Xk-2c	I	223	TU	8975	TURKEY	36	40
8340	3016	Be122-2bc	Be	223	TU	2632	TURKEY	27	40
8342	3027	Bk49-2c	Bk	223	TU	2315	TURKEY	30	40
8353	3027	Bk49-2c	Bk	223	TU	601	TURKEY	27	40
8354	3016	Be122-2bc	Be	223	TU	9074	TURKEY	30	40
8357	3281	Vc62-3a	Vc	223	TU	1111	TURKEY	28	40
8359	3139	Jc49-1/3a	Jc	223	TU	356	TURKEY	27	40
8362	3157	Kh1-2ab	Kh	223	TU	9875	TURKEY	42	40
8364	3100	I-Bk-Kk-2bc	I	223	TU	2106	TURKEY	39	40
8367	3208	Lo91-2bc	Lo	223	TU	2669	TURKEY	27	40
8372	3173	Kk19-2/3b	Kk	223	TU	1466	TURKEY	39	40
8385	3139	Jc49-1/3a	Jc	223	TU	1040	TURKEY	28	40
8388	3208	Lo91-2bc	Lo	223	TU	15597	TURKEY	28	40
8392	6997	WAT	WR	223	TU	154	TURKEY	28	40
8395	3089	I-Bd-2c	I	223	TU	261	TURKEY	26	40
8399	6997	WAT	WR	223	TU	140	TURKEY	29	40
8417	3093	I-Be-c	I	223	TU	7789	TURKEY	43	40

8418	3114	I-Lc-E-2bc	I	223	TU	488	TURKEY	28	40
8420	3026	Bk45-2bc	Bk	223	TU	28438	TURKEY	30	39
8422	3016	Be122-2bc	Be	223	TU	529	TURKEY	26	40
8427	3208	Lo91-2bc	Lo	223	TU	1058	TURKEY	26	40
8436	3307	Xk53-2/3bc	Xk	223	TU	23619	TURKEY	37	39
8437	3288	Xh31-3a	Xh	223	TU	151	TURKEY	45	40
8440	3129	I-Re-Yh-c	I	223	TU	566	TURKEY	44	40
8442	3157	Kh1-2ab	Kh	223	TU	5898	TURKEY	43	40
8446	3306	Xk52-2/3b	Xk	223	TU	3861	TURKEY	37	40
8460	3026	Bk45-2bc	Bk	223	TU	3604	TURKEY	36	40
8461	3027	Bk49-2c	Bk	223	TU	776	TURKEY	26	40
8470	3319	Xl24-2bc	Xl	223	TU	911	TURKEY	34	40
8474	3122	I-Rc-Xk-c	I	223	TU	27347	TURKEY	43	38
8478	3311	Xk59-2/3a	Xk	223	TU	551	TURKEY	31	40
8479	3200	Lo64-3c	Lo	223	TU	18061	TURKEY	39	39
8480	3013	Be115-2/3c	Be	223	TU	10669	TURKEY	41	39
8490	3016	Be122-2bc	Be	223	TU	3526	TURKEY	30	40
8500	3320	Xl24-2bc	Xl	223	TU	1209	TURKEY	35	40
8506	3129	I-Re-Yh-c	I	223	TU	13	TURKEY	45	40
8514	3114	I-Lc-E-2bc	I	223	TU	894	TURKEY	28	40
8520	3121	I-Rc-Xk-2c	I	223	TU	333	TURKEY	34	40
8530	3139	Jc49-1/3a	Jc	223	TU	278	TURKEY	27	40
8533	3093	I-Be-c	I	223	TU	2172	TURKEY	39	39
8538	3093	I-Be-c	I	223	TU	2090	TURKEY	41	39
8558	3288	Xh31-3a	Xh	223	TU	124	TURKEY	44	39
8561	3169	Kk16-2b	Kk	223	TU	15943	TURKEY	43	39
8562	3319	Xl24-2bc	Xl	223	TU	330	TURKEY	34	39
8564	3114	I-Lc-E-2bc	I	223	TU	447	TURKEY	27	39
8577	3114	I-Lc-E-2bc	I	223	TU	6287	TURKEY	28	39
8598	3093	I-Be-c	I	223	TU	1508	TURKEY	38	39
8605	3208	Lo91-2bc	Lo	223	TU	737	TURKEY	31	39
8633	3139	Jc49-1/3a	Jc	223	TU	676	TURKEY	27	39
8647	6997	WAT	WR	223	TU	1664	TURKEY	33	39
8649	3208	Lo91-2bc	Lo	223	TU	1774	TURKEY	27	39
8659	3016	Be122-2bc	Be	223	TU	832	TURKEY	30	39
8666	3311	Xk59-2/3a	Xk	223	TU	3638	TURKEY	33	39
8668	3319	Xl24-2bc	Xl	223	TU	898	TURKEY	34	39
8674	3122	I-Rc-Xk-c	I	223	TU	1018	TURKEY	43	39
8675	3311	Xk59-2/3a	Xk	223	TU	2087	TURKEY	31	39
8680	3139	Jc49-1/3a	Jc	223	TU	3592	TURKEY	28	39
8681	3310	Xk56-2/3ab	Xk	223	TU	969	TURKEY	31	39
8684	3093	I-Be-c	I	223	TU	657	TURKEY	36	39
8688	3121	I-Rc-Xk-2c	I	223	TU	2358	TURKEY	32	39
8694	3288	Xh31-3a	Xh	223	TU	2372	TURKEY	42	39
8701	6997	WAT	WR	223	TU	3699	TURKEY	43	39
8704	3308	Xk54-3ab	Xk	223	TU	3372	TURKEY	38	38
8705	3295	Xh47-2ab	Xh	223	TU	3379	TURKEY	36	38
8708	3016	Be122-2bc	Be	223	TU	8256	TURKEY	28	38
8727	3320	Xl24-2bc	Xl	223	TU	1326	TURKEY	30	39
8735	3261	Re87-1bc	Re	223	TU	1972	TURKEY	35	39
8737	3093	I-Be-c	I	223	TU	29412	TURKEY	39	38
8740	3122	I-Rc-Xk-c	I	223	TU	377	TURKEY	42	39
8750	6997	WAT	WR	223	TU	139	TURKEY	38	39

8752	3093	I-Be-c	I	223	TU	4323	TURKEY	36	38
8755	3308	Xk54-3ab	Xk	223	TU	922	TURKEY	40	39
8757	6997	WAT	WR	223	TU	101	TURKEY	31	39
8758	6997	WAT	WR	223	TU	92	TURKEY	44	39
8761	3310	Xk56-2/3ab	Xk	223	TU	756	TURKEY	31	39
8762	3114	I-Lc-E-2bc	I	223	TU	4114	TURKEY	27	38
8766	3093	I-Be-c	I	223	TU	380	TURKEY	35	39
8768	3308	Xk54-3ab	Xk	223	TU	3436	TURKEY	37	38
8774	3319	Xl24-2bc	Xl	223	TU	1128	TURKEY	34	38
8777	6997	WAT	WR	223	TU	91	TURKEY	31	39
8778	3016	Be122-2bc	Be	223	TU	1392	TURKEY	31	38
8786	3114	I-Lc-E-2bc	I	223	TU	1547	TURKEY	31	38
8787	6997	WAT	WR	223	TU	63	TURKEY	39	38
8794	3026	Bk45-2bc	Bk	223	TU	5681	TURKEY	32	38
8797	3325	Zg15-3a	Zg	223	TU	673	TURKEY	35	38
8813	3191	Lc63-3bc	Lc	223	TU	26043	TURKEY	40	38
8815	3139	Jc49-1/3a	Jc	223	TU	1191	TURKEY	30	38
8829	3139	Jc49-1/3a	Jc	223	TU	1512	TURKEY	28	38
8832	6997	WAT	WR	223	TU	467	TURKEY	31	38
8835	3121	I-Rc-Xk-2c	I	223	TU	1082	TURKEY	33	38
8837	3013	Be115-2/3c	Be	223	TU	5110	TURKEY	36	38
8838	3114	I-Lc-E-2bc	I	223	TU	2654	TURKEY	29	38
8844	3309	Xk55-3ab	Xk	223	TU	21970	TURKEY	39	37
8854	3310	Xk56-2/3ab	Xk	223	TU	1104	TURKEY	30	38
8860	3114	I-Lc-E-2bc	I	223	TU	956	TURKEY	27	38
8861	3311	Xk59-2/3a	Xk	223	TU	3882	TURKEY	33	38
8862	3114	I-Lc-E-2bc	I	223	TU	5733	TURKEY	31	37
8863	3504	I-Be-E-c	I	223	TU	24951	TURKEY	34	37
8875	3139	Jc49-1/3a	Jc	223	TU	2876	TURKEY	28	38
8887	3114	I-Lc-E-2bc	I	223	TU	822	TURKEY	30	38
8898	3280	Vc56-3a	Vc	223	TU	2868	TURKEY	37	38
8904	6997	WAT	WR	223	TU	688	TURKEY	32	38
8916	3016	Be122-2bc	Be	223	TU	11220	TURKEY	28	37
8918	6997	WAT	WR	223	TU	151	TURKEY	30	38
8919	3208	Lo91-2bc	Lo	223	TU	1386	TURKEY	32	38
8928	3139	Jc49-1/3a	Jc	223	TU	770	TURKEY	30	38
8932	3122	I-Rc-Xk-c	I	223	TU	580	TURKEY	40	38
8935	6997	WAT	WR	223	TU	215	TURKEY	30	38
8938	6659	Bk49-2c	Bk	223	TU	3473	TURKEY	31	37
8945	3289	Xh33-3a	Xh	223	TU	14	TURKEY	45	38
8946	3139	Jc49-1/3a	Jc	223	TU	751	TURKEY	32	37
8949	3016	Be122-2bc	Be	223	TU	1479	TURKEY	30	37
8952	3114	I-Lc-E-2bc	I	223	TU	1746	TURKEY	31	37
8958	3325	Zg15-3a	Zg	223	TU	678	TURKEY	34	38
8959	3016	Be122-2bc	Be	223	TU	1029	TURKEY	32	37
8961	3114	I-Lc-E-2bc	I	223	TU	5262	TURKEY	28	37
8969	3193	Lc76-3b	Lc	223	TU	2558	TURKEY	35	37
8978	3276	Vc1-3a	Vc	223	TU	1231	TURKEY	42	37
8982	3504	I-Be-E-c	I	223	TU	344	TURKEY	33	37
8983	3280	Vc56-3a	Vc	223	TU	7096	TURKEY	35	37
8984	6997	WAT	WR	223	TU	63	TURKEY	27	38
8996	3122	I-Rc-Xk-c	I	223	TU	2662	TURKEY	41	37
9020	6997	WAT	WR	223	TU	112	TURKEY	32	37

9027	3279	Vc50-3ab	Vc	223	TU	155	TURKEY	43	37
9030	3289	Xh33-3a	Xh	223	TU	68	TURKEY	45	37
9033	3093	I-Be-c	I	223	TU	0	TURKEY	43	37
9047	6997	WAT	WR	223	TU	200	TURKEY	35	37
9049	3298	Xk26-2/3a	Xk	223	TU	2992	TURKEY	40	37
9051	3114	I-Lc-E-2bc	I	223	TU	8347	TURKEY	30	37
9070	3277	Vc47-3b	Vc	223	TU	189	TURKEY	42	37
9074	3016	Be122-2bc	Be	223	TU	2465	TURKEY	31	37
9075	3108	I-E-Xk-bc	I	223	TU	35	TURKEY	42	37
9079	3137	Jc36-2/3a	Jc	223	TU	453	TURKEY	38	37
9088	3139	Jc49-1/3a	Jc	223	TU	752	TURKEY	31	37
	3093	I-Be-c	I	223	TU	4951	TURKEY	32	37
9107	6997	WAT	WR	223	TU	61	TURKEY	30	37
9109	3192	Lc69-3a	Lc	223	TU	1611	TURKEY	37	37
9116	3280	Vc56-3a	Vc	223	TU	2401	TURKEY	36	36
9123	3312	Xk9-2/3a	Xk	223	TU	1209	TURKEY	39	37
9133	3322	Xy4-2/3a	Xy	223	TU	324	TURKEY	40	37
9137	3133	I-Xk-2c	I	223	TU	132	TURKEY	38	37
9140	3280	Vc56-3a	Vc	223	TU	870	TURKEY	32	37
9146	6997	WAT	WR	223	TU	68	TURKEY	29	37
9151	3139	Jc49-1/3a	Jc	223	TU	719	TURKEY	30	37
9159	3299	Xk27-2ab	Xk	223	TU	414	TURKEY	39	37
9171	3299	Xk27-2ab	Xk	223	TU	7	TURKEY	38	37
9188	3299	Xk27-2ab	Xk	223	TU	230	TURKEY	38	37
9193	3114	I-Lc-E-2bc	I	223	TU	782	TURKEY	30	37
9212	3191	Lc63-3bc	Lc	223	TU	116	TURKEY	37	37
9275	3001	Ao102-2c	Ao	223	TU	2860	TURKEY	33	36
9283	6997	WAT	WR	223	TU	83	TURKEY	36	36
9298	3191	Lc63-3bc	Lc	223	TU	58	TURKEY	37	36
9320	3191	Lc63-3bc	Lc	223	TU	777	TURKEY	36	36
9384	3563	Vp39-3b	Vp	223	TU	74	TURKEY	36	36

APPENDIX C: THE SOIL CONTENT PROPERTIES OF FAO SOIL (DSMW)

Table C.1. The Soil Content Properties of FAO Soil (DSMW).

Soil unit symbol	sand % topsoil	sand % subsoil	silt% topsoil	silt% subsoil	clay % topsoil	clay % subsoil	pH water topsoil	pH water subsoil	OC % topsoil	OC % subsoil
A	53,3	44,3	17,2	17,1	29,5	38,6	5,2	5,2	1,74	0,63
AF	61,7	52,5	14,4	12,9	23,9	34,6	5,4	5,3	0,91	0,34
AF 1	81,1	75,5	8,7	8,9	10,2	15,6	5,7	5,5	0,35	0,2
AF 2	61,7	44,5	14,3	10,8	24	44,7	5,1	5,2	1,05	0,37
AF 3	21,3	13,1	25,7	24,4	52,9	62,3	5	4,9	1,85	0,58
AG	40,9	36,8	27,2	29,7	32,1	33,4	5,1	4,9	2,26	0,34
AG 1	89,3	72,5	7,2	9,5	3,5	17,9	5,5	5,1	0,5	0,16
AG 2	9,6	15,8	75,2	64,7	15,3	19,6	4,4	4,2	3,07	0,25
AG 3	35,2	32	17,9	24,8	47,2	43,2	5,2	5,1	1,99	0,38
AH	31,3	27,1	24,8	25,1	43,8	47,8	5	5,4	3,34	1,49

AH 1	72,8	71,9	14,6	10,6	12,6	17,4	5	5	1,58	0,9
AH 2	52,4	45,4	27,9	33	19,6	21,5	5,1	5,7	4,46	1,95
AH 3	9,2	7,4	26,1	22,2	64,8	70,4	5	5,3	2,88	1,25
AO	53,6	43,4	15,8	16	30,6	40,6	5,1	5,2	2,25	0,75
AO 1	82,3	68,1	8,6	11,4	9,2	20,5	5	5,1	0,3	0,21
AO 2	51	41,3	21,6	17,2	27,4	41,5	5,3	5	1,73	0,73
AO 3	33	28,9	14,2	15,5	52,9	55,6	5,2	5,4	1,84	0,89
AP	57	46,2	15,6	17,1	27,1	36,8	5,3	5	1,09	0,26
AP 1	80	65,1	12	14,6	7,8	20,3	5,6	5	0,69	0,2
AP 2	58,7	45,4	16,3	17,4	25	37,1	5,8	5,6	0,87	0,29
AP 3	10,4	8,8	22,7	22	66,7	69,6	4,5	4,6	2,91	0,49
B	60,4	60	17	16,6	22,5	23,4	6,9	7,2	1,17	0,57
BC	40,1	41,8	21,5	22,7	38,4	35,5	5,7	5,8	1,44	0,74
BC 1	80	60	10	25	10	15	5,6	5,7	1	0,5
BC 2	56,7	56,8	23,6	20,6	19,8	22,5	5,8	5,9	1,22	0,61
BC 3	15,3	19,3	18,5	25,7	66,3	55	5,6	5,6	1,77	0,93
BD	32,7	29,8	30,3	37,6	37,1	32,3	4,9	5,3	3,28	0,87
BD 1	70	65	20	20	10	15	4,8	5,2	3	1
BD 2	39,9	38,2	34,1	38,4	26	22,7	5,4	5,8	4,26	1,33
BD 3	27,8	24,2	27,8	37	44,4	38,8	4,6	5	2,62	0,57
BE	36,4	41,7	37,2	32,1	26,4	26,3	6,9	7,1	1,07	0,51
BE 1	84,5	78,3	6,1	7,6	10,4	15,4	6,7	6,6	0,2	0,2
BE 2	36,4	40,4	41,1	35,2	22,5	24,4	6,9	7	1,26	0,56
BE 3	18,8	22,7	35,7	35,5	45,4	41,6	7,1	7,4	0,68	0,25
BF	34,2	31,5	15,5	18,7	50,2	50	5	5,2	2,76	0,72
BF 1	82,2	89,5	10	8,3	8	3,2	4,6	4,8	2	0,75
BF 2	60	50	12	14	28	36	4,9	5	2,5	0,75
BF 3	22,3	17	16,9	21,3	60,7	61,7	5,1	5,2	3,22	0,75
BG	34,2	35,3	20,4	16,1	45,4	48,4	5,9	5,8	1,82	1,31
BG 1	78,9	76,4	8,2	7,2	12,4	15,6	4,9	4,9	0,9	0,21
BG 2	71,3	75,5	3,7	2,3	25	22,2	7,4	7,6	0,18	0,1
BG 3	6,9	8,3	30	23,7	63,1	68,1	5,8	5,5	2,68	2,09
BH	55,2	60,4	21	16,5	23,8	23,2	5,3	5,8	3,86	1,78
BH 1	82,5	81,1	6,1	2,9	11,6	16,1	5,7	7	0,95	0,25
BH 2	54,2	53,4	25,7	21,1	20,1	25,6	5,2	5,5	5,11	2,52
BH 3	35	34	35	30	30	36	5,7	5,6	3,45	1,12
BK	81,6	81,6	6,8	6,7	11,7	11,8	7,6	8,2	0,44	0,22
BK 1	88,2	86,2	4,2	4,4	7,7	9,4	7,7	8,2	0,26	0,18
BK 2	59,5	66,1	15,1	13,6	25,5	20,3	7,5	8,2	0,77	0,29
BK 3	10,3	13,8	40	41,9	49,7	43,4	8,6	8,7	0,84	0,49
BV	23,3	20	26	26,1	50,7	53,9	7,4	7,4	1,1	0,53
BV 1	35	33	25	25	40	42	7	7	1	0,4
BV 2	25	22	30	30	45	48	7,2	7,2	1,5	0,5
BV 3	23,3	20	26	26,1	50,7	53,9	7,4	7,4	1,1	0,53
BX	42,4	43,2	31,2	29,9	26,4	27	5,3	6,3	1,48	1,26
BX 1	75	71	20,6	24	4,5	5	5,2	5,3	1	0,7
BX 2	50	52	30	28	20	20	5,3	6,3	1,2	0,8
BX 3	26,2	29,3	36,5	32,8	37,4	38	5,3	7,2	1,48	1,26
C	42,9	38,8	27,6	27,1	29,5	34,2	7,3	8,1	1,52	0,56
CG	32	30	45	45	23	25	7	8	3,6	1,8
CG 1	80	70	10	10	10	20	6,5	7,6	3	1
CG 2	30	23	50	55	20	22	7	7,8	3,6	1,5
CG 3	42	38	22	22	36	40	7,2	8	3,6	1,5
CH	32,2	30,8	44,1	45,7	23,7	24	7,1	8	3,04	0,97
CH 1	80	75	10	10	10	15	7	8	2	0,7
CH 2	27,3	24,9	55,1	57,2	17,6	18	7,1	8,1	2,44	0,81
CH 3	42	42,5	22	22,8	36	36,1	7,6	7,7	2,89	0,96
CK	41,6	39,3	26,6	25,4	31,8	35,3	7,5	8,3	1,32	0,51
CK 1	80,5	41,5	8,6	14,7	11	43,9	6,7	8,8	1,01	0,32
CK 2	41,4	47,9	31,7	28,4	26,8	23,8	7,6	8,1	1,47	0,67
CK 3	16,1	17,9	26,8	25,7	57,1	56,3	7,7	8,4	1,17	0,25
CL	46,3	40,2	24,9	24,5	28,8	35,4	7,1	7,9	1,27	0,49
CL 1	79,7	68,7	4,4	3,5	16	27,8	7,2	7,6	0,72	0,35

CL 2	41,2	33,3	33,8	32	25	34,8	7,1	8	1,47	0,56
CL 3	39,9	39,7	17,3	19,9	42,9	40,5	7,1	8	1,22	0,49
D	40,2	35	50,3	47,2	9,6	17,8	5,3	5,2	1,09	0,24
DD	3	2,4	87,8	84,3	9,2	13,3	4,4	4,8	1,14	0,4
DD 1	70	65	18	15	12	20	4,5	4,9	1	0,3
DD 2	3	2,4	87,8	84,3	9,2	13,3	4,4	4,8	1,14	0,4
DD 3	45	40	15	10	40	50	4,6	5	1,5	0,5
DE	71,1	65,5	17,8	15	11,1	19,5	5,3	5,1	1,47	0,2
DE 1	71,1	65,5	17,8	15	11,1	19,5	5,3	5,1	1,47	0,2
DE 2	50	40	40	40	10	20	5,5	5,8	2	0,6
DE 3	45	40	15	10	40	50	5,5	6	2,2	0,7
DG	46,4	37,2	45,2	42,2	8,4	20,6	5,8	5,4	0,65	0,13
DG 1	70	60	20	20	10	20	5,6	5,8	2	0,6
DG 2	46,4	37,2	45,2	42,2	8,4	20,6	5,9	5,4	0,65	0,13
DG 3	50	40	15	10	35	50	5,8	6,2	2	0,6
E	48,5	45	30,8	32	20,7	23	7,6	7,5	1,74	0,9
E 1	70	67	10	11	20	22	7,5	7,8	0,9	0,5
E 2	50	47	25	26	25	27	7,6	8	1,96	0,9
E 3	30	27	35	36	30	32	7,5	8,2	2	1
F	35,7	31,1	16,3	15,8	48	53	5	5,2	1,93	0,75
FA	23,5	22,1	27,4	25,8	49,1	52	5,2	5,4	2,63	0,98
FA 1	83	70,3	5,3	9,4	11,7	20	5,8	5,4	0,62	0,33
FA 2	55	48	9	10	36	42	5,2	5,4	2	0,7
FA 3	13,6	14,1	31,1	28,6	55,3	57,4	5,1	5,4	3,03	1,11
FH	12,8	9,1	21,6	23	65,5	67,8	4,8	5,1	3,49	1,44
FH 1	80	69	6	6	14	25	4,6	5	3	1
FH 2	45	40	25	20	30	40	4,8	5,1	3,5	1,3
FH 3	13	9,1	20,9	23	66	67,8	4,9	5,1	3,64	1,48
FO	28,7	25,8	18,4	17,3	52,9	56,9	5,1	5,3	1,92	0,67
FO 1	79,1	65,5	7	5,6	13,9	29	4,6	4,8	0,65	0,36
FO 2	45,7	44,5	30,1	29	24,2	26,5	5,4	5,5	1,53	0,23
FO 3	15,7	13,9	16,5	15,5	67,8	70,6	5,1	5,3	2,21	0,81
FP	44,7	33,6	20,6	27,4	34,8	38,8	4,8	4,7	1,36	0,55
FP 1	80	63	6	7	14	30	4,8	4,6	1	0,3
FP 2	42	34,5	42	39,4	16	26,1	4,8	4,6	1,04	0,32
FP 3	57,7	32,6	5,8	15,4	36,5	51,5	4,7	4,7	1,69	0,78
FR	40,4	36,8	14,8	13,3	44,6	49,8	5,3	5,4	1,52	0,63
FR 1	80,7	76,2	4,1	4,3	14,6	19,4	5,3	5,1	0,65	0,29
FR 2	69,8	60,3	7,7	7,9	22,5	31,5	5,3	5,4	0,81	0,36
FR 3	23,9	21	18,9	16,9	57,2	61,9	5,2	5,3	1,84	0,83
FX	52,6	47,2	7,8	6,8	39,5	45,9	4,8	4,9	1,23	0,41
FX 1	79	68,6	5,8	6,3	14,8	24,7	5,3	5	0,81	0,3
FX 2	72,9	62,3	5,9	6,7	21,3	31	5	4,9	0,91	0,34
FX 3	8,6	7,5	8,9	7,4	82,4	85	4,4	4,8	1,73	0,58
G	32,9	44,3	23,7	19,7	43,4	37	6,1	6,4	2,02	0,72
GD	18,9	33,9	21,8	18	59,3	48,2	4,7	4,7	2,92	1,63
GD 1	80	80	5	5	15	15	5	5,3	2,3	1,2
GD 2	51,3	53,6	28,1	28,1	20,7	18,3	5,3	6,2	2,59	0,55
GD 3	11,8	30,5	20,5	14,4	67,7	55,1	4,5	4,3	2,96	1,93
GE	42,8	50,3	20,4	18,4	36,8	32,9	6,4	6,8	1,3	0,52
GE 1	82,1	83,2	6,5	4,5	11,4	12,3	6,8	6,9	0,81	0,23
GE 2	51	49,9	24,2	22	28,2	31,5	6,6	7,1	1,41	0,4
GE 3	25,5	38,1	23,1	19,7	51,3	42,3	6,1	6,4	1,35	0,78
GH	40,5	32,6	30,3	27,9	29,2	39,5	5	5,3	6,56	1,91
GH 1	80	80	5	5	15	15	4,6	5,3	5	1,5
GH 2	55,8	46,7	31,7	31,4	12,6	22	4,6	5,5	7,2	2,4
GH 3	25,2	18,6	29	24,5	45,9	57,1	5,4	5,2	5,27	1,42
GK	31,8	46,3	18	14,9	50,2	38,7	7	7,9	0,98	0,21
GK 1	80	80	5	5	15	15	7	7,5	1	0,3
GK 2	63,6	65,6	7,7	3,2	28,7	31,2	7	7,6	0,72	0,26
GK 3	25,6	41,8	21	17,6	53,4	40,5	7	8	1,04	0,2
GM	26,4	50,2	25,9	16,2	47,7	35,7	6	6,4	2,44	0,78
GM 1	81,5	89,4	8,2	5,8	10,4	4,8	7,1	6,5	0,77	0,3

GM 2	41,4	57,4	38,4	20	26,6	33,8	7,4	7,9	2,57	1,08
GM 3	20,5	45,6	25	16,1	54,5	38,4	5,6	6,1	2,54	0,7
GP	17,9	22,9	51,9	40,4	30,1	36,8	5,2	5,2	2,73	0,42
GP 1	40	40	50	45	10	15	5	5,2	2	0,4
GP 2	24,1	24,1	57,1	49,9	18,8	25,9	5,1	5,2	1,3	0,31
GP 3	8,6	21	44,1	26	47	53,1	5,5	5,1	4,88	0,59
GX	50	40	30	30	20	30	6	5,8	4,23	1,18
GX 1	80	80	5	5	15	15	6	5,8	2	1
GX 2	55	45	30	30	15	25	6	5,8	4	2
GX 3	25	20	30	25	45	55	6	5,8	4	2
H	37,3	52	25,7	20,5	37	27,5	6,5	6,8	1,57	0,53
HC	40,8	40,8	22,5	25,7	36,8	33,4	7,9	8,4	2,17	0,8
HC 1	75	70	15	15	10	15	7,2	8,2	2	0,8
HC 2	56,9	56,8	23	21,2	20,2	22	7,8	8,3	1,59	0,59
HC 3	8,5	8,8	21,5	34,9	70	56,3	8,2	8,6	3,33	1,23
HG	34,6	65,2	22,2	13,8	43,3	21	6	6,3	1,82	0,38
HG 1	83	90,8	6,6	3,3	10,3	5,9	5,9	6,9	0,7	0,11
HG 2	64,1	74,8	11,7	5,5	24,2	19,7	6,6	6,4	0,52	0,16
HG 3	13	56,2	29,5	19,3	57,6	24,6	5,6	6	2,72	0,53
HH	37,2	46	31,2	26,7	31,6	27,4	6,7	6,9	1,09	0,5
HH 1	75	70	20	20	5	10	6,5	6,7	1,5	0,5
HH 2	45,5	55,7	30,9	24,7	23,6	19,7	6,6	6,7	1,02	0,3
HH 3	20,7	26,5	31,9	30,8	47,5	42,8	7,3	7,6	1,28	0,92
HL	39,1	46,9	26,5	20,7	34,6	32,4	6,4	6,6	1,46	0,63
HL 1	75	70	15	10	10	20	6,4	6,6	1,5	0,5
HL 2	43,5	53,4	31,2	27,8	25,5	18,8	6,6	6,8	1,23	0,52
HL 3	33,2	38,3	20,2	11,2	46,6	50,5	6,4	6,6	1,8	0,75
I	58,9	56	16,2	17	24,9	27	7,1	7,2	0,97	0,4
I 1	75	72	15	16	10	12	8,3	8,3	0,31	0,2
I 2	65	62	15	16	20	22	7	7,2	1	0,4
I 3	55	52	15	16	30	32	4,8	5,5	2,3	0,8
J	55,8	52,7	22,2	23,5	22	23,8	6,3	6,3	1,32	0,81
JC	39,6	41,7	39,9	39,8	20,6	18,5	8	8,1	0,65	0,24
JC 1	68,9	62,9	16,7	20,1	14,4	17	8	8,2	0,28	0,11
JC 2	20,9	36,4	54	44,8	25,2	18,9	8	8,1	0,84	0,27
JC 3	10	10	50	50	40	40	8	8,2	0,9	0,3
JD	35,9	33,9	39,4	37,2	24,8	28,9	4,5	4,4	2,16	1,3
JD 1	79,5	85,9	13,5	9,3	7	4,8	5,6	5,5	1,31	0,77
JD 2	32,5	25,7	44,1	42,9	23,5	31,5	4,3	4,3	1,68	1,66
JD 3	2,3	6,8	51,3	48,2	46,5	45,1	4,1	3,6	4,47	0,74
JE	70,8	67	12,8	14,1	16,5	18,9	6,6	6,9	1,15	0,67
JE 1	80,1	79,5	8,6	7,6	11,4	12,9	6,4	6,5	0,76	0,25
JE 2	56,2	55,1	19,1	19,6	24,7	25,4	6,8	7,2	0,93	0,29
JE 3	21	21,1	36,9	40,1	42,2	38,9	7,2	7,4	2,61	0,83
JT	11,7	7,8	36,8	40,3	51,5	52	4,1	3,6	2,57	1,67
JT 1	50	50	30	30	20	20	3,5	2,8	2	1
JT 2	30	9,1	36,7	48,6	33,3	42,3	3,6	2,8	3	1,5
JT 3	5,8	7,4	34	37,5	60,2	55,2	4,3	3,8	2,57	1,67
K	39,1	42,6	37	33,9	23,9	23,4	7,6	7,9	1,93	0,89
KH	54,5	60,4	27,3	22,9	18,2	16,7	7,7	8,2	2,16	0,8
KH 1	80	65	10	10	10	25	7,2	8	1,2	0,5
KH 2	54,5	60,4	27,3	22,9	18,2	16,7	7,7	8,2	2,16	0,8
KH 3	40	40	20	20	40	40	7,7	8,5	2	0,8
KK	16,5	20,7	48,9	48	34,4	31,3	8	8,2	1,5	1,01
KK 1	80	70	15	15	5	15	8	8,2	1,5	1
KK 2	18,5	26,9	54,9	47,7	26,7	25,5	8	8,2	1,48	1,11
KK 3	12,5	11,8	37	39,3	50	48,9	7,9	7,9	1,55	0,81
KL	36,7	42,4	40,3	33,8	23,1	23,9	7,1	7,5	2	0,87
KL 1	80	70	5	5	15	25	7,1	7,5	1,6	0,8
KL 2	35,1	50,1	45,8	31,7	19	18,2	7,3	7,7	1,83	0,87
KL 3	41,4	39	23,5	22,8	35,2	38,2	7,3	7,4	1,73	1,01
L	70,4	64,5	10,3	9,9	19,3	25,7	6,7	7,2	0,51	0,27
LA	87,5	81,8	6,2	5,9	6,4	12,3	6,7	7,3	0,47	0,21

LA 1	90,1	84,5	4,5	4,6	5,3	10,9	6,8	7,4	0,28	0,16
LA 2	47,8	40,3	30,3	25,1	21,9	34,6	5,5	4,7	3,2	0,94
LA 3	50	30	25	20	25	50	6	6,5	1,5	0,5
LC	64,3	59	12,2	11,2	23,5	29,8	6,4	6,5	0,63	0,35
LC 1	80,2	73,3	7,7	6,9	12,1	19,8	6,4	6,6	0,3	0,22
LC 2	57,6	51	16,4	15,9	26,1	33,1	6,2	6,3	0,64	0,41
LC 3	29,2	31,4	13,6	12,3	57,3	56,6	6,5	6,8	1,51	0,48
LF	74,6	67,7	9,6	8,9	15,9	23,4	6,4	7	0,39	0,25
LF 1	82,2	75,1	7,3	6,7	10,5	18,3	6,1	6	0,37	0,22
LF 2	64,4	55,8	13,5	12,9	22,1	31,3	6,3	8,9	0,39	0,28
LF 3	26,9	26,1	19,1	18,2	54,1	55,6	5,7	5,6	0,54	0,5
LG	59,9	53,4	13,4	12,6	26,7	34	6,5	6,9	0,73	0,31
LG 1	81,7	71,9	6	5,8	12,3	22,3	6,3	6,7	0,45	0,2
LG 2	55,4	48,5	18,3	17,5	26,3	34,1	6,5	7,1	0,83	0,23
LG 3	42,4	41,3	12,7	10,6	44,9	48,2	6,8	7,2	0,85	0,52
LK	75,4	69,5	7,4	8,2	17,2	22,4	7,7	8,2	0,34	0,23
LK 1	84,3	79,7	5,1	5	10,6	15,4	7,5	8,1	0,26	0,17
LK 2	64	55,3	10,9	12,5	25,2	32,2	7,9	8,3	0,44	0,33
LK 3	46,7	39,1	14,8	17,7	38,6	43,3	8,4	8,9	0,49	0,36
LO	76	71,9	9,9	8,9	14,1	19,2	6,4	6,7	0,41	0,21
LO 1	87,1	81,6	4,2	4,2	8,7	14,3	6,3	6,6	0,33	0,17
LO 2	53,7	49,6	23,3	22,1	23	28,3	6,7	7	0,57	0,28
LO 3	43,5	43,1	13,4	12,3	43,1	44,6	6,3	6,2	0,66	0,4
LP	69,9	57,5	10,5	10,9	19,5	31,6	5,9	5,6	0,73	0,35
LP 1	74,8	65,1	11	11,6	14,2	23,3	5,7	5,5	0,55	0,32
LP 2	65,1	49,9	10,1	10,2	24,9	39,9	6,1	5,7	0,92	0,42
LP 3	45	35	10	10	45	55	6,3	5,6	1	0,4
LV	26,1	26,8	27,3	22,5	46,7	50,9	6,6	7,1	1,86	0,84
LV 1	55	50	20	15	25	35	6,6	7	1	0,4
LV 2	48,4	36,3	28,3	25,1	23,3	38,7	6,6	8,4	0,49	0,19
LV 3	23,8	17,2	28	19,8	48,4	63	6,6	6,5	2,55	1,16
M	37,9	47,9	35	30,4	27,1	21,6	6,6	6,6	3,23	0,78
MG	30	25	50	45	20	30	6,3	6,5	4	1,4
MG 1	75	70	15	10	10	20	6,1	6,3	3	1
MG 2	30	25	50	45	20	30	6,3	6,5	4	1,4
MG 3	40	35	20	15	40	50	6,3	6,8	4,5	1,3
MO	33,3	29,2	46,4	44,2	20,4	26,7	6,1	5,8	3,65	1,11
MO 1	75	70	15	10	10	20	6,1	5,8	3	1
MO 2	33,3	29,2	46,4	44,2	20,4	26,7	6,1	5,8	3,65	1,11
MO 3	40	35	20	15	40	50	6,3	7	4	1,4
N	57,9	46,6	13,3	12	28,9	41,4	6	6,1	1,12	0,46
ND	38,9	31,9	17,6	13,8	43,6	54,4	5,2	5,2	1,57	0,44
ND 1	85,1	78,2	7,3	8,5	7,7	13,3	4,6	4,8	1,04	0,39
ND 2	55	45	20	20	25	35	5,2	5,2	1,5	0,5
ND 3	15,8	13	22,7	15,8	61,6	71,3	5,5	5,4	1,64	0,52
NE	68,4	57,8	10,5	10	21,2	32,2	6,3	6,5	0,6	0,32
NE 1	81,8	72,7	5,9	6,2	12,3	21,1	6,3	6,3	0,34	0,21
NE 2	57,1	46,9	18,1	15,6	24,8	37,3	6,3	6,9	0,89	0,47
NE 3	22,8	13,1	21,2	15,9	55,9	70,7	6,7	6,9	1,33	0,48
NH	6,4	5,4	29,8	21,5	63,9	73,3	5,5	5,4	4,04	1,47
NH 1	80	70	8	5	12	25	5,2	5,4	2	0,8
NH 2	55	45	20	15	25	40	5,3	5,4	3	1
NH 3	6,4	6,3	29,8	24,6	63,9	69,2	5,3	5,2	4,01	1,65
O	35	35	40	40	25	25	4,9	4,6	46,33	49,37
OD	35	35	40	40	25	25	4,2	4,1	47,3	49,76
OD 1	70	70	20	20	10	10	4,2	4,1	50	60
OD 2	35	35	40	40	25	25	4,2	4,1	50	60
OD 3	10	10	45	45	45	45	4,2	4,1	50	60
OE	35	35	40	40	25	25	6,3	5,3	41,46	46,78
OE 1	70	70	20	20	10	10	6,3	5,3	40	45
OE 2	35	35	40	40	25	25	6,3	5,3	40	45
OE 3	10	10	45	45	45	45	6,3	5,3	40	45
OX	35	35	40	40	25	25	4,2	4,1	56,1	55,58

OX 1	70	70	20	20	10	10	4,2	4,1	55	55
OX 2	35	35	40	40	25	25	4,2	4,1	55	55
OX 3	10	10	45	45	45	45	4,2	4,1	55	55
P	69,5	72	23,9	22,2	6,7	7	4,6	4,8	3,86	1,24
PF	64,9	66,9	26,3	23	8,5	10	5	5,4	1,25	0,28
PF 1	94	94,4	3,3	3,6	2	2	5,3	5,6	0,6	0,31
PF 2	35,7	39,4	49,3	42,4	15	17,9	4,7	5,2	1,9	0,25
PF 3	43	40	40	40	17	20	4,8	5,4	2	0,5
PG	87,3	79,9	9,6	15,5	3,2	8,5	4,2	4,6	3,36	1,37
PG 1	87,3	79,9	12,3	15,5	3,2	8,5	4,2	4,6	3,36	1,37
PG 2	60	58	30	27	10	15	4,4	5	3,4	1
PG 3	43	40	40	40	17	20	4,4	5	3,4	1
PH	80,8	84,8	16,5	13,7	2,8	1,6	4,3	4,5	3,18	0,88
PH 1	96	93,9	3	4,9	1,1	1,3	4,3	4,5	1,11	1,2
PH 2	50,4	66,5	43,4	31,4	6,3	2,2	4,4	4,7	7,33	0,24
PH 3	43	40	40	40	17	20	4,5	4,9	5	0,5
PL	51,3	51,3	40,1	41	8,7	7,7	4,1	4,5	4,52	1,41
PL 1	90	90	9	8	1	2	4	4,4	3	1
PL 2	51,3	51,3	40,1	41	8,7	7,7	4,1	4,5	4,52	1,41
PL 3	43	40	40	40	17	20	4,2	4,6	3	1
PO	67,9	74,4	28,7	21,9	3,6	3,7	5	5,2	1,65	0,72
PO 1	91,4	90,9	8,2	7,2	0,8	2	4,7	5,4	0,44	0,28
PO 2	49	58	44	36,6	7	5,4	5,3	4,9	2,47	1,16
PO 3	43	40	40	40	17	20	4,7	5,5	2,5	1
PP	56,5	62,9	28,3	24,8	15,2	12,4	4,7	4,8	8,62	2,68
PP 1	98,6	96	1,1	2	0,3	2	4,9	4,3	0,94	1,75
PP 2	56,7	62,6	32,5	31,3	10,8	6,1	4,7	5,2	15,82	3,15
PP 3	22	30	38	41	40	29	4,6	4,8	1,88	0,9
Q	91,9	91,8	3,2	3	5	5,4	6,2	6,3	0,23	0,13
QA	92,6	92,4	3,6	3,7	3,7	5,8	5,9	5,8	0,87	0,1
QA 1	92,6	92,4	3,6	3,7	5,5	5,8	5,9	5,8	0,87	0,1
QA 2	93	84	3	3	4	8	5,5	5,9	1	0,2
QA 3	89	85	5	5	6	10	5,7	6	1,2	0,3
QB	92	92,4	3,1	2,8	4,9	5	6,4	6,4	0,21	0,12
QB 1	92	92,3	3,2	2,9	4,8	5	6,4	6,4	0,21	0,12
QB 2	89	83	3	5	8	12	6,4	6,6	1	0,25
QB 3	48,5	92,9	16	3	35,6	4,2	6,4	6,9	0,4	0,16
QF	91,7	91,2	3,3	3,1	5,1	5,8	5,9	6,4	0,27	0,15
QF 1	92	91,6	3	3	5	5,5	5,9	6,4	0,27	0,15
QF 2	90	86	3	4	7	10	6	5,5	0,5	0,15
QF 3	85	81	5	7	10	12	5,9	5,4	0,8	0,2
QL	92,8	91,7	2,7	2,9	4,7	5,5	6,3	6,1	0,2	0,12
QL 1	92,6	91,7	2,7	2,9	4,8	5,5	6,3	6	0,2	0,12
QL 2	87	80	3	5	10	15	6,3	6,1	0,8	0,2
QL 3	83	75	5	7	12	18	6,3	6,1	0,8	0,2
R	70,6	71,9	14,1	13,7	15,4	14,3	6,7	7	0,57	0,43
RC	63,5	62,8	19,2	18,4	17,3	18,7	7,6	7,6	0,76	0,41
RC 1	82,2	82,1	6,9	6,9	10,9	11,1	7,5	7,6	0,33	0,33
RC 2	38,7	37,1	35,5	33,8	25,8	28,8	7,5	7,6	0,58	0,52
RC 3	30	35	40	33	30	32	7,5	7,6	0,8	0,6
RD	82,1	79,2	6,7	5,7	11,3	15,1	7	6,8	0,27	0,15
RD 1	83	79,2	6,5	5,7	10,5	15,1	7	6,8	0,27	0,15
RD 2	40	44	37	38	23	18	6,2	5,6	0,5	0,16
RD 3	30	35	40	33	30	32	6	5,8	0,7	0,23
RE	68,3	71,6	15,1	15,2	16,6	13,2	6,4	6,8	0,5	0,45
RE 1	82,8	79,9	7,5	8,2	9,7	11,7	6,4	6,6	0,29	0,23
RE 2	38,7	43,8	36,9	38,2	24,6	17,9	6,9	7,1	0,82	1,04
RE 3	30	35	40	33	30	32	6,1	6,5	0,99	0,3
RX	82,5	87,5	9,9	6,3	7,7	6,3	5,4	5,5	1,7	0,77
RX 1	82,5	87,5	9,9	6,3	7,7	6,3	5,2	5	1,7	0,77
RX 2	40	44	37	38	23	18	5,4	5,5	2	0,8
RX 3	30	35	40	33	30	32	5,4	5,6	2,2	0,8
S	55,4	47,3	20,4	19,8	24,2	32,8	8,2	8,6	0,65	0,48

SG	53,9	37,7	25,5	26,2	20,6	36,1	8	8,7	0,67	0,45
SG 1	79,7	58	8,9	10,9	11,5	31,2	7,9	9,5	0,26	0,1
SG 2	35,4	21,5	44,9	40,3	19,5	38,1	7,1	7,7	0,5	0,2
SG 3	39,3	29,5	19,7	28,5	41	42	9,9	9,2	1,82	1,31
SM	51,7	59,7	31,9	21	16,4	19,2	7,6	8,5	1,14	0,46
SM 1	80	60	10	15	10	25	7,5	8,5	1,2	0,4
SM 2	55,4	59,7	25	21	19,6	19,2	7,6	8,5	1,14	0,46
SM 3	40	35	20	15	40	50	7,8	9	1,5	0,5
SO	57,6	47,2	13,5	16,8	29	35,9	8,5	8,7	0,39	0,51
SO 1	86,6	69,4	9,6	13,2	3,7	17,5	6,6	7,1	0,44	3,06
SO 2	59,5	47,7	16,4	20,5	24,4	31,6	8,8	9,4	0,4	0,19
SO 3	40,4	35,4	11,2	13	48,5	51,6	9,2	8,2	0,37	0,19
T	42,1	43,1	38,1	38,3	19,8	18,7	5,8	6,1	5,23	2,63
TH	41	42,6	41,3	41	17,7	16,4	5,4	5,7	7,03	3,66
TH 1	72,8	74,4	19,3	18,2	8	7,3	5,4	5,9	9,57	2,32
TH 2	34,3	36,2	49,5	49,9	16,2	13,9	5,3	5,7	6,97	4,42
TH 3	7,6	8,1	40,8	35	51,7	57	4,9	5	9,65	5,16
TM	31,2	27,5	39,6	42,8	29,2	30	6,3	6,5	3,95	1,93
TM 1	70	75	20	20	10	5	6,3	6,5	3,5	1,5
TM 2	38,5	34	44,5	49	17	17,3	6,5	6,9	4,35	2,37
TM 3	9,3	7,7	24,9	24,2	66	68,1	5,5	5,2	2,36	0,72
TO	38,2	41,6	36,6	35	25,2	23,5	6	6,4	3,02	1,08
TO 1	45	50	50	45	5	5	6	6,4	2,5	1
TO 2	43,5	48,1	41,1	39	15,5	12,9	6,4	6,8	3,31	1,15
TO 3	12	9,1	14	14,7	74	76,1	4,3	4,5	1,57	0,74
TV	64,5	67	26,2	26,3	9,3	6,7	6,3	6,5	1,4	0,84
TV 1	75,5	69	19,5	25,5	5	5,6	6,5	6,5	0,87	0,38
TV 2	42,5	63	39,7	27,9	18	9,1	5,8	6,3	2,3	0,74
TV 3	40	50	35	30	25	20	5,8	6,3	3	1
U	50,8	47	16,8	18	32,3	35	4,1	4,2	2,38	2
U 1	70	67	10	11	20	22	4,1	4,2	2	1,5
U 2	50,8	47	16,8	18	32,3	35	4,2	4,2	2,38	2
U 3	30	27	30	31	40	42	4,2	4,3	3	2
V	24,6	22,4	14,4	13,4	61	64,2	7,3	7,7	0,68	0,51
VC	22,4	20,8	24,5	23,5	53	55,7	7,8	8	0,69	0,46
VC 1	44	40	30	34	26	26	7	7,5	1	0,5
VC 2	43,7	39,4	28,6	33	27,3	27,6	7,8	7,9	1,43	0,76
VC 3	20,2	18,8	23,9	22,5	55,8	58,6	7,8	8	0,61	0,43
VP	25,1	22,8	12,2	11	62,7	66,1	7,2	7,6	0,68	0,52
VP 1	55	45	15	17	30	38	7	7,5	1	0,5
VP 2	53,2	44,2	15,9	16,5	31,1	39,4	7,8	7,8	0,76	0,57
VP 3	24,4	22,4	11,5	10,9	64,2	66,7	7,2	7,6	0,67	0,52
W	61,4	51,3	21,9	18,1	16,7	30,6	6,3	6,8	1,25	0,41
WD	19,8	15,2	55,2	47,5	24,8	37,3	4,7	5,1	4,27	0,53
WD 1	90	75	5	5	5	20	4,5	5	1,2	0,2
WD 2	28,5	23,5	61,5	55,5	9,8	21	4,5	4,5	1,5	0,13
WD 3	11,1	6,2	49	45,1	39,9	48,8	4,9	5,7	4,63	0,81
WE	76,6	68,9	10,3	7,5	13,1	23,4	6,2	6,4	0,46	0,24
WE 1	88,9	77,8	4,6	3,7	6,6	18,3	6,3	6,4	0,23	0,15
WE 2	52,1	47,4	24,4	16,3	23,5	36,3	5,7	6,5	1,06	0,59
WE 3	40,2	53,4	19,7	15,6	40,2	31	6,6	6,7	0,53	0,13
WH	60	50	10	10	30	40	4,8	5,4	2	0,5
WH 1	85	70	5	5	10	25	4,5	5,2	1,5	0,3
WH 2	65	50	10	10	25	40	4,8	5,4	2	0,5
WH 3	40	35	15	15	40	50	5,2	5,6	2,2	0,55
WM	21,1	16,6	56,8	41,6	22,2	41,8	5,9	6,6	2,02	0,65
WM 1	85	70	5	5	10	25	5,6	6,4	1,5	0,5
WM 2	21,1	16,6	56,8	41,6	22,2	41,8	5,9	6,6	2,02	0,65
WM 3	40	35	15	15	40	50	6	6,8	2,2	0,7
WS	69,1	57,6	16,7	14,1	14,3	28,3	6,9	7,8	0,72	0,34
WS 1	78,2	65,3	13	11,6	8,9	23,1	7,1	8,4	0,65	0,3
WS 2	50,3	42,1	25,3	19,3	24,4	38,7	6,7	7,4	0,87	0,46
WS 3	40	30	20	20	40	50	7	8,5	0,9	0,4

WX	65	50	10	10	25	40	5	5,6	2	0,5
WX 1	85	70	5	5	10	25	4,8	5,4	2	0,5
WX 2	65	50	10	10	25	40	5	5,6	2	0,5
WX 3	40	35	15	15	40	50	5,2	5,8	2	0,5
X	72,8	67,7	10,5	11	16,8	21,4	7,2	7,4	0,36	0,25
XH	54,8	52,4	20,6	21,5	24,9	26,3	7,7	8,2	0,53	0,24
XH 1	75,9	75,8	12,5	12,1	11,7	12,3	7,8	8,7	0,65	0,23
XH 2	55	52	21	21	24	27	7,7	8,2	0,5	0,25
XH 3	33,8	28,9	28,8	31	38,2	40,3	7,9	8,1	0,44	0,27
XK	48,7	37,4	29,9	36,4	21,6	26,1	8,2	8,4	0,64	0,36
XK 1	85,8	77,9	3,8	7,8	10,3	14,3	8,4	9,2	0,5	0,25
XK 2	20,5	18,2	57,9	54,6	21,8	27	8,3	8,3	0,67	0,34
XK 3	47,5	54,2	12,9	10,5	39,6	35,3	7,6	8,1	0,83	0,37
XL	76	70,8	8	8,4	16,1	20,9	7,1	7,3	0,32	0,24
XL 1	83,3	79,3	6,5	6,2	10,3	14,5	7,1	7,2	0,22	0,17
XL 2	66,7	62,3	10,8	10,8	22,7	27,1	7	7,3	0,39	0,3
XL 3	38,2	27	12,7	16,2	49,2	56,9	7,9	8,2	0,58	0,45
XY	64,6	56,3	21,1	23,5	14,4	20,2	8,4	8,1	0,38	0,22
XY 1	96,7	86,6	1,3	5,3	2	8,1	8,8	8,4	0,23	0,12
XY 2	32,4	26	40,9	41,7	26,7	32,3	7,9	7,8	0,52	0,31
XY 3	40	35	22	23	38	42	8,5	8,2	0,5	0,25
Y	49,2	42,4	26	27,9	24,8	29,3	7,7	7,8	0,33	0,23
YH	50,4	40,8	29	38,9	20,6	20,3	6,6	6,8	0,3	0,2
YH 1	75	75	12	12	13	13	6,4	6,8	0,3	0,2
YH 2	50,4	40,8	29	38,9	20,6	20,3	6,6	6,8	0,4	0,25
YH 3	35	30	27	30	38	40	6,8	7	0,4	0,25
YK	63,5	51	17,9	21,1	18,7	27,5	8	8,2	0,26	0,2
YK 1	82,4	76,7	10,4	15	7,6	8,4	7,7	7,9	0,12	0,13
YK 2	57,7	47,3	25,7	30,3	16,6	21,9	8,2	8,2	0,3	0,24
YK 3	31,4	3,3	25	24	43	71,3	8,4	8,6	0,5	0,29
YL	69,8	53	5,7	8,3	24,4	38,7	6,3	7	0,4	0,2
YL 1	80	75	6	6	14	19	6,3	6,8	0,35	0,2
YL 2	69,8	53	5,7	8,3	24,4	38,7	6,3	7	0,4	0,25
YL 3	35	30	12	16	53	54	6,5	7,2	0,4	0,3
YT	10	5	40	40	50	55	8	7,4	0,41	0,4
YT 1	50	45	25	25	25	30	7,8	7,2	0,3	0,3
YT 2	45	40	28	33	27	27	8,2	7,6	0,4	0,3
YT 3	9	2	35	40	56	58	8,2	8	0,4	0,3
YY	49	48,5	10,7	9,4	40,3	41,8	8,3	8	0,13	0,16
YY 1	96	94,7	3	4,1	1	1,2	8	7,7	0,13	0,16
YY 2	35	30	40	40	25	30	8,3	8	0,15	0,15
YY 3	2	2,3	18,3	14,7	79,5	82,4	8,5	8,3	0,12	0,12
Z	39,5	36,7	23,4	24,8	37,2	38,6	9	9,2	0,49	0,36
ZG	47,8	41,7	8,5	11	43,8	47,4	9,2	9,2	0,38	0,35
ZG 1	78,1	62,1	8,2	13,9	13,7	23,9	10,6	10,2	0,2	0,2
ZG 2	65,9	66,5	3,6	5,1	30,5	28,8	10,4	10,4	0,11	0,23
ZG 3	23,6	19,2	11	12,4	65,5	68,5	8,7	8,7	0,41	0,35
ZM	48,4	48,9	34,1	36,9	17,5	15,3	8,5	8,7	1,83	0,97
ZM 1	85	75	5	5	10	20	8,2	8,5	1,5	0,7
ZM 2	48,4	48,9	34,1	36,9	17,5	15,3	8,5	8,7	1,83	0,97
ZM 3	30	20	30	25	40	55	8,7	8,7	1,8	0,9
ZO	43,2	37,2	24,6	24,5	32,4	38,2	9,3	9,5	0,4	0,28
ZO 1	95,6	75,9	0,8	2,5	4,2	21,3	8,9	10,1	0,18	0,07
ZO 2	37,9	34,7	45,6	46,2	16,6	19,2	9,5	9,4	0,49	0,24
ZO 3	22,2	20,5	15,7	13,7	62,2	65,7	9,3	9,4	0,42	0,42
ZT	19,2	25,2	37,6	39,6	43,1	35,2	8,4	8,7	0,39	0,31
ZT 1	50	45	35	45	15	10	8,2	8,5	0,3	0,25
ZT 2	46,9	63,9	30,7	24,6	22,1	11,5	8,3	8,6	0,25	0,23
ZT 3	5,4	5,8	41,1	47,2	53,6	47,1	8,4	8,7	0,46	0,36